



Publication No. WI-2021-02

16 January 2022

The Watershed Institute

Applied Environmental Science

California State University Monterey Bay

<https://csumb.edu/watershed/>

100 Campus Center, Seaside, CA, 93955

Central

Coast

Watershed

Studies

CCoWS

**Eleven Year Summary of Watershed Studies
at Hollister Hills
State Recreational Vehicle Area:
Fall 2010 to Fall 2021**

Douglas Smith (PhD)
Jamie Schnieders (MS)
Mikaela Bogdan (MS)
Joey Klein (MS)
Kaitlyn Chow (MS)
Taylor Luna (MS)
Katherine Melchor
Lauren Marshall
Skylar Wolfe

Author Contact
dosmith@csumb.edu

Acknowledgements

Thanks to:

- Wes Grey, Nicholas Somilleda, Scott Soares, Matthew Allen and Hollister Hills SVRA Park Staff.
- Colin Nicol, John Silveus, Aimee Teaby, Andrea Goodmansen, and Carrie Williams (CSUMB Watershed Geology Lab).
- CSUMB's Geomorphic Systems and River Hydrology students from 2010 to 2021.

Cite this report as:

Smith D., Schnieders, J., Bogdan, M., Klein, J., Chow, K., Luna, T., Melchor, K., Marshall, L., and Wolfe, S. 2021. Eleven Year Summary of Watershed Studies at Hollister Hills State Recreational Vehicle Area: Fall 2010 to Summer 2021. The Watershed Institute, California State Monterey Bay, Publication No. WI-2021-2, pp 115.

Executive Summary

Off-highway vehicle (OHV) use and the attendant environmental impacts are managed in California by State Recreational Vehicle Areas. In 2010, Hollister Hills State Recreational Vehicle Area (HHSVRA) commissioned a study of erosion and sediment transport processes to improve resource stewardship practices. This report summarizes 11 years of study. The culminating product is a sediment budget that provides an estimate of the relative importance of OHV use in the overall watershed.

Our work focuses on the Bird Creek watershed, which drains most of the park. We summarize data and qualitative observations from the following Bird Creek watershed sediment sources: OHV use, stream channels, county roads, cattle, campgrounds, and landslides. Stream gages assess the sediment transport into and out of the park. We also describe best management practices that either reduce OHV sediment production or trap the sediment before it leaves the park. We create a sediment budget by extrapolating well constrained measures of both the trail erosion and sediment retention to the entire HHSVRA property (within the Bird Creek watershed).

Given certain assumptions (described in the text), OHV use erodes approximately 3392 metric tonnes/yr of sediment from trails. Sediment basins retain approximately 2262 tonnes/yr. The difference between those two values (1130 tonnes) represents sediment trapped on hillslopes before reaching a stream channel. The other sediment sources and sinks contribute very little to the budget, except for natural landslides that contribute sediment downstream of the park. The other sediment sources we assessed included stream bank erosion, stream channel erosion and storage, cattle impacts, campground runoff, and county road impacts. Nearly all of the OHV erosion and much of the county road impacts are located upstream of sediment basins, so they contribute almost no sediment directly to Bird Creek.

A seven-year trail erosion study determined that trails with condition indices of green and yellow erode at the same rate, while red-rated trails have significantly more erosion. We found that erosion rate does not depend on rainfall (inches/yr or inches/hour), soil type (granitic and clay), or use type (single track, ATV, or road). Trail management measurably decreases erosion rate.

We note that gully restoration, trail narrowing projects and trail decommissioning have been successful at reducing erosion. A detailed sediment source inventory of

Hidden Springs watershed indicates the need for one trail decommissioning and some general water bar maintenance

We estimated the sediment entering and leaving the park through stream gaging in bird Creek. Seven of the eleven study years did not have enough rain to generate significant sediment transport. Over the 11-year study, the average values were 6 tonnes/yr entering the park and 45 tonnes/yr leaving the park. Those are minimum values because of equipment failure during 2017, the rainiest year of the study.

Bird Creek contributes to the San Benito River. The San Benito is listed as impaired by excess suspended sediment. The proposed future target for annual suspended load in the watershed is 93,460 tonnes. Based on proportional drainage areas, Bird Creek within, and upstream, of the park is currently far below its target share (proportioned on watershed area) of 2060 tonnes/yr.

Table of Contents

| | |
|---|-----------|
| Acknowledgements..... | ii |
| Executive Summary..... | iii |
| 1 Introduction | 7 |
| 1.1 Geologic Setting | 10 |
| 1.2 Goals | 12 |
| 1.3 Hydrology | 13 |
| 1.4 Sediment Transport..... | 13 |
| 1.5 Sediment Sources..... | 14 |
| 1.6 Best Management Practices | 17 |
| 2 Methods..... | 18 |
| 2.1 Hydrology | 20 |
| 2.1.1 Precipitation | 20 |
| 2.1.2 Streamflow | 20 |
| 2.2 Sediment Transport..... | 21 |
| 2.3 Sediment Sources..... | 21 |
| 2.3.1 Off Highway Vehicle Use | 21 |
| 2.3.2 Campgrounds | 22 |
| 2.3.3 Stream Bank and Channel Erosion | 22 |
| 2.3.4 Cattle | 22 |
| 2.3.5 County Road Culverts | 22 |
| 2.3.6 Landslides and Colluvial Processes..... | 23 |
| 2.4 Best Management Practices | 23 |
| 2.4.1 Sediment Retention Basins..... | 23 |
| 2.4.2 Hidden Springs..... | 23 |
| 2.4.3 Coyote Trail Erosion Control..... | 24 |
| 3 Results | 24 |
| 3.1 Hydrology | 24 |
| 3.1.1 Precipitation | 24 |
| 3.1.2 Streamflow | 26 |
| 3.2 Sediment Transport..... | 28 |
| 3.2.1 Bed Load | 28 |
| 3.2.2 Suspended Load | 28 |
| 3.3 Sediment Sources..... | 30 |
| 3.3.1 Off Highway Vehicle Use | 30 |
| 3.3.2 Campgrounds | 37 |

| | | |
|------------|---|------------|
| 3.3.3 | Stream Bank and Channel Erosion | 39 |
| 3.3.4 | Cattle | 44 |
| 3.3.5 | County Road Culverts | 46 |
| 3.3.6 | Landslides and Colluvial Processes..... | 60 |
| 3.3.7 | Landslide Causes..... | 83 |
| 3.4 | Best Management Practices | 86 |
| 3.4.1 | Sediment Retention Basins..... | 86 |
| 3.4.2 | Hidden Springs Sediment Inventory..... | 94 |
| 3.4.3 | Gully Management: Example BMP..... | 98 |
| 4 | Discussion | 103 |
| 5 | References | 107 |
| 6 | Appendix A..... | 114 |

1 Introduction

Off-highway vehicle use has a long history in western states. Increased popularity in the 1960's led to mounting environmental damage in public lands. The problem was first addressed in California in 1971 with the California Off-Highway Vehicle (OHV) Recreation program and the Chappie-Z'berg Off-Highway Motor Vehicle Law (Bedrossian and Reynolds 2007a). The law ensured stewardship of the land through maintenance and oversight while providing ample designated riding areas for enthusiasts (Bedrossian and Reynolds 2007a). The resulting State Vehicular Recreation Areas (SVRAs) are managed by the Off-Highway Motor Vehicle Recreation (OHMVR) Division of California State Parks, which was established by the OHMVR Act of 2003 to foster "education, conservation, and enforcement efforts that balance OHV recreation impacts with programs that conserve and protect natural resources" (California State Parks 2009). The OHMVR Act was renewed and revised in State Bill 247 in 2017. Among other provisions, it restated the importance of documenting the efficacy of soil conservation measures—annually in some cases (CA 2017).

Early studies documented significant erosion impacts of OHV use both in unregulated wilderness (Wilshire 1983) and within the SVRA system (Griggs and Walsh 1981). In response to these studies, ideas about best management practices (BMPs) began to emerge (Tuttle and Griggs 1987).

Soil conservation standards and guidelines for OHV use in California were published in 1991 (and updated in 2006) in response to a 1987 mandate (Bedrossian and Reynolds 2007a and 2007b). The standards require maintenance of OHV areas and trails, use of an erosion hazard rating system, and annual monitoring that would allow for "feasible rehabilitation by resource managers" (Bedrossian and Reynolds 2007a). The updated soil conservation standards stimulated SVRA managers to improve and expand best management practices (BMPs) and restoration efforts. In particular, they aimed to reduce soil loss and eliminate off-site sediment transport. While there is an encyclopedic inventory of the volumes written about OHV impacts (Ouren et al. 2007), there is scant literature on the appropriate methods for documenting the improvements that result from BMP implementation and environmental restoration efforts. Thus, the requirement in SB 249 (CA 2017) to report on the effectiveness of soil conservation efforts is problematic.

This report is an eleven-year study of watershed processes, focusing on sediment erosion, transport, and management within the Bird Creek watershed portion of the Hollister Hills SVRA (HHSVRA). The HHSVRA is located near Hollister, CA (Fig. 1). Park environmental scientists contracted the Watershed Geology Lab at California State University Monterey Bay to provide a variety of watershed studies focused on evaluating sediment sources, sediment

BMPs, and the net impact on local waterways. The monitoring work spanned from Fall 2010 to Fall 2021.

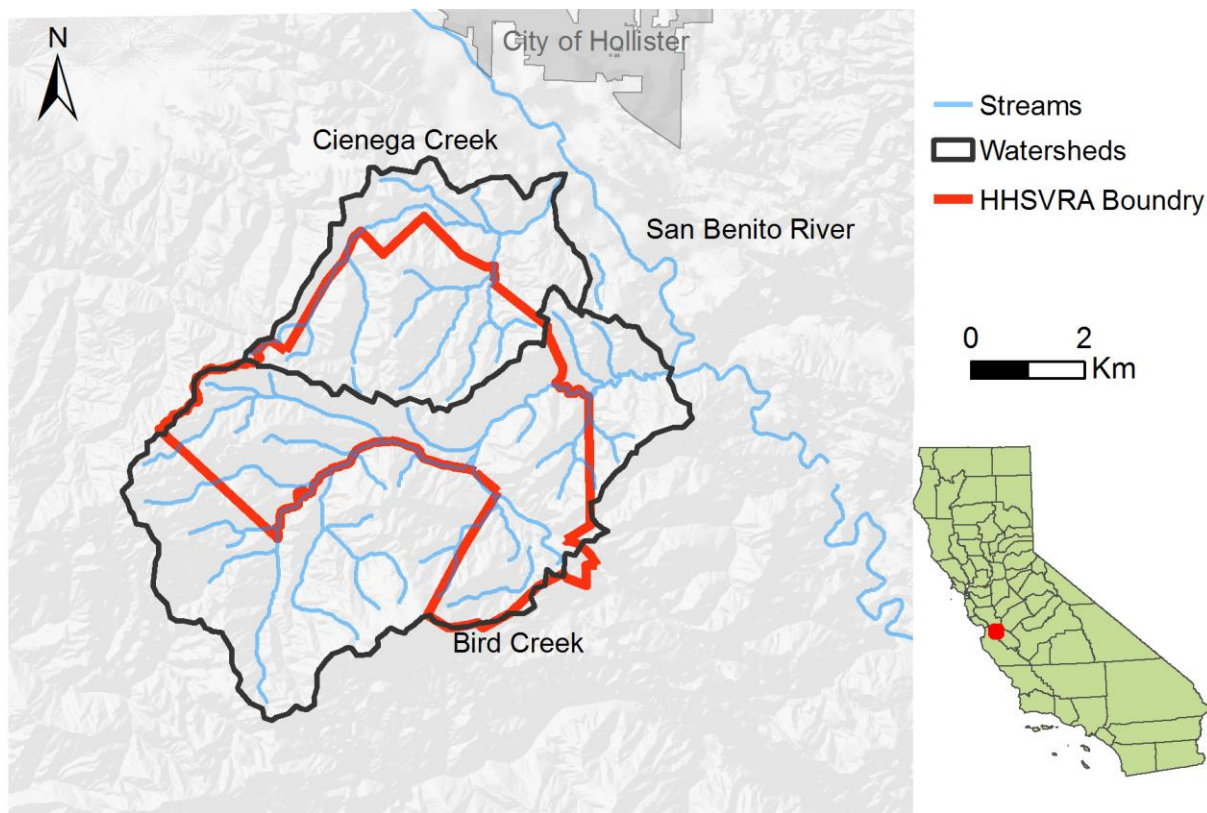


Figure 1. Hollister Hills State Vehicular Recreation Area in San Benito County, California. The park spans portions of Cienega Creek and Bird Creek watersheds.

Runoff from the HHSVRA enters the San Benito River via Bird Creek and Cienega Creek (Fig. 1). The San Benito River was 303(d) listed in 1998 for suspended sediment and siltation (RWQCB 2006). While the relative importance of individual suspended sediment sources in the San Benito watershed is not well established (ESA PWA 2013), the range of possible sources includes a variety of agricultural activities, timber harvesting, grazing upon pasture and range lands, urban and rural residential development, paved and unpaved roads, farm animal and livestock, off-highway recreational vehicle areas, uncontrolled off-highway trails, sand and gravel mining, various other hydro-modifying activities, and natural erosion and landslides (Figs. 2 and 3; RWQCB 2005). The San Benito River sediment impairment was addressed by the Total Maximum Daily Loads (TMDL) process. In that process, TMDLs were very roughly estimated for various activities in the watershed, and a watershed-scale limit and timeline were established. The goal for the entire San Benito Watershed is to not exceed 93,460 tonnes/yr by approximately 2050 (RWQCB 2005). On

the other hand, actual, calculated sediment transport (via rated stream gages) in the San Benito River has not happened in recent years, so there are no updates on achieving that goal. The only recent suspended sediment study in the San Benito River (ESA PWA 2013) was not useful because it was conducted in a dry year (WY 2012).

One goal of this study is to explore the sediment budget of Bird Creek and the HHSVRA within the context of the broader San Benito watershed sediment problem.

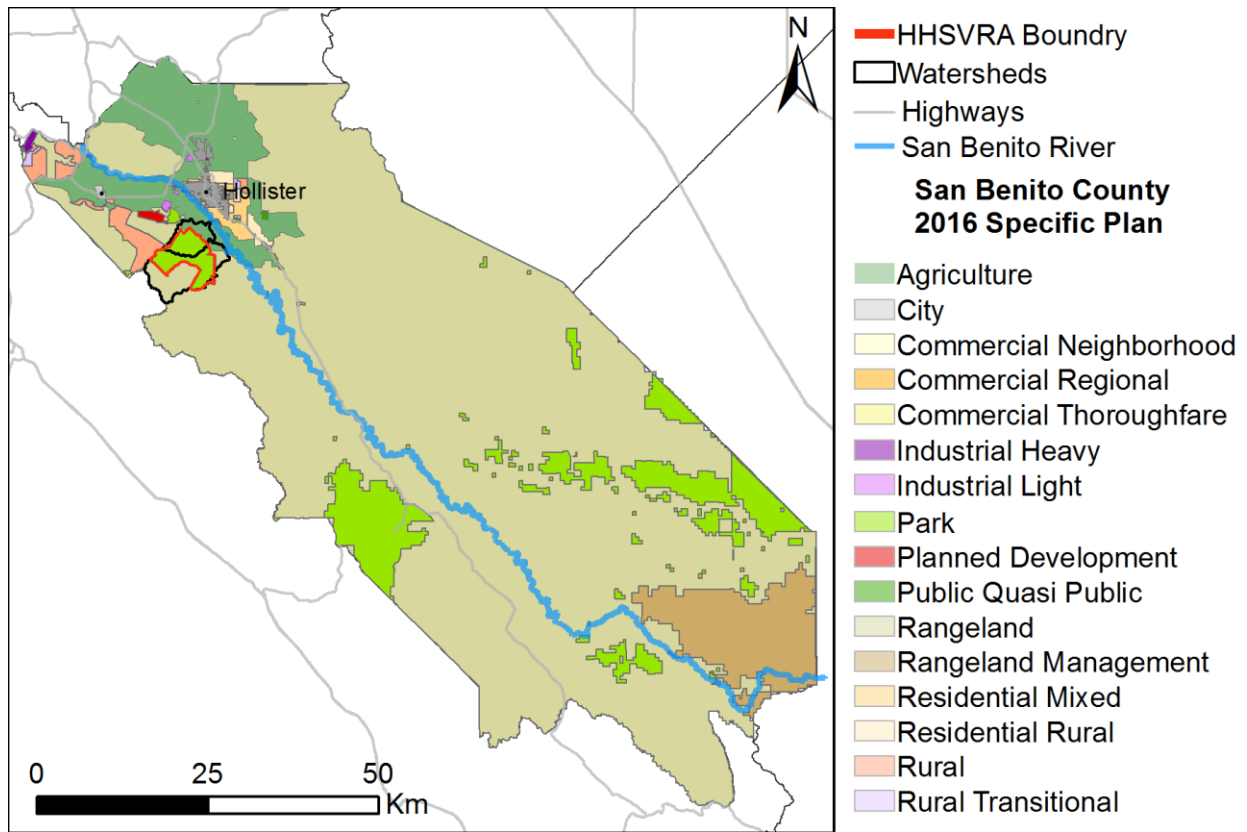


Figure 2. San Benito County 2016 Specific Plan. Data from San Benito Count 2016.

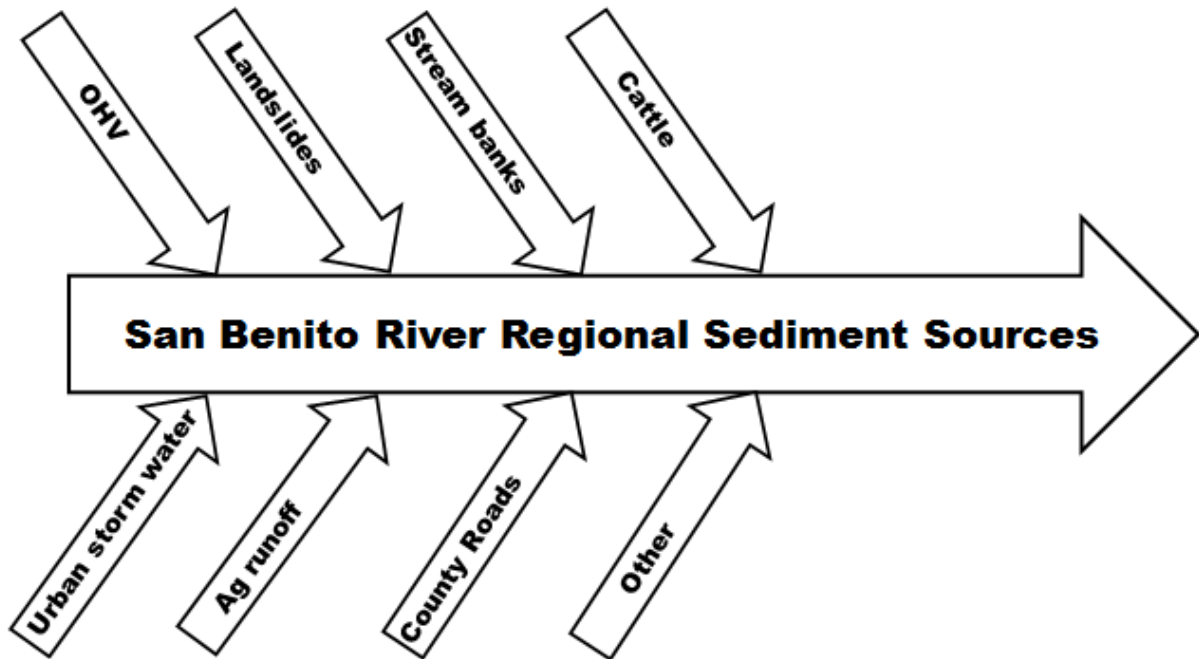


Figure 3. There are many sediment sources in the San Benito River watershed.

1.1 Geologic Setting

The San Andreas Fault bisects the park into two regions with contrasting substrate and soils (Figs. 4 and 5). The northeastern portion of the park is underlain by fine-grained Miocene and Pliocene marine and non-marine sedimentary rocks (Harden et al. 2001; Wagner et al. 2002; Graymer et al. 2006) that produce clay-rich soils (NRCS 2011). Our experience indicates that the clay-rich soils are prone to slope failure and deep erosion in wet weather. The southwestern portion of the park is underlain by pervasively fractured Cretaceous granite and older dolomitic marble that produce well drained granular soils (Harden et al. 2001; Wagner et al. 2002; Graymer et al. 2006; NRCS 2011). These soils are typically less erodible than the clay-rich soils in wet weather, but can form significant gullies on steeper slopes.

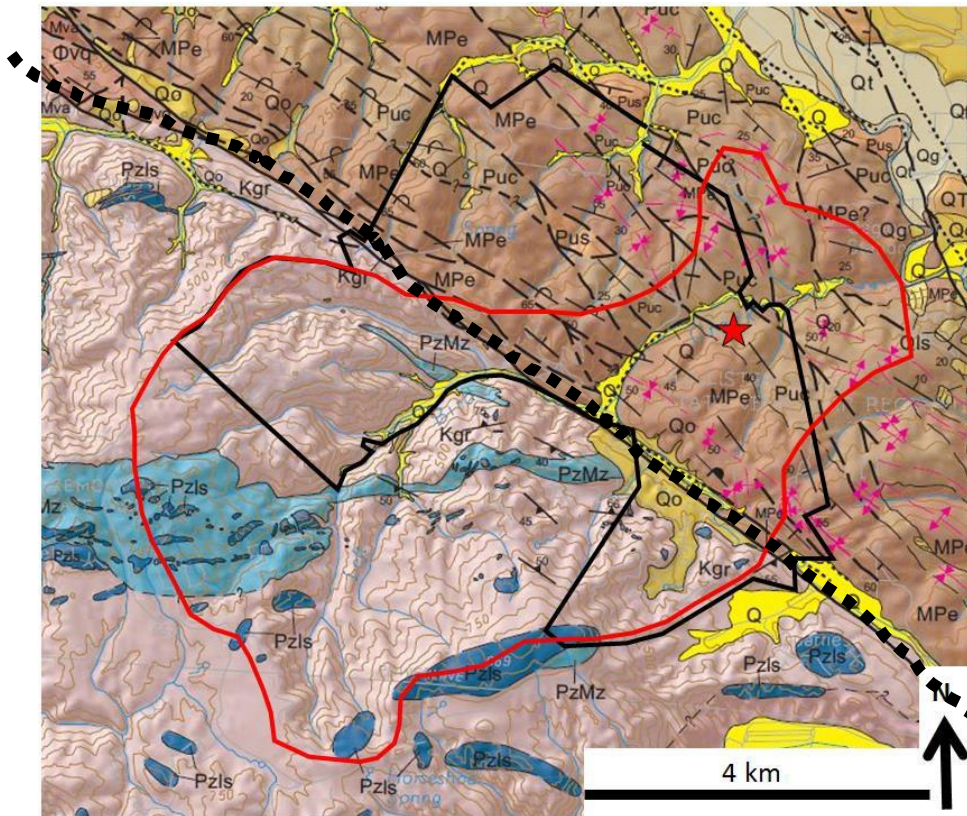


Figure 4. Geologic units within the HHSVRA boundary (black line) and Bird Creek watershed (red line) include Paleozoic limestone (Pzls) and marble (PzMz), Cretaceous granite (Kg), Miocene/Pliocene shallow marine sandstone (MPe), Pliocene continental sandstone (Pus) and mudstone (Puc), and various Quaternary alluvial deposits (Qx). From Wagner et al. (2002). San Andreas Fault is dotted black line

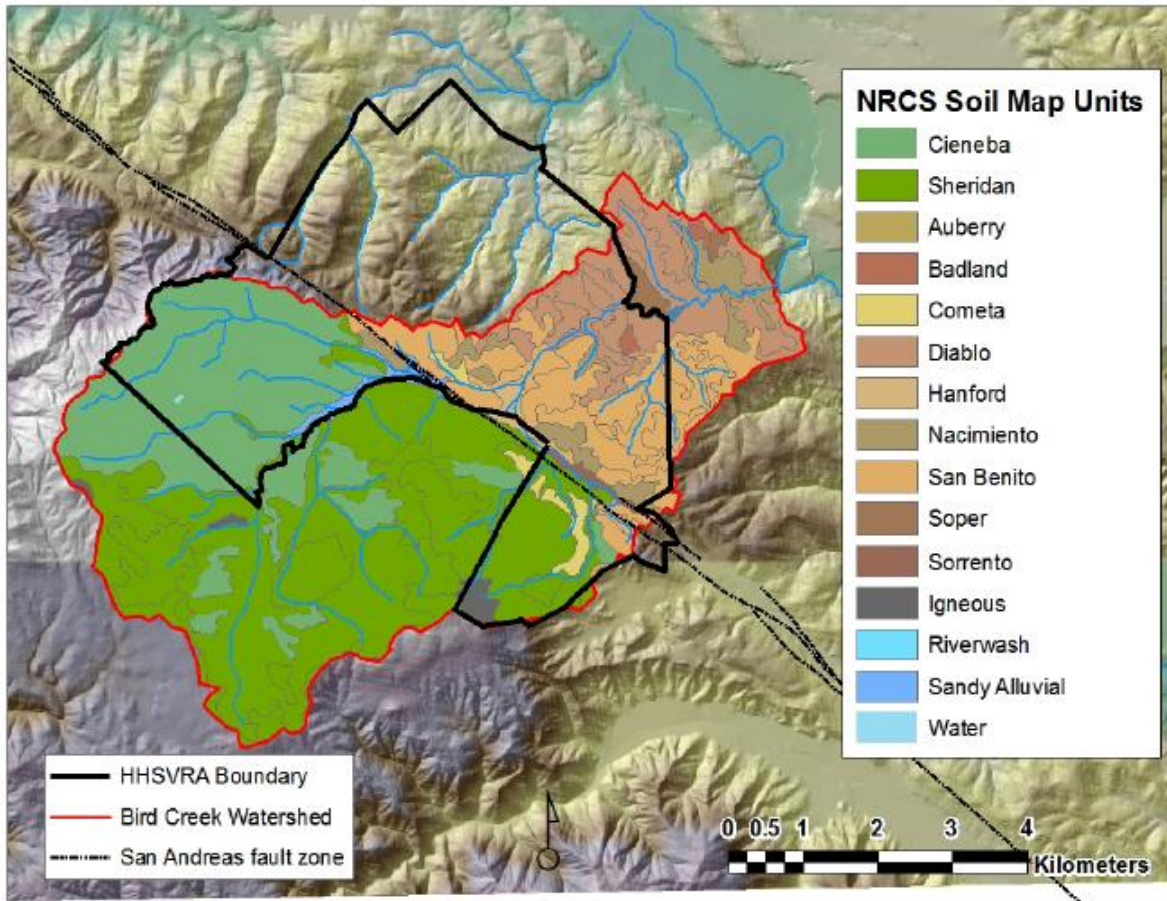


Figure 5. Soil map of Hollister Hills State Vehicular Recreation Area and the Bird Creek watershed. Note the change in soil type from the northeastern to the southwestern side of the San Andreas Fault.

1.2 Goals

The specific goals of our work were to:

- estimate the amount of sediment transported by Bird Creek,
- create an inventory of sediment sources within the watershed,
- generally assess the relative importance of each sediment source,
- explore the general efficacy of sediment control measures at HHSVRA, and
- evaluate the need for a sediment retention basin in Hidden Springs watershed.

The general approach for this work was to gage the Bird Creek channel for water and sediment discharge and to monitor a range of potential sediment sources at least once, and annually in some cases. Most of the data were collected and analyzed by paid student research assistants, and in some cases, classes of students would study specific topics in

greater detail as part of a class project. This report summarizes all the results, including class projects that had sufficient quality control.

1.3 Hydrology

Bird Creek responds to a Mediterranean climate in which most of the precipitation falls between October and April. The long-term average annual precipitation for Bird Creek is 419 mm (16.5 in), ranging from 397 mm (15.6 in) in the lower watershed to 491 mm (19.3 in) at the ridge tops (Prism 2004). The rainfall in Central California is dominated by drought interspersed with years with high-magnitude rain events, commonly delivered by atmospheric rivers in El Niño winters. The high magnitude events can have a dramatic and lasting impacts on landscapes and infrastructure, especially following wildfire (Smith et al. 2021)

Small streams in Central California often have a “flashy” hydrograph, in which short term large flow events account for a large portion of annual stream discharge. Most storm runoff events can be expected to last less than 24 hours, although multiple rain events within a short period of time may lead to longer lasting (and relatively higher) flows. Rain events late in the season will disproportionately generate larger runoff events because the soils tend to be more saturated. Hot and dry summers typically lead to ephemeral streamflow in the regional waterways, including Bird Creek. Ephemeral streams typically dry up in summer and fall after the water table has dropped too far to produce baseflow conditions. Bird Creek is ephemeral, except in two short reaches that have nearly perennial flow because of locally active springs. The perennial channel reaches are located 50 m downstream of the bridge leading to ranger residences and in the Hudner Ranch area. During serial drought years, even the spring-fed stream reaches dry up.

1.4 Sediment Transport

Sediment transport within the park mainly starts when either natural processes or human impacts (OHV use, cattle, etc.) dislodge sediment from hill slopes or stream banks where it can advance downslope under the influence of gravity, flowing water, or both. Once sediment reaches a 1st order channel, it moves as either bedload or suspended load along the channel network. Bedload is classified as the portion of sediment that moves on, or near, the stream bed by rolling, sliding, or skipping. Suspended sediment is the portion of fine particles, which is transported within the water column, suspended above the bed by water turbulence (Leopold et al. 1964). We assessed both bedload and suspended load transport rates in Bird Creek.

1.5 Sediment Sources

Sediment sources that we assessed at least qualitatively in the past eleven years include: off highway vehicle use, campgrounds, stream bank and channel erosion, cattle, county road culverts, and colluvial processes such as landslides (Fig. 6).

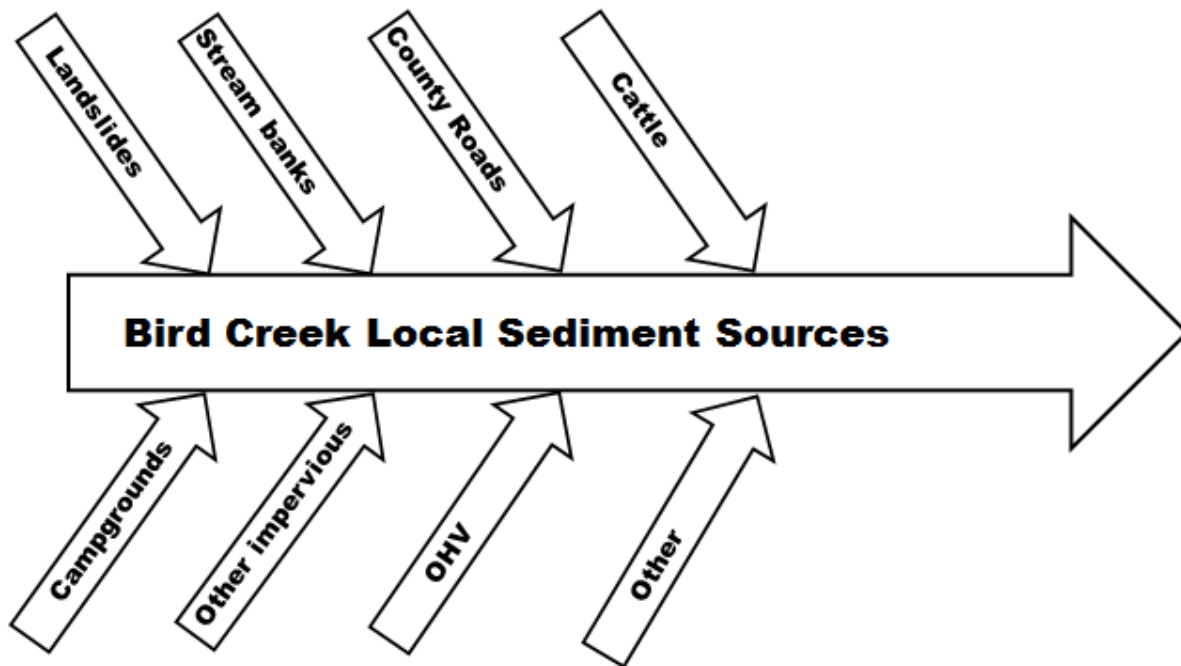


Figure 6. Potential sediment sources in the Bird Creek watershed.

HHSVRA comprises over 150 miles of dirt trails for 4-wheel drive, ATV, and motorcycle recreation. Past studies have shown that even though unpaved trails may only compose a small percentage of a watershed they might contribute a disproportionate amount of sediment runoff (Turton et al. 2009).

Campgrounds, staging areas, and roads that are only indirectly related to OHV activities were explicitly called out as commonly overlooked sediment sources in OHV parks (Bedrossian and Reynolds 2007b). HHSVRA contains seven campgrounds with compacted dirt areas. Compacted dirt in the campgrounds, staging areas, and near administrative and maintenance buildings can act as an impervious cover causing runoff to flow into adjacent streams. Likewise, county roads unrelated to the park are present in the watershed. San Juan Canyon Road bounds the park on the northwest and Cienega Road crosses the park lower in the watershed, near the park entrance. These roads are impervious surfaces that concentrate runoff onto park property. The roads also employ a great number of culverts that further concentrate flow into jets that can erode the down-gradient slopes. Impervious

surfaces and culverts inevitably lead to an increase in surface runoff, slope destabilization, and sediment load (Montgomery 1994, Luce and Wemple 2001).

Stream channels and banks naturally transport, store, and release sediment to reach equilibrium with watershed conditions (Wynn and Mostaghimi 2006). Stream systems that have been destabilized by chronic excess runoff can become long-term sources of non-point source sediment as they undergo a well-documented cycle of incision and re-equilibration (Harvey and Watson 1986; Hawley et al. 2012). Sediment contributions from these sources can be quantified with bank pin and cross section studies (Harrelson et al. 1994). Stream banks along Bird Creek vary greatly in height and material strength. For example, a marked change in geology occurs across the San Andreas Fault (Fig. 4). West of the fault, in the granitic part of the watershed, the soil along Bird Creek is sandy alluvial loam. East of the fault, where the watershed is underlain by weaker sedimentary rocks, the Creek runs through diablo clay and gravelly loam (NRCS Website; Fig. 5). Clay, having low bulk density, is not only a suspended sediment component but also prone to subaerial erosion (Prosser et al. 2000).

HHSVRA grazes cattle during certain times of the year on the Hudner Ranch area to reduce the coverage of invasive perennials and grass species (CDPR 2012). Cattle are agents of geomorphic change, trampling and reshaping the landscape with their hooves. While upland grazing compacts and disturbs the soil, the greatest water quality impacts occur when cattle have access to the streambanks and channel (Trimble and Mendel 1995). Grazing is restricted to certain times and areas in the HHSVRA, and riparian areas are fenced to keep cattle out of the channel. Cattle on properties that border the park have free access to stream banks and channels.

Colluvial processes (e.g., creep, landslides, debris flows) are the main natural mechanism by which soil and rock move down from hillslopes to waterways. Landslides are defined as the downward and outward movement of a mass of rock, earth, or debris under the influence of gravity (Dikau et al. 1996). Their distinctive morphology make them simple to identify in the landscape (Fig. 7). Scheingross et al. (2012) recognized that much of the substrate along the San Andreas Fault near the HHSVRA is susceptible to slow land sliding (earthflow) processes that are prevalent along regions with fine-grained sediment, steep slopes, and a lack of high-magnitude earthquakes. These conditions prevail in the Bird Creek watershed, east of the San Andreas Fault (Fig. 7). Landslides can be a major source of excess sediment in rivers if they are hydraulically connected to a river channel (Davies and Korup 2006). Landslides are abundant in the HHSVRA; we assess whether or not they are volumetrically important to the annual sediment load of Bird Creek, or if they are active on a much longer (geologic) time frame that is of less interest to resource managers.

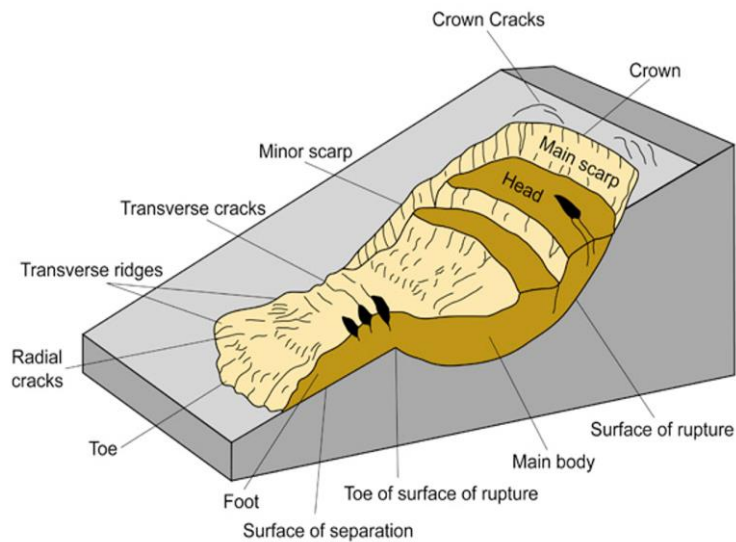


Figure 7. Typical landslide morphology.

Scheingross et al. (2012) recognized that much of the substrate along the San Andreas Fault near the HHSVRA is susceptible to slow land sliding (earthflow) processes that are prevalent along regions with fine-grained sediment, steep slopes, and a lack of high-magnitude earthquakes. These conditions prevail in the Bird Creek watershed, east of the San Andreas Fault (Fig. 8). Landslides can be a major source of excess sediment in rivers if they are hydraulically connected to a river channel (Davies and Korup 2006). Landslides are abundant in the HHSVRA; we assess whether or not they are volumetrically important to the annual sediment load of Bird Creek, or if they are active on a much longer (geologic) time frame that is of less interest to resource managers.

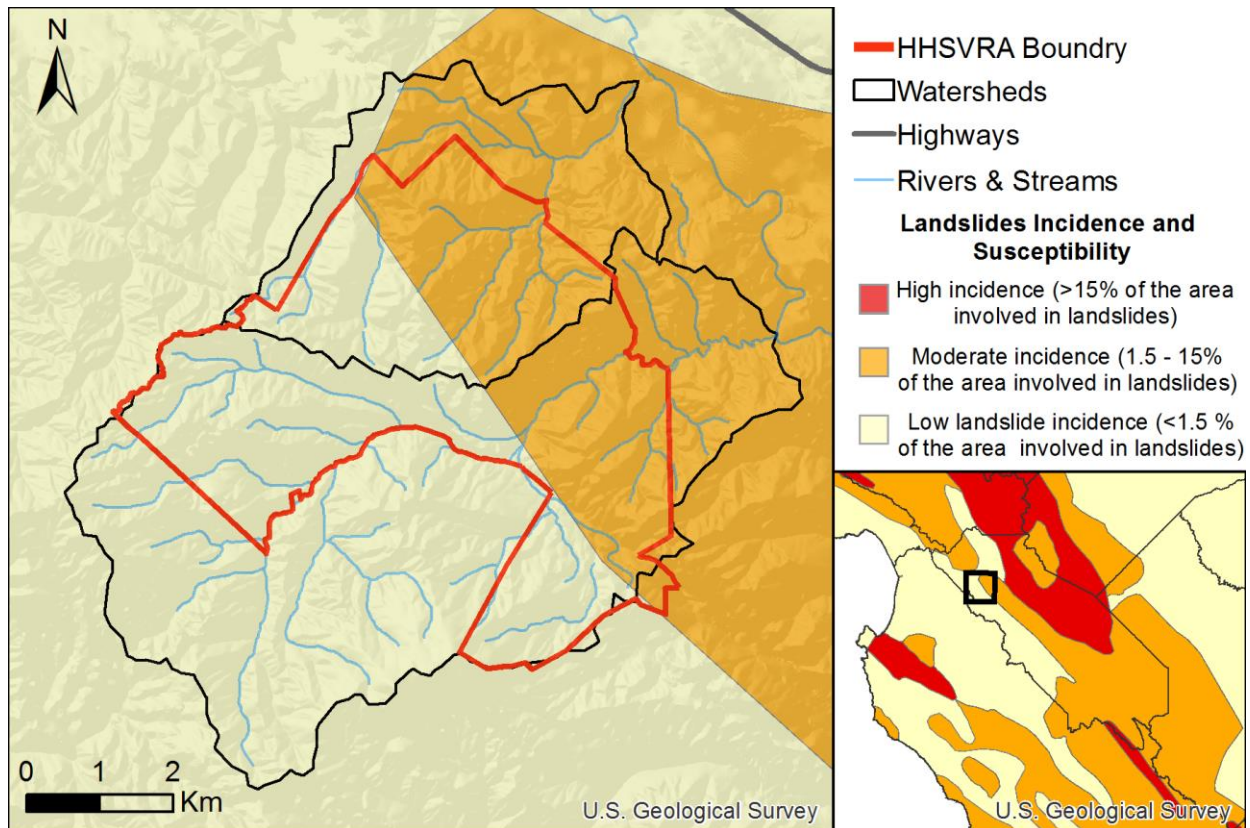


Figure 8. Landslides susceptibility within San Benito County and HHSVRA. Data from USGS 2016.

1.6 Best Management Practices

HHSVRA best management practices (BMPs) include trapping eroded sediment in 25 retention basins located throughout the park. Sediment is removed from the basins on a multi-year time frame as part of long-term sediment management. These basins were constructed in the Bird Creek tributaries many years ago to retain sediment eroded by OHV use. The sediment volume retained by the basins is typically estimated by the number of “truckloads” that are excavated from time to time. We began more detailed sediment volume estimates during our study using topographic surveys.

Other best management practices (BMPs) employed by the park include narrowing trails, outsloping trails, planting native plants on hillslopes, and decommissioning and restoring trails that are deemed to be unsustainable or that pose extreme erosion hazards (Fig. 9). These practices have been ongoing for decades at HHSVRA. Another best management practice is gully stabilization. To reduce erosion, gullies are filled and graded. In some

cases rock berms or other hard engineering is used for stability while native plants establish natural strength. We monitored a gully restoration site from 2012 to 2021.



Figure 9. Example of BMP that includes trail narrowing, outsloping, and planting (A). Decommissioned part of trail has rock drainage and native plantings. Vegetation is sparse because it was recently planted on the newly graded slope. Planted and volunteer native vegetation is still filling in the graded slope after 10 years of maturation.

2 Methods

General methods are described below. More detailed methods can be found in the past reports and in the results section of this report. Table 1 is a timeline indicating when various data sets were collected. Figure 10 shows where most studies are located.

Table 1. Timeline of HHSVRA study type and year.

| Study | Year | | | | | | | | | | | |
|-------------------------|------|------|------|------|------|------|------|------|------|------|------|---|
| | 2011 | 2012 | 2013 | 2014 | 2015 | 2016 | 2017 | 2018 | 2019 | 2020 | 2021 | |
| Precipitation | | | | | | | | | | | | |
| Radio Ridge | | X | X | X | X | X | X | X | X | X | X | X |
| Grand Prix 1 | | X | X | X | X | X | X | X | X | X | X | X |
| Gauges | | | | | | | | | | | | |
| Qw & Qsus | | | | | | | | | | | | |
| Nature | X | X | X | X | X | X | X | x | X | X | X | X |
| Hudner | X | X | X | X | X | X | X | x | X | X | X | X |
| Bedload | | | | | | | | | | | | |
| Nature | X | | | | | | | | | | | |
| Hudner | X | | | | | | | | | | | |
| Bank pins | | | | | | | | | | | | |
| Bird Creek | X | X | | X | X | X | | | | | | |
| Landslide Pegs | | | | | | | | | | | | |
| Colluvial Landslides | X | X | X | X | | X | X | X | X | | | X |
| Hudner Landslides | | | | | | X | X | X | X | | | X |
| Trails | | X | X | X | X | X | X | X | X | X | | |
| Sediment Basins | | | | | | | | | | | | |
| Gilmore | | X | X | | | | X | X | | | | |
| Grand Prix 1 | | X | X | X | X | X | | | | | | |
| Grand Prix 2 | | | | | | | X | X | | | | |
| Lodge | | | | | X | | | | | | | |
| Office | | X | | | | X | X | X | | | | |
| Scandia | | | X | | | X | X | X | | | | |
| Super Hill | | | X | | | X | X | | | | | |
| Sycamore | | | | | | | | | | | | |
| Vineyard | | | X | | | | | | X | | | |
| Whoopdeedoo | | X | | | | | | | | | | |
| Woodwardia | | X | | | | X | X | X | | | | |
| Cross Sections | | | | | | | | | | | | |
| Bird Creek | X | X | X | X | X | X | X | X | X | | | X |
| Colluvial Creek | X | X | X | X | | X | | X | | | | X |
| Coyote | | X | | X | X | X | | | | | | |
| Misc | | | | | | | | | | | | |
| Campgrounds | | X | | | | | | | | | | |
| Cattle Impact | | X | | | | | | | | | | |
| San Juan Grade Culverts | | | | X | | | | | | | | X |
| Cienega Culverts | | | X | | | X | | X | | | | X |

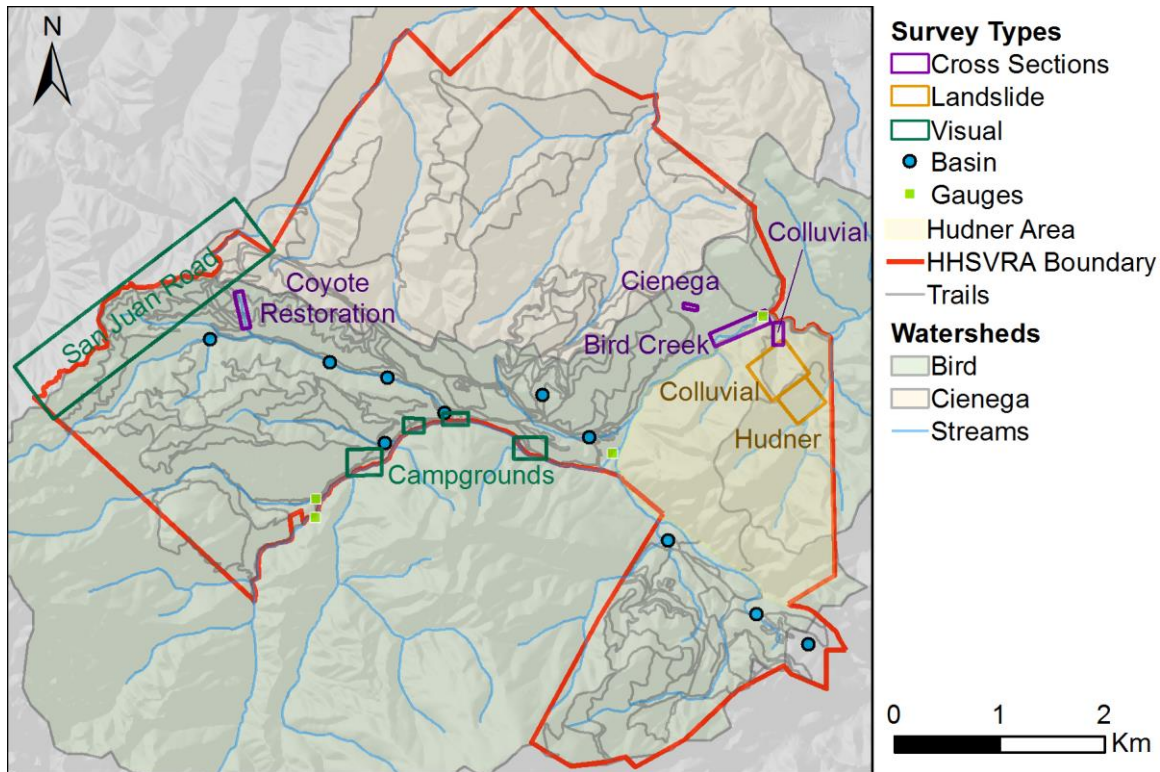


Figure 10. Spatial distribution of all HHSVRA monitoring sites and type of study.

2.1 Hydrology

2.1.1 Precipitation

Local precipitation was monitored from 2011 – 2021 through Western Weather Group’s web-based platform. Hourly data were collected from HHSVRA meteorological stations at Radio Ridge and the Gran Prix Track (WesternWeather 2021).

2.1.2 Streamflow

In 2010, two gaging sites—Nature and Hudner—were established on Bird Creek in areas with adequate accessibility and hydraulic control (Fig. 11). Streamflow and sediment transport was estimated using a variety of gaging instruments.

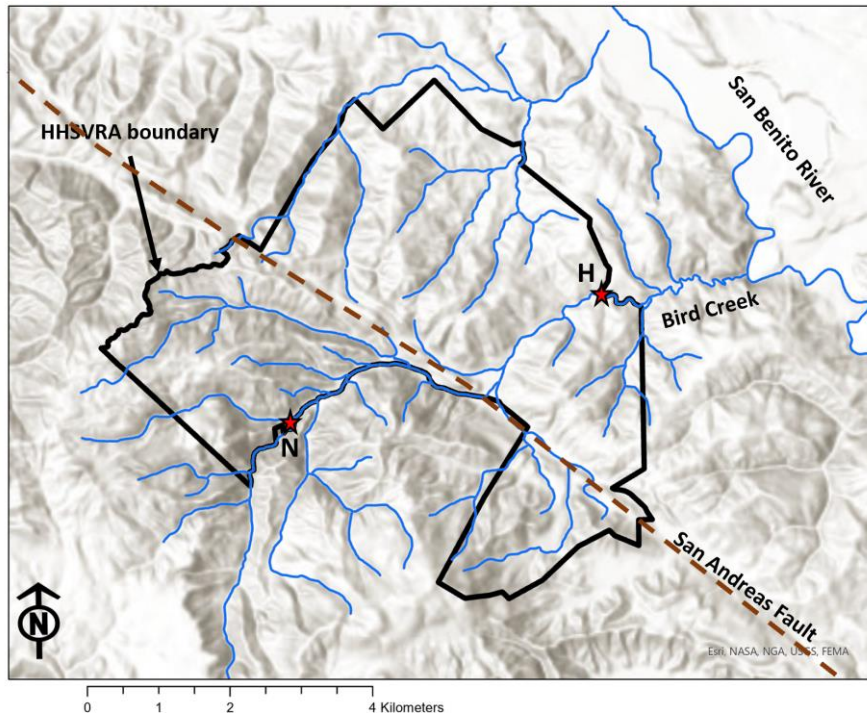


Figure 11. Two stream gaging sites located on Bird Creek Watershed. Nature (N) and Hudner (H) record sediment entering and leaving the park, respectively.

2.2 Sediment Transport

Sediment transport was estimated at the Nature and Hudner gage sites. The Nature gage is located near the upstream boundary of the HHSVRA, and Hudner gage is located near the downstream boundary of the park. Subtracting the Nature sediment yield from the Hudner sediment yield gives an approximation of the sediment entering Bird Creek from all sources along the length of the HHSVRA. This above–below experimental design was complicated by the presence of non–state lands bordering the creek as well.

2.3 Sediment Sources

2.3.1 Off Highway Vehicle Use

In 2013 we began measuring annual trail erosion at 18 sites throughout the park. Trail sites were chosen in collaboration with HHSVRA natural resource managers based upon soil type, trail use, and trail condition. Trail use types include off road vehicle (4x4), all–terrain vehicle (ATV), and single–track (motorcycle). Trail condition was determined by park environmental scientists based upon visual inspection (HHSVRA 2012). Trail condition rating includes red, yellow, and green for highly eroded, moderately eroded and no erosion

respectively. The locally-surveyed erosion rates were extrapolated to the unsurveyed trails and roads in the park within the Bird Creek watershed.

2.3.2 Campgrounds

Assessment of unpaved recreational areas included field reconnaissance, GPS data collection, GIS map production, and literature review. Sediment erosion and transport was photo documented.

2.3.3 Stream Bank and Channel Erosion

Stream channels and banks were monitored in the Hudner Ranch reach of Bird Creek because it has the largest watershed drainage area, while still located within the HHSVRA boundary. Given the relatively lower gradient, the site should be most responsive to watershed conditions, exhibiting aggradation in the context of excess bedload, or incising because of excess runoff.

Aggradation and degradation were monitored in the Hudner Ranch reach by establishing nine benchmarked cross sections that were surveyed approximately annually during the study. Several other cross sections were monitored for shorter periods upstream of those cross sections, and in granitic soils located west of the San Andreas Fault near Walnut Camp.

2.3.4 Cattle

Upland cattle impacts were not directly assessed. The impacts of riparian cattle access were documented during creek walks, and in a study comparing impacted and unimpacted reaches of Bird Creek within the Hudner Ranch area. The comparative study collected photographic and channel substrate data in 2012 in a location where cattle had accidental creek access, and a reach immediately upstream that had no cattle access (GEOL 460 2012).

2.3.5 County Road Culverts

The California Department of Transportation (CDOT) installs many different types of road drainage systems (CDOT 2014). Two such drainage features found in HHSVRA are asphalt berm confined spillways and culverts that process runoff on Cienega Road and San Juan Canyon Road (Fig. 10).

2.3.6 Landslides and Colluvial Processes

Landslides were identified by visual reconnaissance in the watershed and through aerial photography. General sediment transport processes were evaluated by inspection, and several landslides were selected for longer-term study to determine if they were active, and to estimate the current rates of motion and sediment contribution to Bird Creek. Five landslides in Colluvial Creek, and one landslide in Hudner Creek watershed were monitored for movement by resurveying a series of iron rods driven into the slide bodies (Fig. 10). Time series cross sections on Colluvial Creek helped constrain how actively the system is exporting sediment to Bird Creek. Deeper studies of Hudner landslide quantified the export of sediment from the toe of the slide to Hudner Creek and Bird Creek.

2.4 Best Management Practices

2.4.1 Sediment Retention Basins

One measure of effective sediment management at HHSVRA is the volume of sediment trapped by retention basins. Sediment retention has been a long-term BMP at HHSVRA. Nearly all of the trails in HHSVRA are located upstream of sediment basins that catch sediment eroded from the trails. Some tributaries have more than one basin in series along the length of the channel. The basins are large enough to allow typical storm runoff to pond. The low energy and large capacity ensure that they capture 100% of the bedload that would have entered Bird Creek. The basins have enough residence time to allow the silt fraction to settle as well. We periodically surveyed a subset of basins to quantify the volume and mass of retained sediment. The average annual retention was extrapolated to the unsurveyed basins based upon soil type in the watershed and drainage area feeding the basin. The estimated watershed-scale volume was used in the sediment budget.

2.4.2 Hidden Springs

Most sediment generated in HHSVRA is trapped by sediment basins. Hidden Springs creek is the only major Bird Creek tributary that does not have a sediment basin. In 2019, park staff directed us to evaluate the need for a sediment basin. Our methods included a sediment source inventory, a map of sediment pathways and storage areas, visual assessment of sediment transport during runoff events, and channel grain size analyses.

2.4.3 Coyote Trail Erosion Control

The Coyote Trail erosion control project was monitored for general effectiveness and stability. Each berm and intervening slope facet were periodically inspected for signs of renewed erosion and geomorphic stability. Six berms were selected for further study. Six benchmarked cross sections were established at each of the 6 berms for a total 36 transects that were periodically resurveyed to monitor project success. Surveys are conducted with autolevel and meter tape. The site was also periodically inspected to evaluate vegetative recovery, with the last inspection in 2021.

3 Results

3.1 Hydrology

3.1.1 Precipitation

During the study, average annual rainfall was 14.27 in (Table 2; Fig. 12). The site exhibited high inter-annual variability, ranging from 6.05 in to 26.09 in. The variability is both because the site is within the Mediterranean climate of central California, but also because it is located in the rain shadow of Fremont Peak, the tallest peak of the Gabilan Range. The majority of the rain occurred from October to May, while the remaining months are typically dry.

Table 2. Precipitation record (2011–2021) for Radio Ridge located in Hollister, California. Data from Western Weather Group (2021).

| Water Year | Oct | Nov | Dec | Jan | Feb | Mar | Apr | May | Jun | Jul | Aug | Sep | Total |
|------------|------|------|------|------|------|------|------|------|------|------|------|------|-------|
| 2011 | 0.89 | 2.29 | 4.15 | 1.81 | 4.07 | 4.57 | 0.20 | 1.11 | 0.37 | 0.00 | 0.00 | 0.00 | 19.46 |
| 2012 | 0.83 | 1.96 | 0.11 | 2.28 | 0.62 | 2.62 | 2.18 | 0.03 | 0.06 | 0.03 | 0.00 | 0.00 | 10.72 |
| 2013 | 0.27 | 2.54 | 4.35 | 0.98 | 0.75 | 0.60 | 0.21 | 0.00 | 0.00 | 0.00 | 0.00 | 0.08 | 9.78 |
| 2014 | 0.11 | 0.28 | 0.34 | 0.20 | 2.72 | 1.56 | 0.76 | 0.00 | 0.00 | 0.00 | 0.00 | 0.08 | 6.05 |
| 2015 | 1.05 | 0.51 | 5.23 | 0.00 | 1.26 | 0.17 | 1.14 | 1.24 | 0.00 | 0.02 | 0.06 | 0.08 | 10.76 |
| 2016 | 0.18 | 3.42 | 2.97 | 5.67 | 0.88 | 5.23 | 0.87 | 0.08 | 0.00 | 0.00 | 0.00 | 0.00 | 19.30 |
| 2017 | 2.76 | 1.53 | 2.20 | 9.70 | 6.27 | 1.91 | 1.55 | 0.06 | 0.06 | 0.00 | 0.00 | 0.05 | 26.09 |
| 2018 | 0.23 | 1.43 | 0.29 | 2.48 | 0.27 | 4.62 | 1.43 | 0.00 | 0.00 | 0.00 | 0.00 | 0.00 | 10.75 |
| 2019 | 0.30 | 3.78 | 1.94 | 3.54 | 7.56 | 2.35 | 0.30 | 1.48 | 0.00 | 0.00 | 0.00 | 0.00 | 21.25 |
| 2020 | 0.00 | 1.62 | 6.62 | 1.00 | 0.00 | 3.00 | 1.51 | 0.36 | 0.00 | 0.00 | 0.00 | 0.00 | 14.11 |
| 2021 | 0.00 | 0.53 | 0.9 | 5.19 | 0.49 | 1.58 | 0 | 0 | 0.00 | 0.00 | 0.00 | 0.00 | 8.69 |

| | | | | | | | | | | | | |
|------------------------|-------------|-------------|-------------|-------------|-------------|-------------|-------------|-------------|-------------|-------------|-------------|-------------|
| Monthly Average | 0.60 | 1.81 | 2.65 | 2.99 | 2.26 | 2.56 | 0.92 | 0.40 | 0.04 | 0.00 | 0.01 | 0.03 |
|------------------------|-------------|-------------|-------------|-------------|-------------|-------------|-------------|-------------|-------------|-------------|-------------|-------------|

Annual Average 14.27

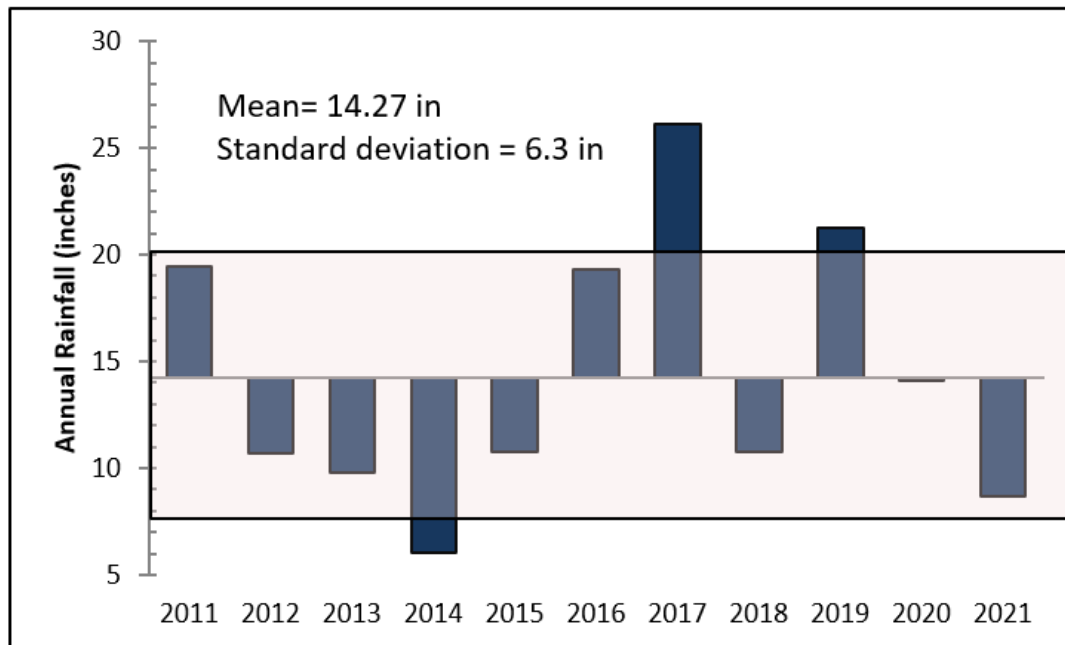


Figure 12. Annual precipitation at Hollister Hills SVRA. Values shown with respect to the mean value of 14.27 in (horizontal line). The colored box spans one standard deviation above and below the mean rainfall value.

Most of Bird Creek dries each summer. In most years during the study, the channel did not develop enough flow to carry water or sediment beyond the park boundary. A plot of daily rain values shows that sustained flow in Bird Creek requires considerable rainfall early in the season (Fig 13). The year with the highest single daily rainfall (2021) did not have enough antecedent moisture to develop sustained runoff. During our study, only four years produced the conditions that could transport sediment from the park (Fig. 13).

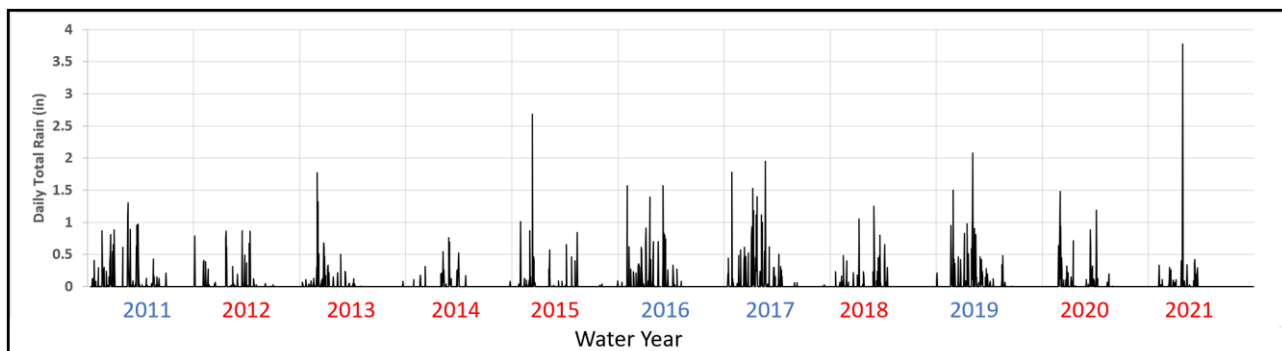


Figure 13. Daily total rainfall at the Radio Ridge gage during the study period. Blue water years produced sustained flow through the park, while the red water years did not.

3.1.2 Streamflow

In 2010, the Hudner and Nature gages included telemetered YSI multi-parameter water quality sondes to record water pressure and water quality parameters. These units were replaced in fall 2015 with DTS-12 digital turbidity sensors and SDI pressure transducers that are telemetered by GOES satellite. There was a LevelTroll pressure transducer deployed at each site for backup data. Data were variously recorded at 5, 10 or 15-minute intervals and stage values were converted to discharge values using event-based discharge measurements and a rating curve developed from field measurements.

In years with run-off events, flow measurements were taken near the gauge sites using various instruments including Pygmy, Price AA, and Flowtracker Acoustic Doppler current meters, and 3" orifice Parshall flume. We modified the U.S. Geological Survey guidelines to account for narrower cross-sectional widths of the streams (Nolan and Shields 2000).

Water discharge was gaged at Nature and Hudner areas of the HHSVRA (Fig. 11; Nicol et al 2011; Smith et al. 2016). Variability in flow correlates directly with rainfall, but is also highly related to antecedent soil moisture (Fig.14). The soils are very dry at the start of each water year, so the first several rainfall events infiltrate without producing sustained surface runoff. Stream flow and winter base flow only occur after several storms have saturated the soils. In the drought years, the clay soils developed exceptionally deep polygonal cracks, locally up to 0.4 m deep. The resulting macroporosity infiltrated nearly all the precipitation, leaving little for runoff in Bird Creek (Fig. 15). Base flow typically ended at Nature in April, but continued throughout the year at Hudner when there was enough groundwater to serve the spring located upstream from the gage. In water years 2012, 2013, 2014, 2015, 2018, 2020, and 2021 Bird Creek had either no, or very brief, continuous flow between the Nature and Hudner gages. For those years, virtually no sediment entered or left the park in Bird Creek.

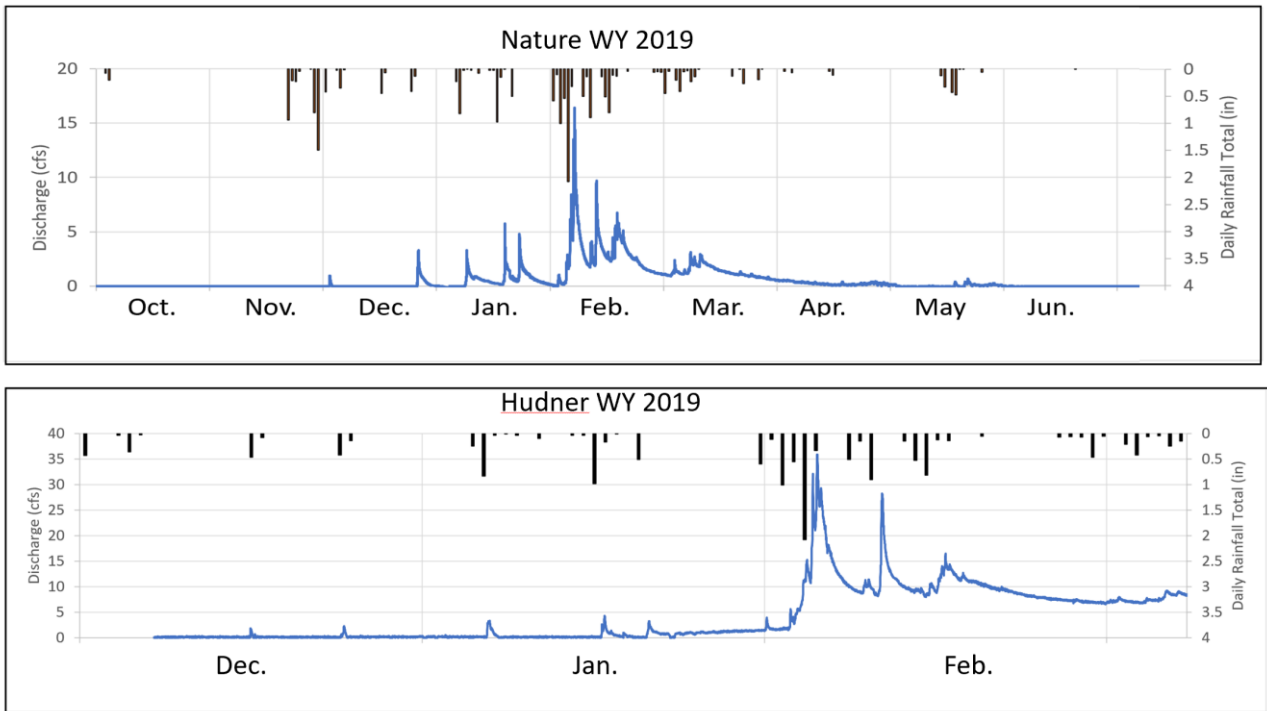


Figure 14. Rainfall at the Radio Ridge gage is plotted with stream discharge measured at the Nature and Hudner gages. Hudner main pressure gage and backup gage malfunctioned in March. Water year 2019 shows as an example.



Figure 15. Deep, polygonal cracks form during the dry months. In 2013, the cracks formed prematurely in March. View west toward Cienega Road.

3.2 Sediment Transport

Sediment transport rates were determined using a 3-inch Helley–Smith sampler for bedload and a DH–48 depth–integrated sampler for suspended load at the same time that water discharge measurements were taken at Nature and Hudner gages. In water year 2011, the pressure gage record was rated for suspended and bedload sediment discharge using event–based sediment transport measurements. Following the 2011 Water Year, bedload was no longer measured because it was virtually absent in our initial studies (Nicol et al. 2011). Following 2011, a time series of turbidity was rated for suspended sediment concentration to create a time series of suspended sediment transport rate (Minella et al. 2008; Wass et al. 1997).

3.2.1 Bed Load

Bed load was sampled in the 2011 Water Year at Nature and Hudner gage locations (Fig. 20). Total mass of bedload passing Nature and Hudner gage locations was approximately 21 kg and 176 kg respectively. Bedload was not sampled in subsequent years because the transport volume was clearly an insignificant proportion of the total load. Apparently, sediment basins employed in the region are very efficient bedload traps.

3.2.2 Suspended Load

The Nature gage was rated for suspended sediment transport in WY 2011, 2016, and 2019 (Fig. 16). There was insufficient flow for rating in the intervening drought years, and the gage was damaged in high flows of 2017. Peaks in suspended sediment transport generally correspond to storm runoff peaks, but turbid water spikes are also present between storms. Sporadic turbidity can arise from small landslides, bank failure, and events on tributary streams.

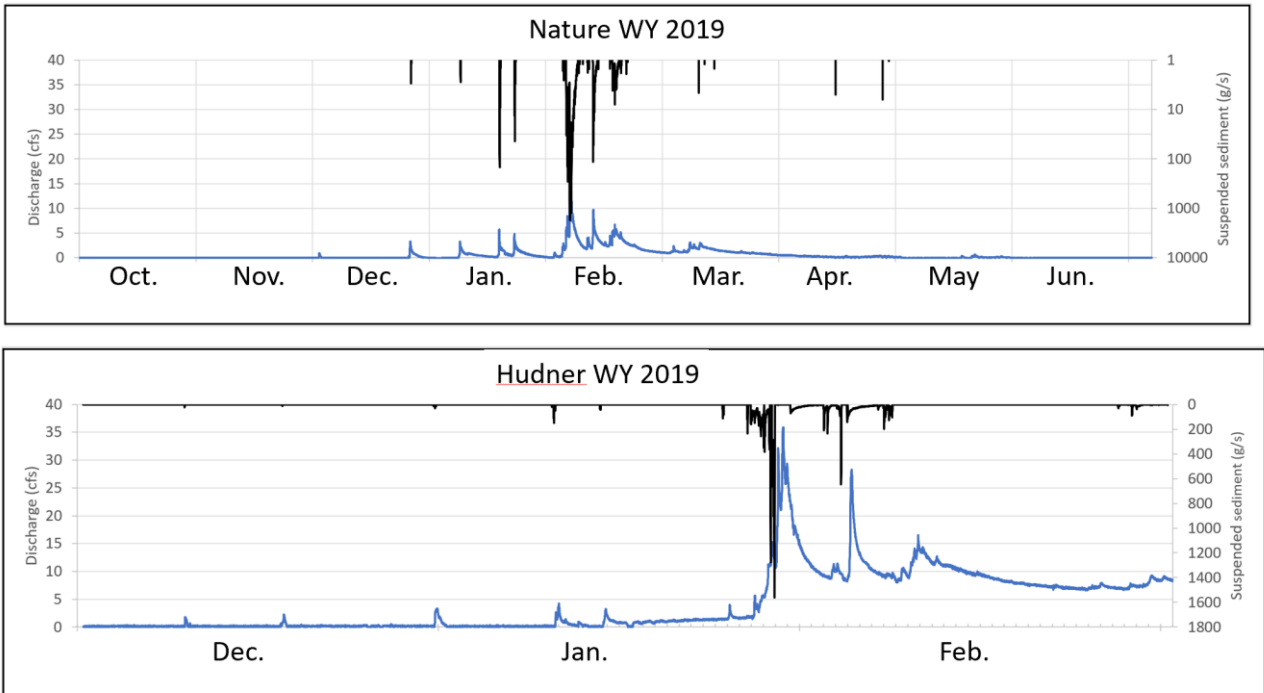


Figure 16. Water discharge (blue) and suspended sediment discharge (black) at Nature gage. Water 2019 shown as an example.

The Hudner gage was rated for suspended sediment in WY 2011, 2012, 2016, and 2019 (Fig. 16). There was no measurable sediment transport in the intervening drought years, and the gage equipment was damaged in high runoff of 2017. Table 3 summarizes the estimates of sediment mass transported into the park (Nature) and leaving the park (Hudner) for each year of the study, based upon the gaging effort. The values listed for 2017 are minimum values, drawn from the highest values recorded for those gages during the study.

Table 3. Estimate of total sediment transport (tonnes/yr) past the Nature and Hudner gages during the 11-year study period.

| | 2011 | 2012 | 2013 | 2014 | 2015 | 2016 | 2017 | 2018 | 2019 | 2020 | 2021 | 11 year average |
|--------|-------|------|------|------|------|------|--------|------|------|------|------|-----------------|
| Nature | 12.3 | 0 | 0 | 0 | 0 | 17.2 | >19.1 | 0 | 19.1 | 0 | 0 | 6 |
| Hudner | 183.2 | 11.2 | 0 | 0 | 0 | 66.8 | >183.2 | 0 | 56.4 | 0 | 0 | 45 |

3.3 Sediment Sources

3.3.1 Off Highway Vehicle Use

Trail erosion was assessed for seven years by subtracting precise DEMs surveyed at 18 sites throughout the park (Fig. 17; Teaby et al. 2013a; Silveus et al. 2014; Chow et al. 2015 & 2016; Morris et al. 2018; Smith et al. 2018; Bogdan et al. 2018; Schnieders et al. 2021). Sites were categorized by use designation, soil type and a three-level, visually assessed, erosion potential index (red, yellow, green; HHSVRA 2012).

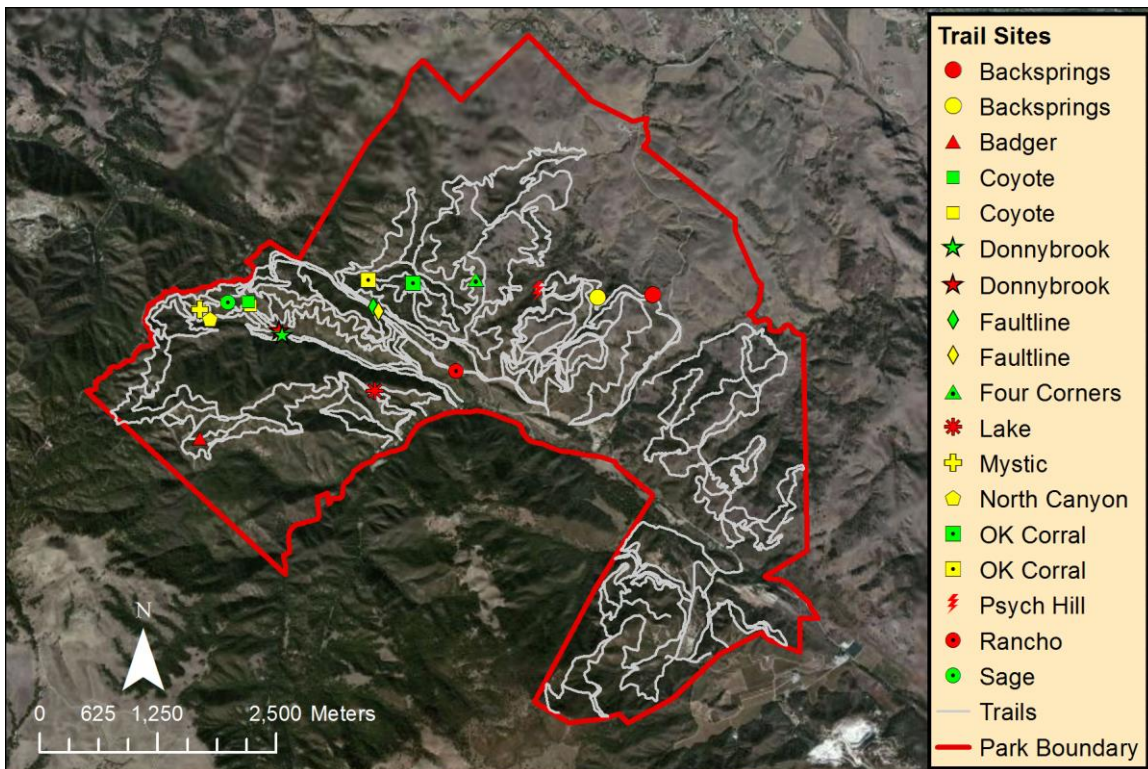


Figure 17. Trail erosion site locations within Hollister Hills State Vehicular Recreation Area, Hollister, CA. Color of symbol represents rating index classification as red, yellow, or green.

Two benchmarks (BM) were established at each monitoring site for annual survey reproducibility. The 2013 & 2014 surveys were conducted using a Trimble s6 robotic total station with surface scanning capability. Digital elevation models (DEMs) were then created using ArcGIS.

Starting in 2015, trail surveys used photogrammetry to develop DEMs. A 3” Nikon total station was used to scale and orient aerial photos shot with a gimbaled Hero 3+ GoPro in a “mowing-the-lawn” pattern. Ground control points (GCPs) were placed within the sample

sites to improve the product accuracy. DEMs and orthomosaic photos were created in both Agisoft Photoscan and Pix4D Software.

Annual trail erosion and deposition (change in surface elevation) was determined in ArcGIS using the *Raster Calculator* tool to subtract consecutive annual DEMs. The *Cut and Fill* tool and summary statistics were used to determine total volume of eroded or deposited sediment. A mask was created in ArcGIS to exclude vegetation and DEM imperfections from the analysis.

The elevation change detected by the surveys was multiplied by local trail width to calculate erosional volume per unit length of trail. That value was extrapolated to the total length of trails in the park to estimate the annual volume of OHV derived erosion.

In 2016, OHV staff began trail management to mediate areas of high erosion. Site management was then added as a variable to analyze annually and cumulatively. Data for all years are in Table 4.

Table 4. Annual elevation change at each trail assessment site. Site condition is from HHSVRA (2012). Positive numbers indicate deposition and negative numbers indicate erosion. Grey indicates sites that were managed before the annual survey. Blue value is site with imported material—excluded from 2016 analysis.

| Trail Location | Condition | Usage | Soil Type | 19-20 | 18-19 | 17-18 | 16-17 | 15-16 | 14-15 | 13-14 |
|----------------|-----------|--------------|-----------|--------|--------|--------|--------|--------|--------|--------|
| OK Corral_1 | Green | Single Track | Clay | -0.011 | 0.020 | -0.031 | 0.037 | -0.039 | 0.000 | -0.007 |
| Donnybrook_2 | Green | Single Track | Granite | -0.010 | -0.001 | 0.022 | -0.016 | 0.007 | -0.036 | -0.045 |
| Four Corners | Green | ATV | Clay | -0.012 | -0.012 | -0.092 | 0.082 | 0.009 | -0.085 | -0.009 |
| Coyote_1 | Green | ATV | Granite | 0.007 | -0.016 | -0.050 | 0.033 | -0.031 | -0.001 | -0.023 |
| Faultline_2 | Green | Road | Clay | -0.051 | -0.048 | -0.020 | 0.046 | -0.026 | -0.044 | -0.019 |
| Sage | Green | Road | Granite | 0.000 | -0.023 | -0.007 | 0.031 | -0.026 | -0.001 | -0.008 |
| OK Corral_2 | Yellow | Single Track | Clay | 0.002 | -0.053 | -0.009 | -0.009 | -0.079 | -0.001 | -0.022 |
| Mystic | Yellow | Single Track | Granite | 0.018 | -0.008 | -0.023 | 0.010 | -0.021 | -0.016 | -0.002 |
| Backsprings_2 | Yellow | ATV | Clay | -0.019 | -0.035 | -0.016 | -0.014 | 0.065 | -0.005 | -0.012 |
| Coyote_2 | Yellow | ATV | Granite | 0.024 | -0.010 | 0.066 | -0.018 | 0.029 | -0.016 | -0.016 |
| Faultline_1 | Yellow | Road | Clay | -0.030 | -0.022 | -0.050 | 0.021 | -0.031 | -0.052 | -0.041 |
| North Canyon | Yellow | Road | Granite | -0.003 | -0.027 | 0.001 | 0.035 | 0.079 | -0.021 | -0.060 |
| Psych Hill | Red | Single Track | Clay | 0.012 | -0.064 | N/A | -0.171 | 0.040 | 0.040 | 0.040 |
| Donnybrook_1 | Red | Single Track | Granite | 0.002 | -0.013 | -0.023 | 0.008 | -0.170 | -0.055 | -0.038 |
| Backsprings_1 | Red | ATV | Clay | -0.016 | 0.022 | -0.226 | 0.191 | -0.173 | 0.000 | -0.006 |
| Badger | Red | ATV | Granite | 0.019 | -0.031 | 0.011 | 0.006 | -0.170 | -0.036 | -0.038 |
| Rancho | Red | Road | Clay | 0.020 | -0.036 | -0.013 | -0.025 | 1.286 | -0.031 | -0.023 |
| Lake | Red | Road | Granite | -0.028 | -0.058 | 0.013 | -0.020 | 0.022 | -0.039 | -0.083 |

No statistical differences between the trail sustainability categories are present when analyzing annual average change ($p=0.3$; Table 5; Fig. 18). When considering the cumulative change after 7 years of trail use, red sites erode significantly more than green or yellow sites when all sites are grouped ($p=0.02$; Table 5; Fig. 18). Red sites also appear to have more cumulative erosion when considering just unmanaged sites ($p=0.07$; Table 5). The cumulative erosion of managed sites does not correlate with sustainability index ($p=0.4$; Table 5). This result suggests that management reduces erosion in red sites. Green and yellow sites have mutually indistinguishable annual and cumulative erosion rates (Table 5; Fig. 18).

Table 5: Summary of seven-year average annual and cumulative elevation changes (m) for all study sites. Notes match those from Table 4.

| Averages | Overall | red | yellow | green | clay | granite | ST | ATV | Road |
|-----------------|---------|-------|--------|-------|-------|---------|-------|-------|-------|
| All Sites | -0.02 | -0.03 | -0.01 | -0.01 | -0.02 | -0.01 | -0.02 | -0.01 | -0.01 |
| Managed Sites | -0.01 | -0.02 | 0.01 | 0.00 | 0.00 | -0.02 | -0.01 | 0.00 | 0.00 |
| Unmanaged Sites | -0.02 | -0.05 | -0.01 | -0.01 | -0.03 | -0.01 | -0.02 | -0.03 | -0.02 |

| Cumulative | Overall | red | yellow | green | clay | granite | ST | ATV | Road |
|-------------------|---------|-------|--------|-------|-------|---------|-------|-------|-------|
| All Sites | -0.11 | -0.21 | -0.07 | -0.07 | -0.13 | -0.10 | -0.12 | -0.10 | -0.10 |
| Managed Sites | -0.03 | -0.08 | 0.05 | -0.01 | 0.02 | -0.10 | -0.03 | -0.01 | -0.02 |
| Unmanaged Sites | -0.15 | -0.37 | -0.09 | -0.08 | -0.21 | -0.09 | -0.12 | -0.19 | -0.10 |

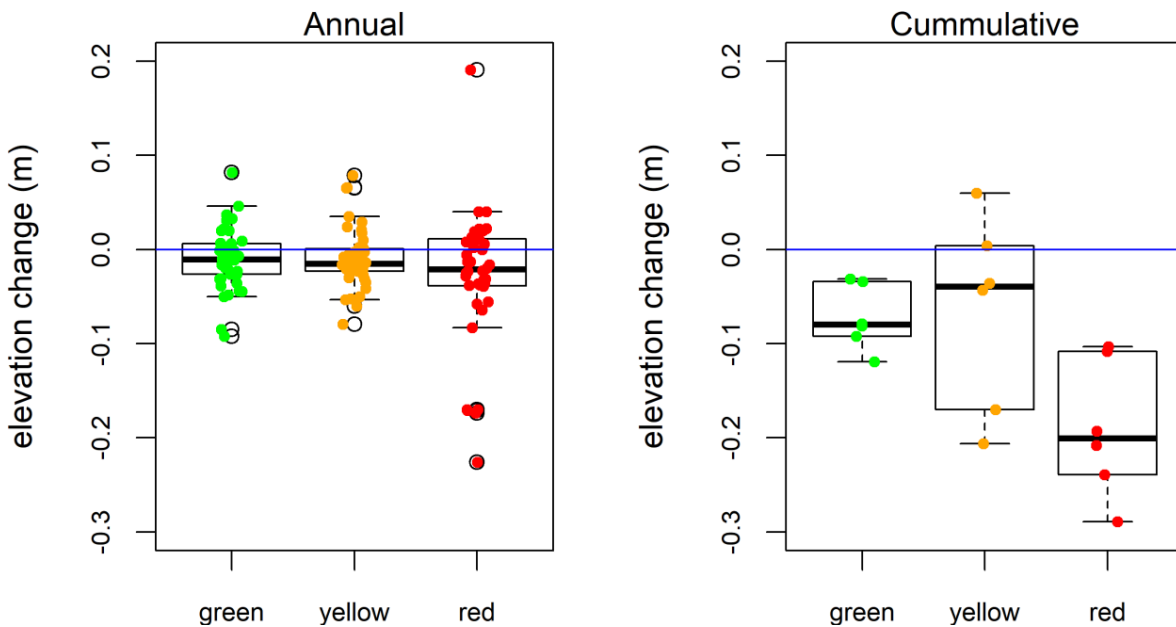


Figure 18. Boxplots of all study sites parsed by sustainability index. (Left) Annual elevation change of all sites (ANOVA $p = 0.3$). (Right) seven-year cumulative elevation change of all sites (ANOVA $p=0.02$).

Soil type and trail use classification did not appear to impact erosion rates. Clay and granite sites erode at approximately equal rates whether considered at the annual or cumulative timeframe (Fig. 19; Table 5). Differences in trail classification did not influence erosion rates cumulatively or annually (Fig. 20; Table 5).

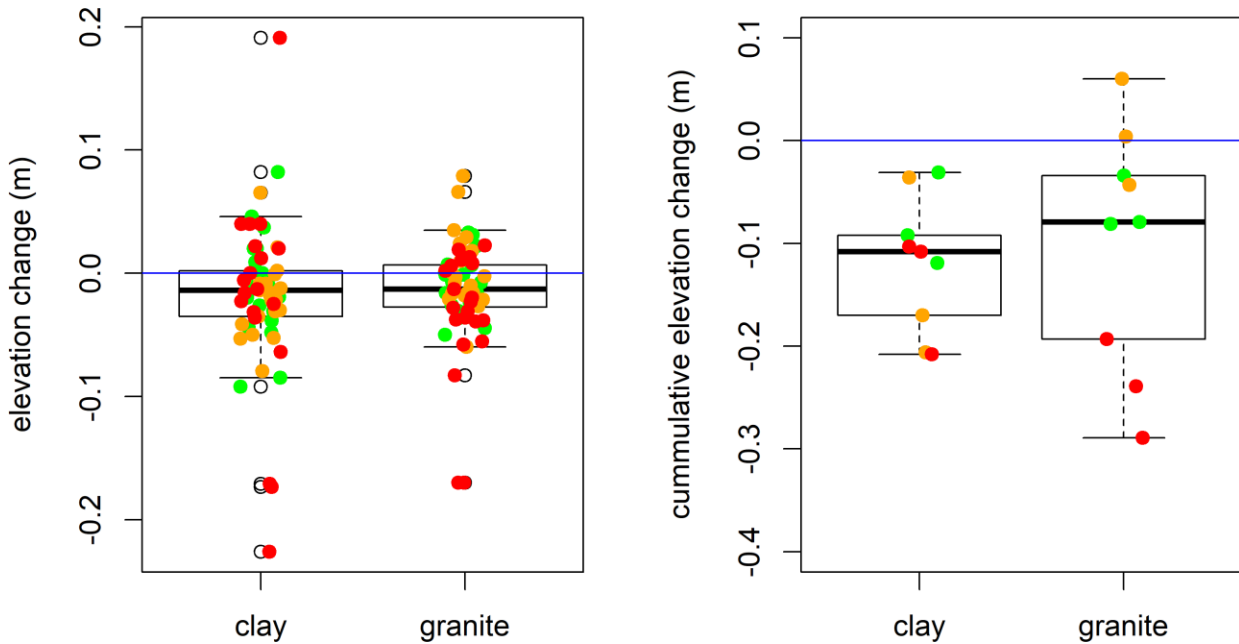


Figure 19. (Left) Annual elevation change of all sites separated by soil type. (Right) Cumulative elevation change of all sites separated by soil type. Dots show individual sites colored by sustainability index (green, yellow, red).

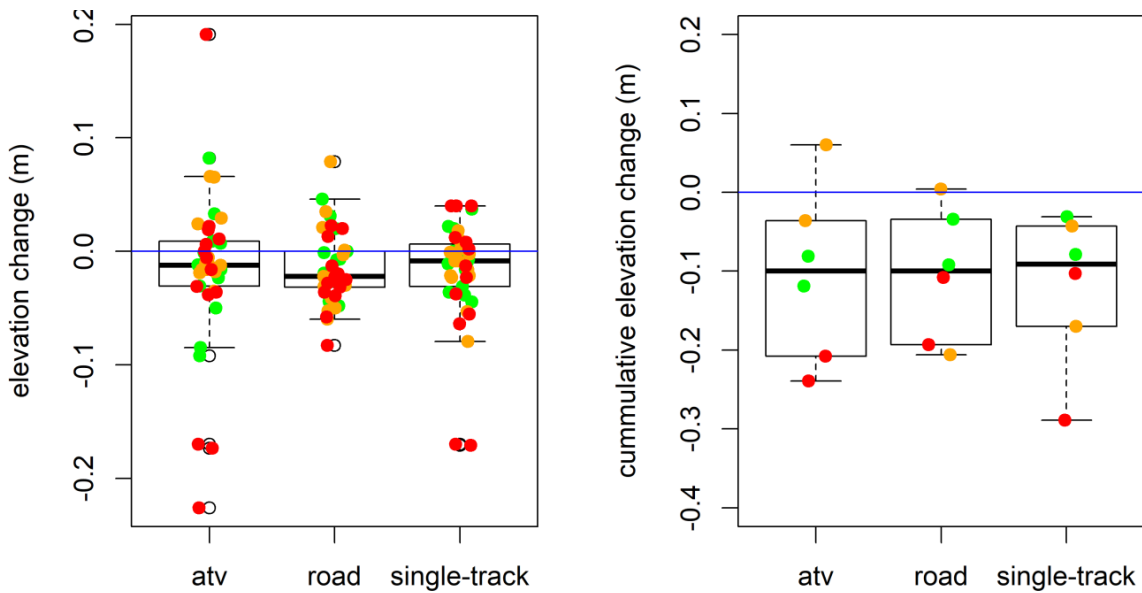


Figure 20. (Left) Annual elevation change of all sites separated by trail use. (Right) Cumulative elevation change of all sites separated by trail use. Dots show individual sites colored by sustainability index (green, yellow, red).

Trail management that mainly consists of replacing the side-cast berm back into the trail tread is an effective strategy for reducing erosion. The net effect of this type of management has been to reduce erosion in nearly all categories and in both annual and cumulative analyses, especially in red sites (Table 4; Fig. 21). Managed red sites eroded 0.29 m less than unmanaged red sites when viewing cumulative seven-year erosion (Table 4).

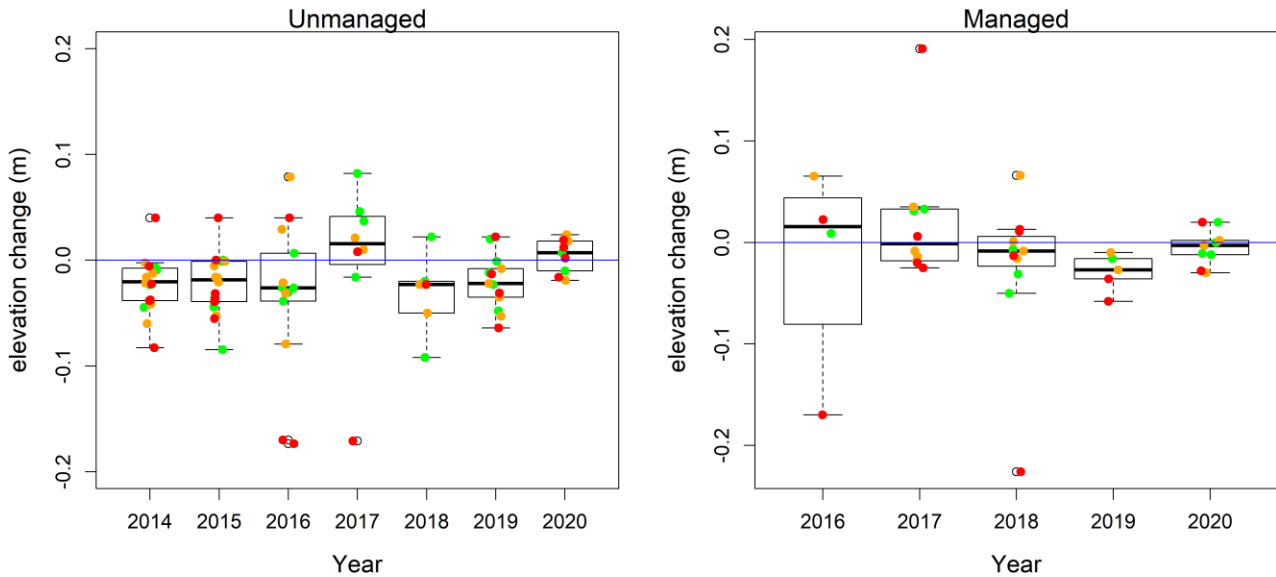


Figure 21. Boxplots of annual elevation change for all sites separated by year and management activity. Dotsshow individual sites colored by sustainability index (green, yellow, red).

The Universal Soil Loss Equation and other soil conservation models logically predict higher soil erosion rates with higher rainfall and rainfall intensity. Rainfall has varied from 6 inches to 26 inches during the study, but there appears to be little correlation between total annual rainfall and erosion rates (Fig. 22). In general, a better predictor of erosion than total rainfall is rainfall intensity (in/hr). Even during a drought year, one intense event can trigger significant geomorphic change (Smith et al. 2021). A review of the four most intense rain events of each year in the study does not reveal a clear pattern between annual rain and erosion (Fig. 22).

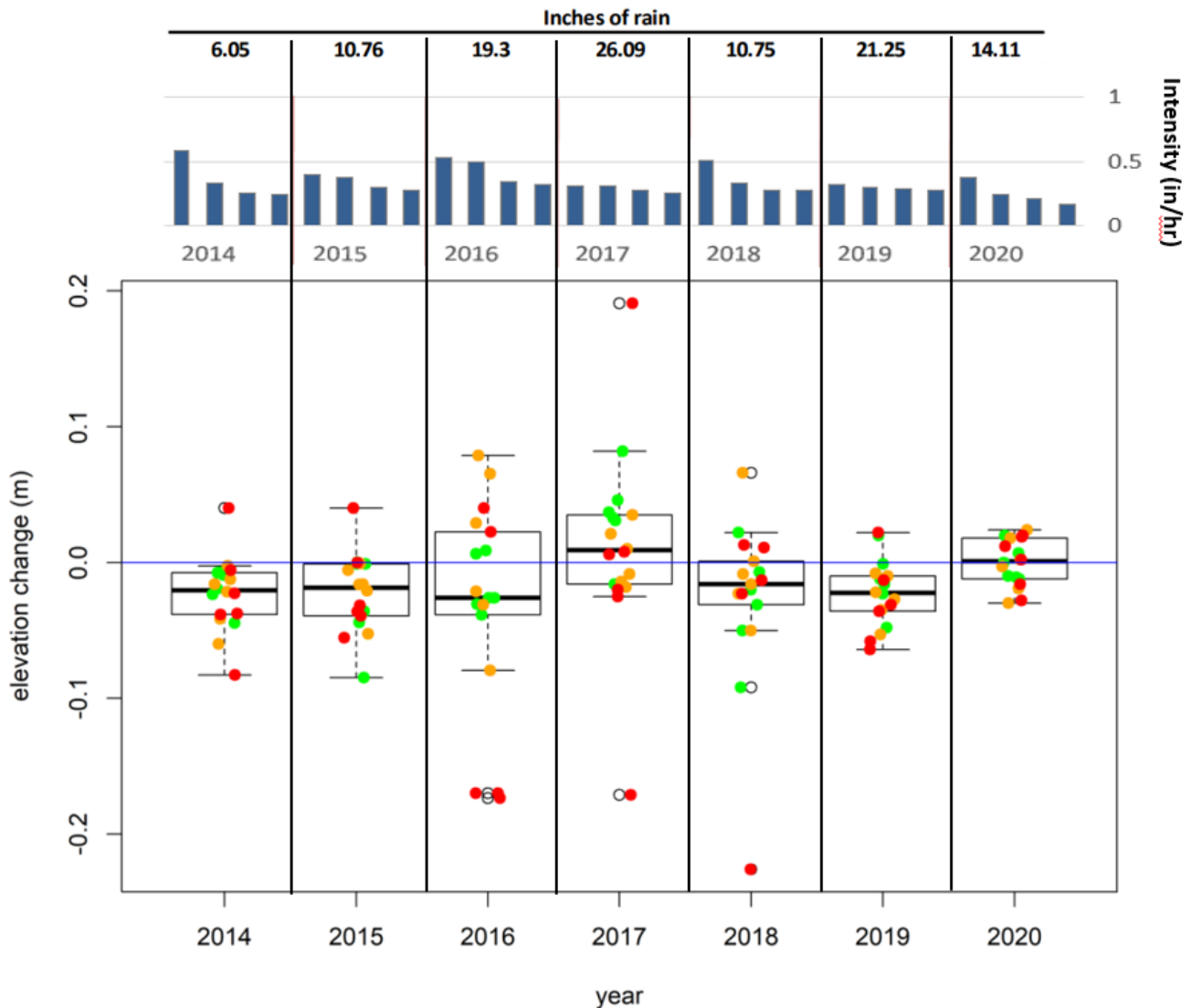


Figure 22 Annual elevation change for seven years of assessment at all sites. Total rainfall (in) and the four most intense precipitation events (in/hr) are shown for each year. Dots show individual sites colored by sustainability index (green, yellow, red). Kruskal-Wallis test indicates inter-year variability ($P = 0.007$).

During our study, cumulative erosion values were calculated by adding annual erosion values. Given that many annual values were very close to our tolerance to identify erosion, that approach might have led to inaccurate sums, where the relative error was high. To test for that effect, we reanalyzed cumulative erosion by directly subtracting the 2013 and 2020 DEMs. There was no significant difference between the methods.

We estimated the annual volume and mass of OHV erosion in Bird Creek watershed by extrapolating a single average erosion rate, calculated from our survey results, to all trails in the park. The single value was a weighted average of the erosion for the three condition indices. The weighting was an estimate of the relative abundance of each trail condition

category in the park (Tables 6 and 7). We did not include soil type or trail use in the weighting because they had no influence on erosion variability (Figs. 19 and 20)

Table 6: Weighted average of erosion per meter of trail length. Annual erosion is from our 7-year study (Table 5). Average widths were estimated at our study sites. Line four is the length-normalized erosion volume (product of the first one, two and three). Line five is the relative abundance of each trail condition throughout the park (HHSVRA (2012)). That proportion is multiplied by line four to derive the relative contribution of erosion (per unit length) from each trail type throughout the park (line six).

| | Condition | | |
|--|-----------|--------|--------|
| | Red | Yellow | Green |
| 1-annual erosion (m) | 0.040 | 0.010 | 0.010 |
| 2-average width (m) | 3.58 | 2.08 | 1.67 |
| 3-unit length (m) | 1 | 1 | 1 |
| 4-volume (m ³) / length (m) | 0.143 | 0.021 | 0.017 |
| 5-proportion of condition in the park | 0.07 | 0.52 | 0.41 |
| 6-weighted volume (m ³) / length (m) | 0.0100 | 0.0108 | 0.0068 |

Table 7: Annual mass of material eroded from trails. Line one is the average of the weighted volumes listed in line 6 of Table 6. Total trail length includes all roads and trails sanctioned by the park. The total annual volume is the product of lines one and two. The annual eroded mass is the product of volume and density.

| | |
|--|---------|
| 1-average weighted volume (m ³) / length (m) | 0.0092 |
| 2-total trail length (m) | 183,700 |
| 3-total annual volume (m ³) | 1,696 |
| 4-density (tonne/ m ³) | 2 |
| 5-annual eroded mass (tonne) | 3,392 |

We estimate trail erosion to be approximately 3390 tonnes/yr in the park. We made several assumptions for the extrapolation.

- 1) The relative abundance trails with green, yellow, and red conditions in the park are approximately the abundance reported in HHSVRA (2012).
- 2) The relative abundance of managed and unmanaged trails in the study sites represents the relative abundance throughout the park.
- 3) The average climate during the study reflects the long-term average.
- 4) The trail material has an average density of 2 tonnes/m³.

The first assumption was based on a 2012 report. Conditions may have improved or worsened on some trails. The third assumption would be stronger if the study had spanned several decades to capture the decadal climate variability related to El Niño and La Niña conditions. We note that our seven-year study fortuitously included two El Niño and two La Niña years as well as years with no ENSO anomalies. The fourth assumption represents a compromise between the density of loose sandy soil (1.6 tonnes/m³) and quartzo-feldspathic bedrock (2.65 tonnes/m³).

3.3.2 Campgrounds

A CSUMB student study in 2012 evaluated runoff pathways from campgrounds and parking lots located along the banks of Bird Creek. Madrone and Bee campgrounds featured frequently disturbed landscaped with rolling terrain, heavy vehicular traffic, and deeply incised channels. Lodge and Walnut campgrounds featured gentle slopes and long winding channels leading to Bird Creek (Fig. 23, 24, 25, GEOL 460 2012).

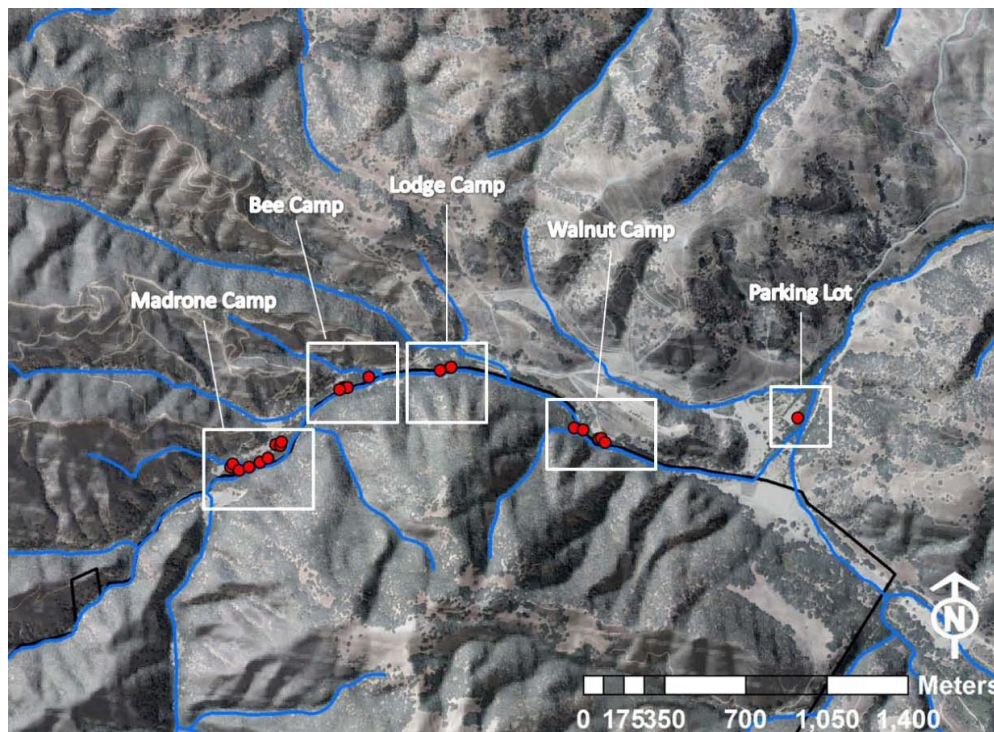


Figure 23. Location of Drainage pathways relative to Lower Ranch Campgrounds and parking lots at HHSVRA (GEOL 460 2012).



Figure 24. Rill channel pathways at Madrone (MC) and Bee Camp (BC) (GEOL 460 2012).



Figure 25. Rill channel pathways at Lodge (LC) and Walnut Camp (WC) (GEOL 460 2012).

Major upgrades to all campgrounds during the course of our study, including adding some concrete pad parking options, have reduced the impacts on Bird Creek. HHSVRA staff continue to visually assess the grounds during rain events as they consider further improvements.

3.3.3 Stream Bank and Channel Erosion

Bank pins were installed at 8 locations along the Hudner Ranch reach of Bird Creek in March 2011 to estimate the contribution of bank erosion to Bird Creek (Figs. 26 and 27). This study only extrapolated the results to the reach of Bird Creek that has similar morphology and geology to the reaches with bank pins. The extrapolation included 2800 m of stream located between the downstream boundary of the HHSVRA and the San Andreas Fault, where the watershed geology and topography significantly change. Pin sets 5 and 8 had upstream and downstream sets. Each bank pin set consisted of 2 to 3 rebar stakes inserted into the channel bank. Bank pin exposure was measured to the closest millimeter. Total volume of stream bank erosion was calculated by multiplying the average pin exposure by 2800 m stream length and the estimated average bank height (1.2 m). That erosion volume was multiplied by two to account for left and right stream banks. The mass of eroded

material was estimated by multiplying the volume of eroded material by an approximate bulk density 1370 kg/m³, a value for typical floodplain deposits (Dumikh 2014).

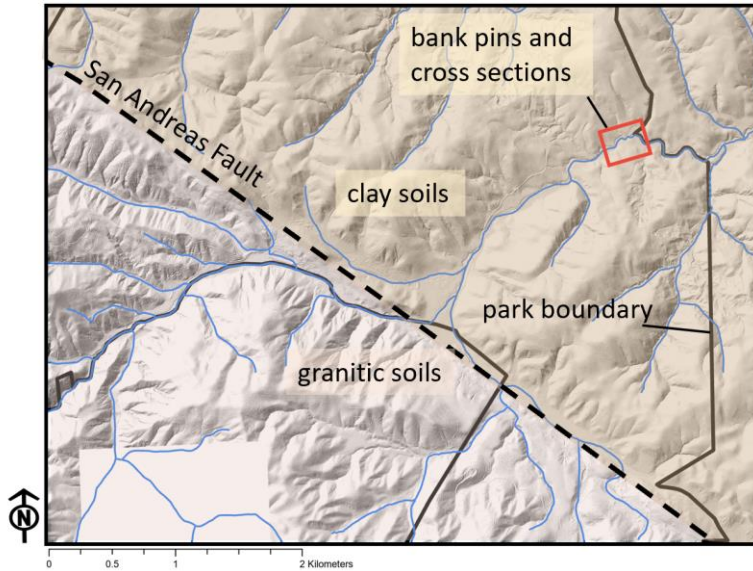


Figure 26. Red box is general location of bank pin and cross section study on Bird Creek (Figs. 27 and 28)



Figure 27. Bank pins located along Bird Creek (GEOL 460 2012). See Figure 26 for setting.

Bank pin exposure was used to calculate volume and mass of sediment eroded from Bird Creek stream banks in 2011, 2012, 2014, 2015, and 2016 (Table 8). The resulting masses

are highly variable from year to year, in keeping with the sporadic nature of both the spatial and temporal controls on bank erosion. The annual average rate of bank erosion measured on just the 2800 m of Bird Creek between the San Andreas Fault and the park boundary was 109 tonnes. This value underestimates the total contribution of bank erosion to Bird Creek because there are 10's of kilometers of stream channel located upstream of the fault that were not assessed. Given the results of cross section surveys provided below, there is no recent chronic channel incision events that would have led to the measured bank erosion. Therefore, the bank erosion is probably typical of the region, rather than being driven by excess runoff from the park, or other runoff sources.

Table 8. Volume and mass of bank erosion in Bird Creek (east of San Andreas Fault).

| 2011 | 2012 | 2014 | 2015 | 2016 | | | |
|--|-------------|-------------|-------------|-------------|----------------|------------------------------|--|
| 0.028 | 0.007 | 0.022 | 0.001 | 0.001 | m | Average pin exposure | |
| 188 | 47 | 146 | 8 | 9 | m ³ | Volume of stream bank eroded | |
| 258 | 64 | 200 | 11 | 12 | tonne | Mass of stream bank eroded | |
| Annual average mass of bank erosion | | | | | 109 | tonne | |

In addition to the stream bank survey, nine benchmarked cross sections of Bird Creek at the Hudner area were surveyed approximately annually since fall 2011 to capture major geomorphic changes that would indicate whether the creek is storing, sourcing, or transporting sediment (Fig 28). Natural streams gradually shift their positions, and temporarily store and erode sediment in small amounts as they transport the varying annual sediment load. Between 2011 and 2016, and between 2017 and 2018, all transects were either unchanging or varied in magnitudes typical of natural stream adjustment to annual sediment load (Fig. 29). Some between-survey variability is assignable to survey precision as well. During that time, local cattle-derived fine sediment locally covered the channel bottom with a few centimeters of fine sediment, but the mud veneer washed through the system once stream discharge renewed, leaving no lasting geomorphic changes.

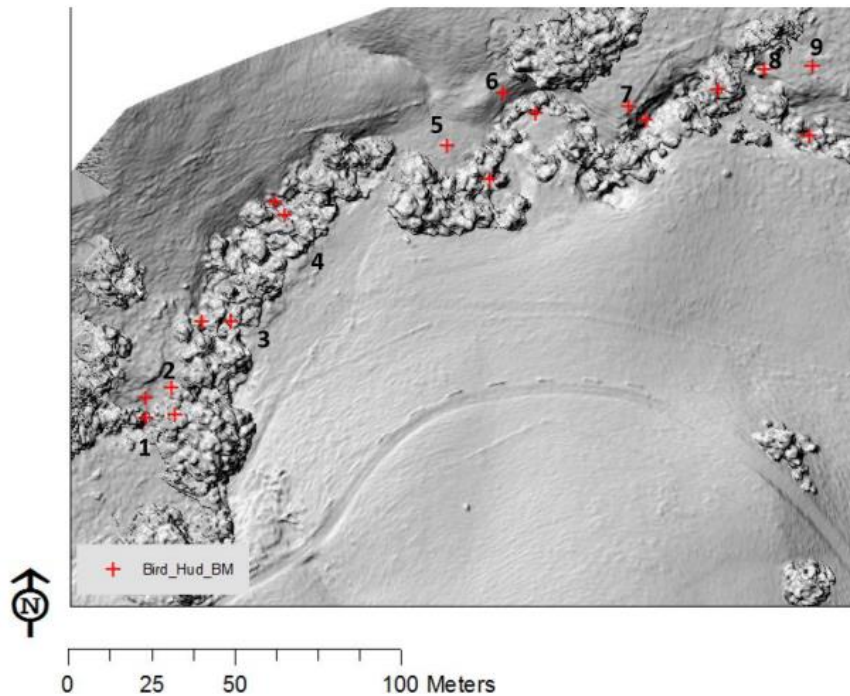


Figure 28. Nine benchmarked cross sections (1–9) (from upstream to downstream) were resurveyed approximately annually to assess channel processes. See Figure 26 for setting.

High magnitude storm runoff events generate high shear stress, and sometimes high sediment loads from the watershed, which can impact stream morphology. The extreme rain events of winter 2017 provided such a test of channel stability and function. All transects maintained their pre-2017 geometry except for transects 3, 4, and 5 (Figs. 28 and 29). The reach of river that starts between transects 2 and 3 and ends between 5 and 6 experienced varying amounts of significant aggradation of sand-sized bed material in 2017. We estimate the volume of sand and small gravel stored in the channel to be approximately 320 m³ (420 yd³) by averaging the change in cross sectional areas between adjacent cross sections and multiplying by the distance between cross sections. That volume is the same order of magnitude estimated to have been input directly to the channel in 2017 by a small landslide located just 90 m upstream of transect 1 (Smith et al. 2019). The channel is relatively straight and narrow between the slide and transects 1 and 2. Therefore, interruption of sediment deposition is unlikely in this reach. A 90-degree left bend in the Bird Creek channel just after transect 2 apparently slowed the flow enough to trigger a pattern of aggradation in the reach just downstream, measured in transects 3 to 5. The volume of sediment deposited gradually tapered downstream until the 320 m³ of sand from the slide was exhausted just downstream of transect 5. If averaged over the 11 years of survey data, and using a loose sand density of 1800 kg/ m³, the study reach stored 58 tonne/yr.

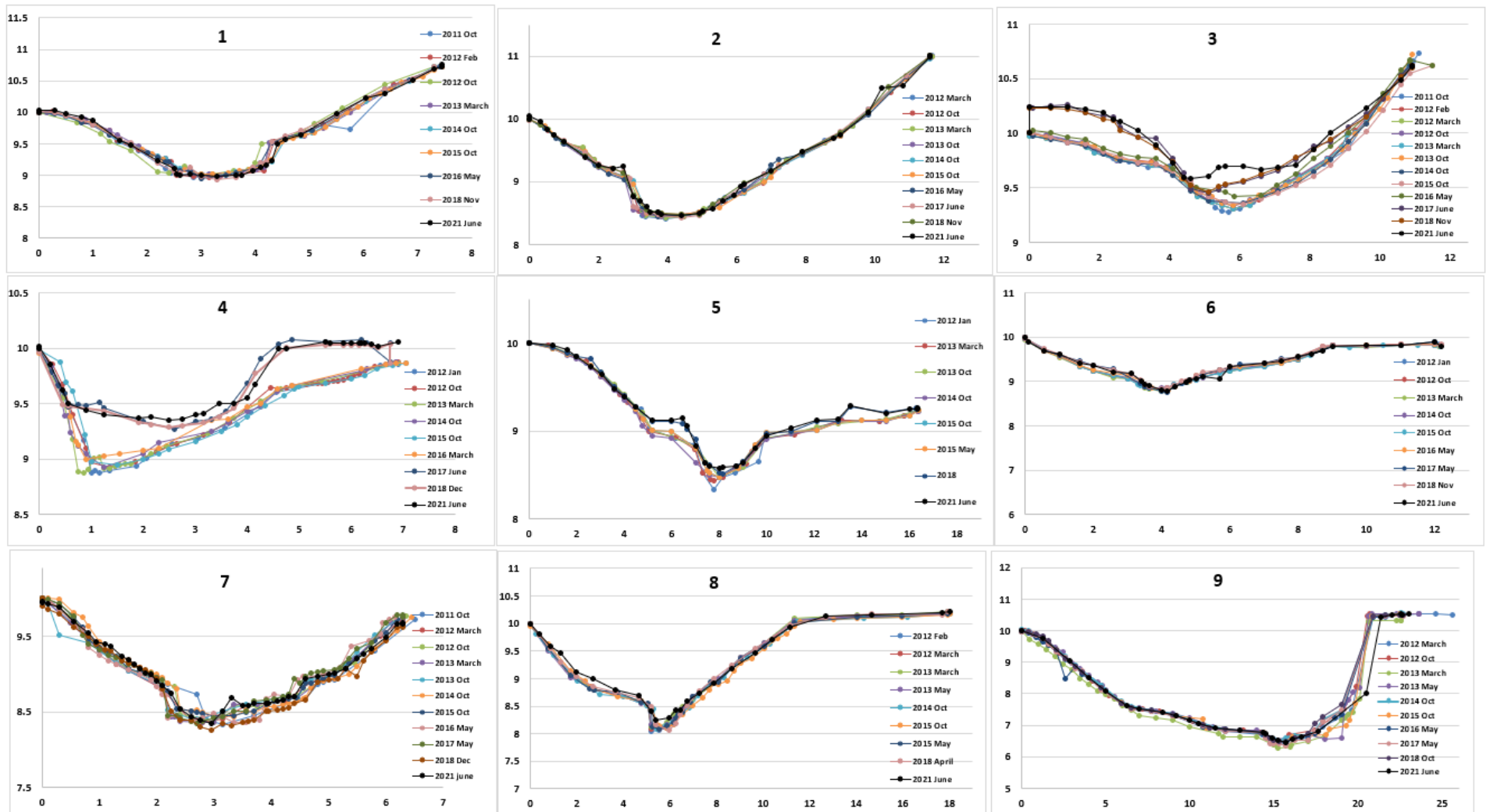


Figure 29: Time-series of Bird Creek cross section geometry near Hudner Ranch. Axial values are meters.

Benchmarked cross sections were also measured from time to time on Bird Creek near Walnut Camp (Fig. 23). This reach is located in the granitic soils, rather than the clay soils of Hudner Ranch. Cross sections did not change significantly during the study period, and a minor knick point at that site did not significantly erode, so we interpret the stream channel to be relatively stable—neither sourcing nor storing a significant volume of sediment (GEOL 460 2012).

3.3.4 Cattle

Direct cattle impact on the banks and bed of Bird Creek include sporadic, rare access when riparian cattle fencing within the HHSVRA is accidentally breached by cattle. A comparative study of one such incident indicated that the cattle hooves sheared fine-grained sediment in the stream banks, leaving a several-centimeter thick veneer of mud blanketing the previously gravelly channel bottom (Fig. 30; GEOL 460 2012). Drought years followed that accidental breach, and the mud veneer covered 350 m of channel until minor runoff of WY 2015 washed it downstream.



Figure 30. Hoof prints are visible in the mud in Bird Creek following an accidental breach of riparian fencing in 2012.

The HHSVRA property line splits Bird Creek along much of its length southwest of the San Andreas Fault (Fig 11). However, the park fence is located high on the stream bank within the park property, leaving the stream channel and riparian areas open to neighboring properties. Along this reach, neighboring cattle enjoy unimpeded access to the riparian zone and channel invert (Fig. 31). Sheared stream banks and manure are a chronic problem along this reach (Fig. 32), but are not caused by park activities or management.



Figure 31. Upstream view of Bird Creek in March 2012, downstream of Walnut Camp. Cattle impact from neighboring property is indicated by sheared muddy stream banks.



Figure 32. A) Cow in riparian terrace adjacent to park fence at Faultline Store. B) Manure in Bird Creek channel at same location as figure A.

Cattle located downstream of the park enjoy continuous, unimpeded access to Bird Creek in the clayey soils east of the San Andreas Fault. During intense rains, the cattle trails likely contribute muddy water mixed with manure to the Bird Creek flow that enters the San Benito River. Similar cattle impacts are likely pervasive in the San Benito River watershed, given the proportion of land intended for that use on similarly fragile soils (Fig. 2).

In summary, we do not have a numerical measurement of the cattle-generated sediment, but it is clearly a chronic source that could be better controlled, especially on neighboring properties and property downstream of the park.

3.3.5 County Road Culverts

Two county roads contribute impervious area runoff to the HHSVRA via a variety of drainage control structures and from uncontrolled runoff. San Juan Grade Road borders the park and Bird Creek watershed divide along the western edge of the park (Fig. 10). Cienega Road bisects HHSVRA land as it crossed from the Cienega watershed to the Bird Creek watershed close to the eastern edge of the park (Fig. 10).

3.3.5.1 San Juan Grade Road Drainage

Visual inspection of oblique aerial photography indicates that hydraulic flow concentration below road–draining culverts erodes HHSVRA hillslopes below San Juan Grade Road, producing a long–term chronic sediment source for Bird Creek (Fig. 33). A review of 1979 USDA aerial photographs indicate that the sediment pathways have been active and visible from the air since at least that time.



Figure 33. Oblique aerial photograph of hillslope erosion concentrated below a subset of culverts along San Benito County's San Juan Grade Road. White arrows point to vertical runoff paths delivering hydraulically concentrated culvert flow onto the HHSVRA slopes. Google Earth image from 2015.

Bedrock material underlying San Juan Grade Road is pervasively fractured, deeply-weathered granitic rock that generally produces small gravel (Fig. 34). The small gravel is either transported directly to channels, or stored on colluvial slopes. The bedrock does not produce much suspended sediment.

We made a qualitative evaluation of erosion hazard of the culverts draining San Juan Grade Road in 2014 (Table 9; Fig. 35). Eleven of the 25 culverts were in either fair or poor condition, two of the culverts showed erosion near the culvert exit from the limited perspective of the top of the slope, and ten culverts had high enough modeled peak flows to transport gravel down the steep hill slopes (Table 9). While only two of the culverts had

erosive features visible from the road, many of them are chronically generating erosive runoff on the hillslopes below the road (Fig. 35)

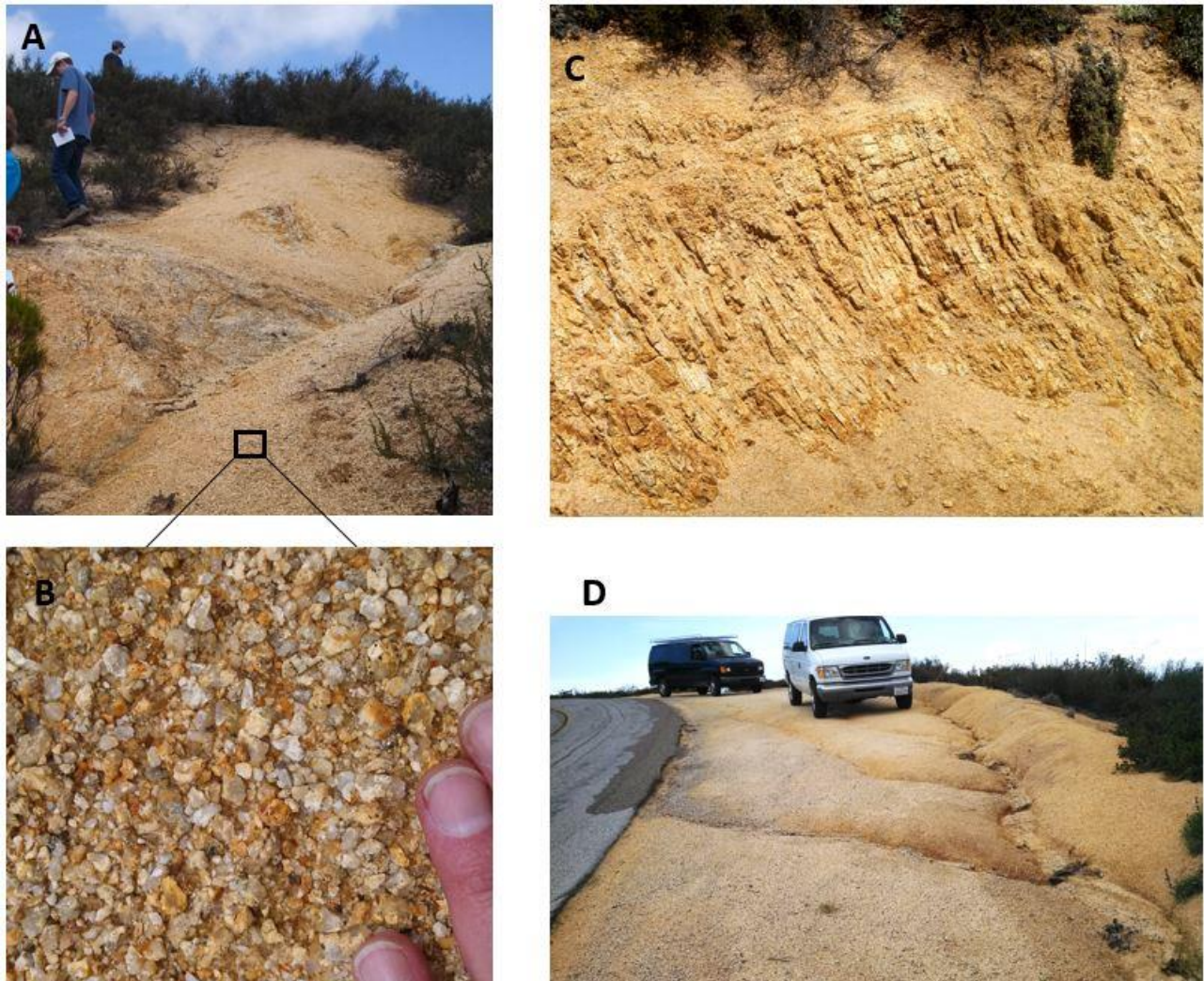


Figure 34. Source material west of the San Andreas Fault is granule and small pebble-sized quartz and feldspar derived from highly weathered bedrock. A) Bedrock outcrop of granitic material. B) close up of bedrock surface showing granule-sized crystals that are easily scraped from the outcrop by hand. C) Bedrock fractures shown in road cut are pervasive throughout the watershed. The fracturing and weathering produces only small diameter gravel for transport down the watershed drainage network. D) Unprotected shoulders are a chronic source of small gravel. Photos from spring 2014 along San Juan Grade Road.

Table 9. Stormwater Diversion Attributes observed in 2014. Diversion number (Div#) is in the order 1 to 25 from high elevation (SW) to lower elevation (NE) in Figure 35. Colors in the table correspond to qualitative erosion hazard based upon modeled peak discharge values (25 yr, 1.04 in/hr storm). Colors are the same in Figure 35. Peak discharge was estimated using the rational method.

| Diversion Number | Diversion Type | Armored | Diversion Condition | Visible Erosion | Watershed Area (ft ²) | Peak Discharge (cfs) |
|------------------|---------------------------------------|---------|---------------------|-----------------|-----------------------------------|----------------------|
| 1 | Natural (no man made diversion) | No | N/A | No | 31677 | 0.57 |
| 2 | Natural (no man made diversion) | No | fair(fresh) | No | 5565 | 0.10 |
| 3 | Natural (no man made diversion) | No | good | No | 16162 | 0.20 |
| 4 | Natural (no man made diversion) | No | N/A | No | 6816 | 0.09 |
| 5 | Asphalt Berm Confined Spillway+Sluice | No | fair | No | 6860 | 0.08 |
| 6 | Asphalt Berm Confined Spillway | No | fair | No | 3777 | 0.05 |
| 7 | Asphalt Berm Confined Spillway | Yes | good | No | 8370 | 0.08 |
| 8 | Culvert | Yes | fair | Yes | 30064 | 0.35 |
| 9 | Asphalt Berm Confined Spillway+Sluice | No | good | No | 11418 | 0.12 |
| 10 | Asphalt Berm Confined Spillway+Sluice | Yes | poor | No | 10682 | 0.12 |
| 11 | Asphalt Berm Confined Spillway+Sluice | No | fair | No | 8701 | 0.10 |
| 12 | Decommissioned Diversion | No | poor | Yes | 18982 | 0.22 |
| 13 | Asphalt Berm Confined Spillway | No | N/A | No | 3099 | 0.05 |
| 14 | Asphalt Berm Confined Spillway | No | fair | No | 1643 | 0.03 |
| 15 | Asphalt Berm Confined Spillway | Yes | good | No | 5122 | 0.06 |
| 16 | Asphalt Berm Confined Spillway | No | good | No | 4081 | 0.06 |
| 17 | Asphalt Berm Confined Spillway+Sluice | Yes | fair | No | 11007 | 0.14 |
| 18 | Natural (no man made diversion) | N/A | N/A | No | 2838 | 0.05 |
| 19 | Natural (no man made diversion) | No | fair | No | 13526 | 0.18 |
| 20 | Natural (no man made diversion) | No | N/A | No | 14033 | 0.24 |
| 21 | Sluice | No | N/A | N/A | 45365 | 0.45 |
| 22 | Top of Culvert | Yes | fair | No | 32721 | 0.39 |
| 23 | Natural (no man made diversion) | No | good | No | 17042 | 0.18 |
| 24 | Natural (no man made diversion) | No | good | No | 4450 | 0.07 |
| 25 | Natural (no man made diversion) | No | good | No | 6115 | 0.06 |

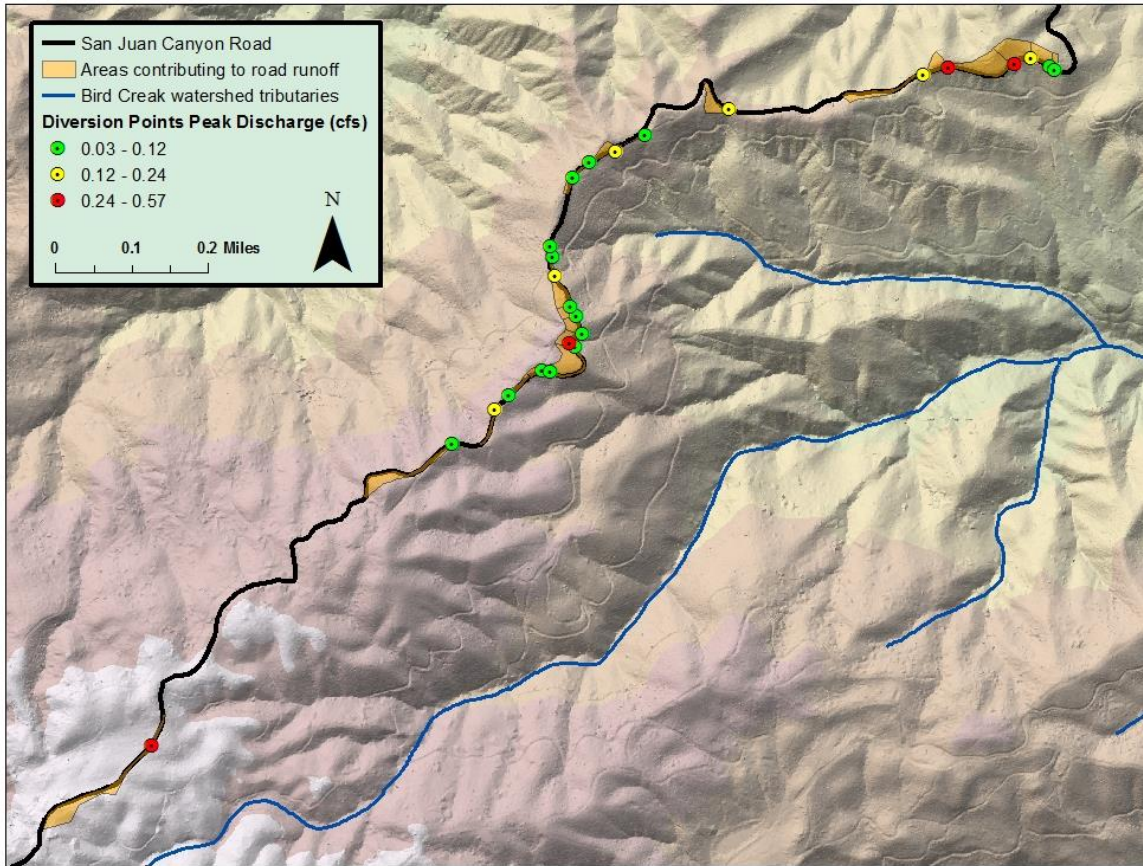


Figure 35. Peak Discharge (Q Peak) of diversions relating to relative areas contributing to San Juan Canyon Road runoff derived by rational method model. See attributes in Table 9. Culverts are numbered in order with descending elevation in Table 9, so culvert #1 is the southwestern red dot.

Our reinspection of the San Juan Grade diversions in 2021 produced the following updates since 2014. Recent asphalt and runoff-controlling berm were present along much of the road, and several diversion outlets had been recently reinforced with new asphalt. Diversion 8 had been removed, with the runoff now directed to diversion 9. Approximately half of the diversions had evidence of beneficial diffuse flow downslope from the road, rather than evidence of flow concentration and erosion. Diversions 17 and 20 (Table 9) are located upslope from the Coyote Trail restoration site. They require maintenance or re-engineering to prevent downslope erosion in the park. In general, conditions along the county road were improved in 2021 as compared to 2014. If any bedload generated by these diversions makes its way past the trail system into a Bird Creek tributary channel, it would be trapped by sediment basins before the confluence with Bird Creek.

3.3.5.2 Cienega Road Drainage

Drainage networks grow from budding of new side channels and headward growth of those new channels through up-slope erosion. This process can be both a chronic sediment source and a hazard when the resulting gully intersects a road. Along Cienega Road, several gullies are the direct result of poorly-engineered culverts that concentrate flow into erosive flows that erode the downslope side of the road during intense rain events. The following observations are summarized from Smith et al. (2018).

The culvert labeled “2” in Figure 36 is the source of water that has produced a large gully and ravine system that includes the features labeled “4”, “5”, and “6” in Figure 36. Feature “4” is a tributary gully that has cut several meters downward in response to base-level drop in the main valley fed by this culvert. The head of that tributary gully is deep, and is growing close to the Cienega Road (Figs. 38, 39 and 40). Cross section transects through the high-resolution digital surface model (DSM) shows that gully depth increases rapidly down gradient (Fig. 39). Steep walls with bare soil indicate the tributary is a chronic and significant source of sediment (Figs. 40 and 41).

The feature labeled “6” in Figure 36 is the second tributary to the main drainage below Culvert two. Serial images indicate this tributary experienced significant new erosion in winter 2017. A new gully grew headward 31 m up the drainage (Fig. 42). It is not visible in fall 2016 aerial imagery but appears for the first time in spring 2017 (Fig. 42). The gully is generally between 0.5 m and 2 m deep, and is 2 m to 3 m wide. It is not a threat to Cienega Road but will likely remain a new chronic source of sediment in high rainfall years. The gully also shows that gully budding and headward growth related to road culvert impact will continue to increase the sediment yield in this region.

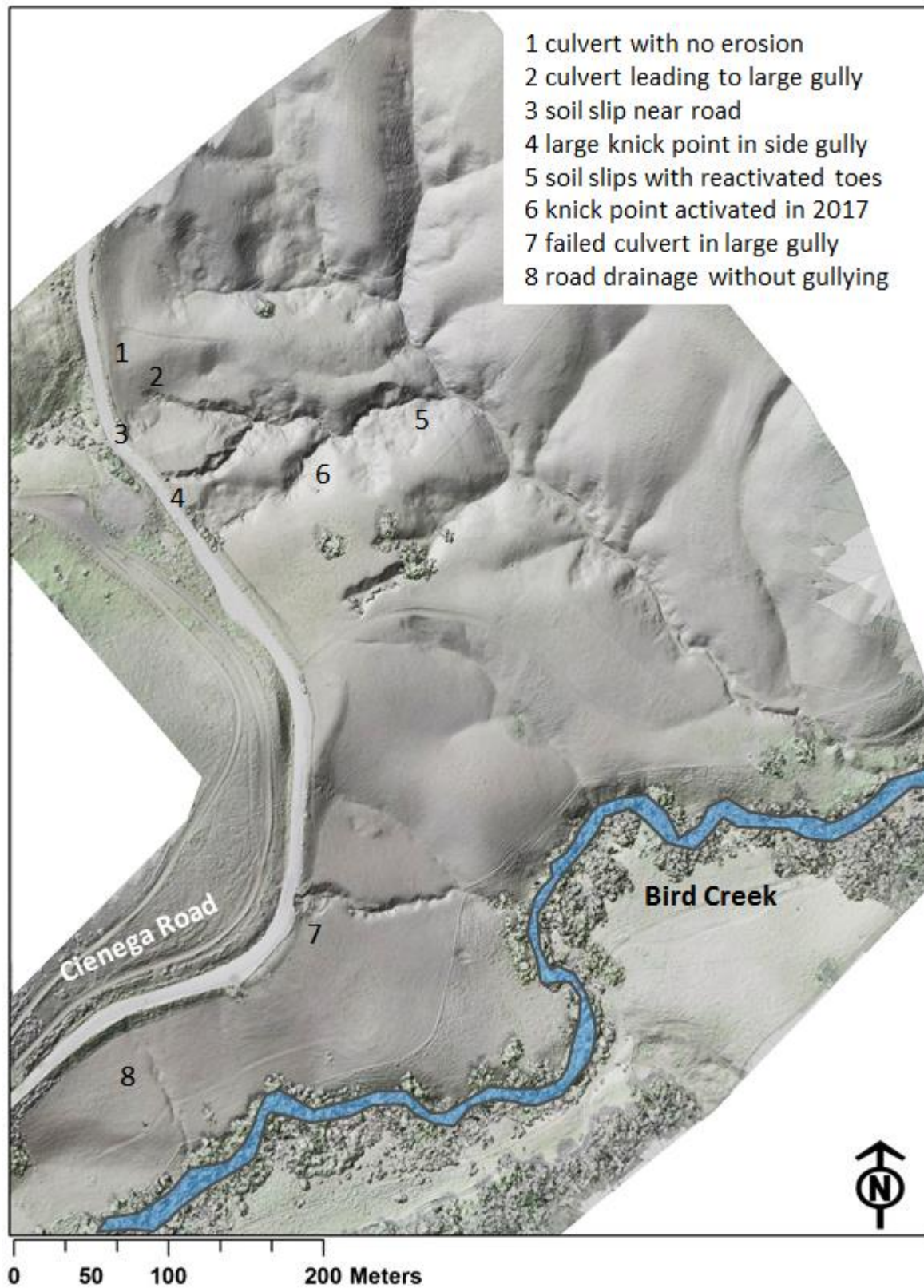


Figure 36. Culverts and erosional features along Cienega Road. Image is blended hillshade and orthophoto from sUAS flight.

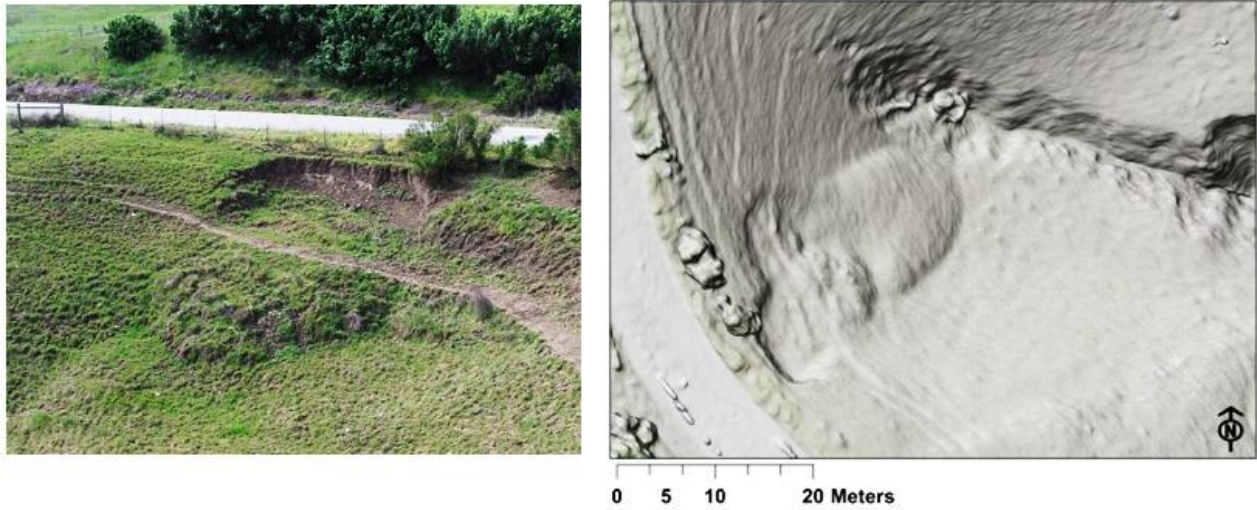


Figure 37. Oblique aerial photograph and hillshade from spring 2018 show soil slip that was reactivated in winter 2017. Location shown in Figure 36, feature number “3.” Culvert labeled number “2” in Figure 36 is visible in hillshade, 5 m north of soil slip toe.



Figure 38. Oblique aerial photograph from sUAS showing active gully near Cienega Road. Feature is labeled “4” in Figure 36. Hillshade of feature is Figure 39. Ground-based photo is Figure 40.

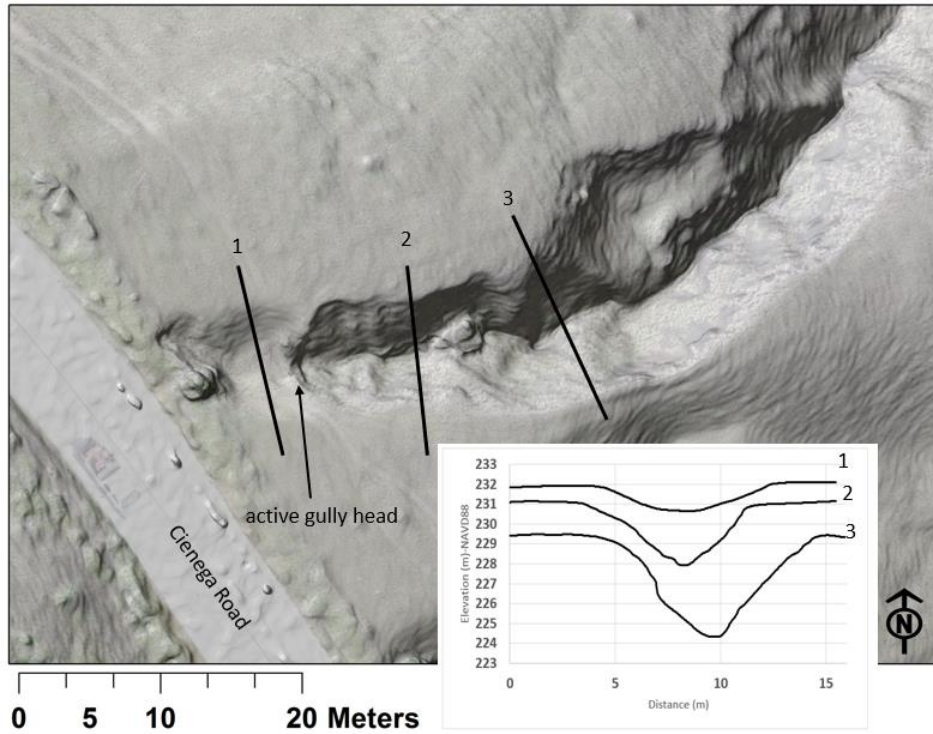


Figure 39. Hillshade showing active gully feature near Cienega Road. Location shown in Figure 36, feature number four. Data from sUAS flight.



Figure 40. Gullies related to culvert drainage erosion. Right gully with surveyors terminates at the culvert labeled “2” in Figure 36. Broken white culvert pipe visible in thalweg is also visible in Figure 38. Left gully is feature number four in Figure 36, also shown in Figure 39.



Figure 41. Close-up of gully walls seen in Figure 40.

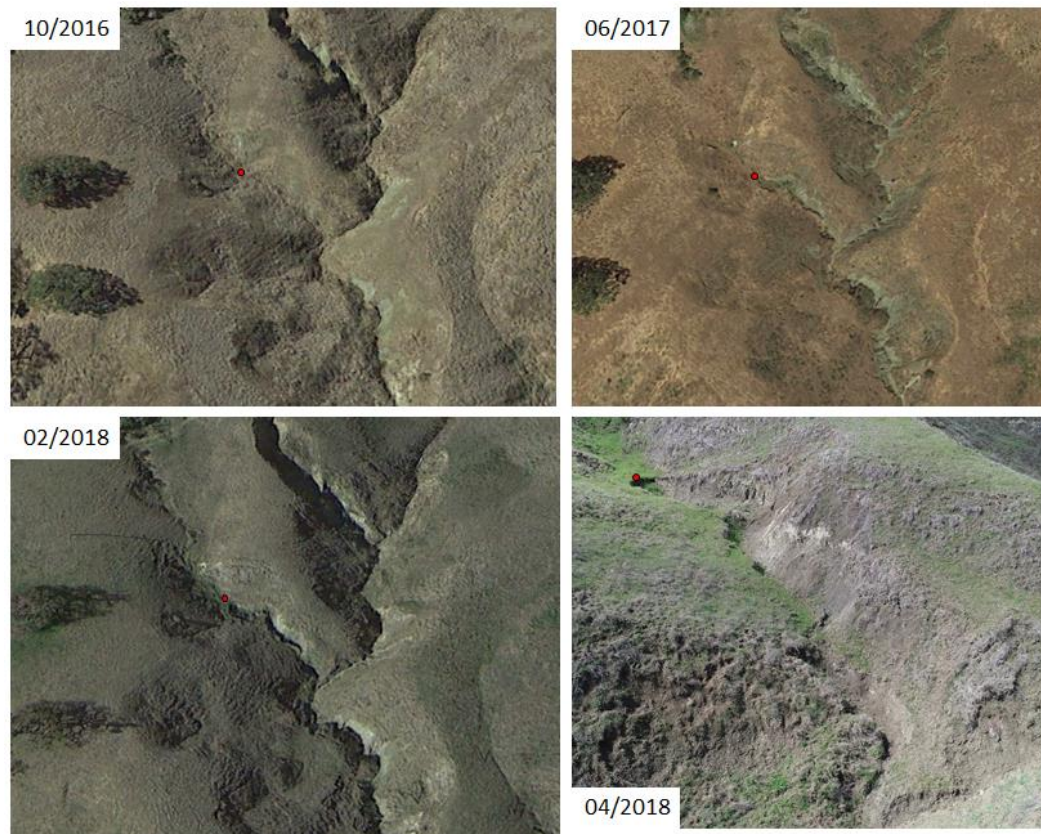


Figure 42. Time series images from Google Earth showing gully formed in 2017. Lower right image is oblique aerial view from sUAS. View is up-gradient. Red dot in all images is the location of the gully head in 2018. Gully is feature “6” in Figure 36.

Innumerable small soil slip features are located along the walls of the main gully below culvert two (Fig. 36). Visual observations indicate the toes of many slips were reactivated in winter 2017. One of those is labeled in Figure 43. Reactivation of gullies in the tributaries and reactivation of slide toes is evidence that the main gully incised in Winter 2017, lowering local base level for adjacent hill slopes. The system generated significant sediment that was transported to Bird Creek in winter 2017 (Fig. 44).



Figure 43. Down gradient view showing unstable slopes in gully system below culvert labeled “2” in Figure 36. Image is oblique aerial view from sUAS. Scene depicts feature five in Figure 36.

Despite the obvious instability low in gully two during the span of our studies (e.g., Fig. 43), repeat benchmarked cross section surveys show that the head of the gully has remained stable (Fig. 45).



Figure 44. Upgradient view of sediment in ravine bottom downstream of Cienega Road gullies. Photograph from 1/25/2017.

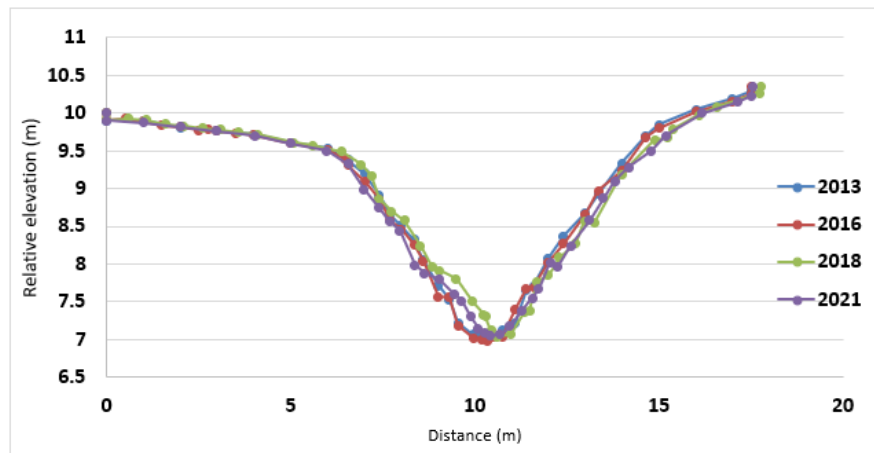


Figure 45. Time series of cross section geometry in gully located within feature “2” (Fig. 36).

The feature labeled “7” in Figure 36 is a road culvert that has accelerated erosion downslope from Cienega road (Fig. 46). The head of the resulting gully is eroding the edge of Cienega

Road, and will pose a continued threat to the road in high-intensity rains. Sediment eroded from the gully bottom and walls can reach Bird Creek along a well-established channel (Fig. 36). While this gully appears to have been active in recent years, it is not a new feature. The feature is visible in aerial images from 1976, but it does not appear to impose a threat to the road at that time. Images from 1996 show the head eroding into the roadway, and it has remained a concern since that time.

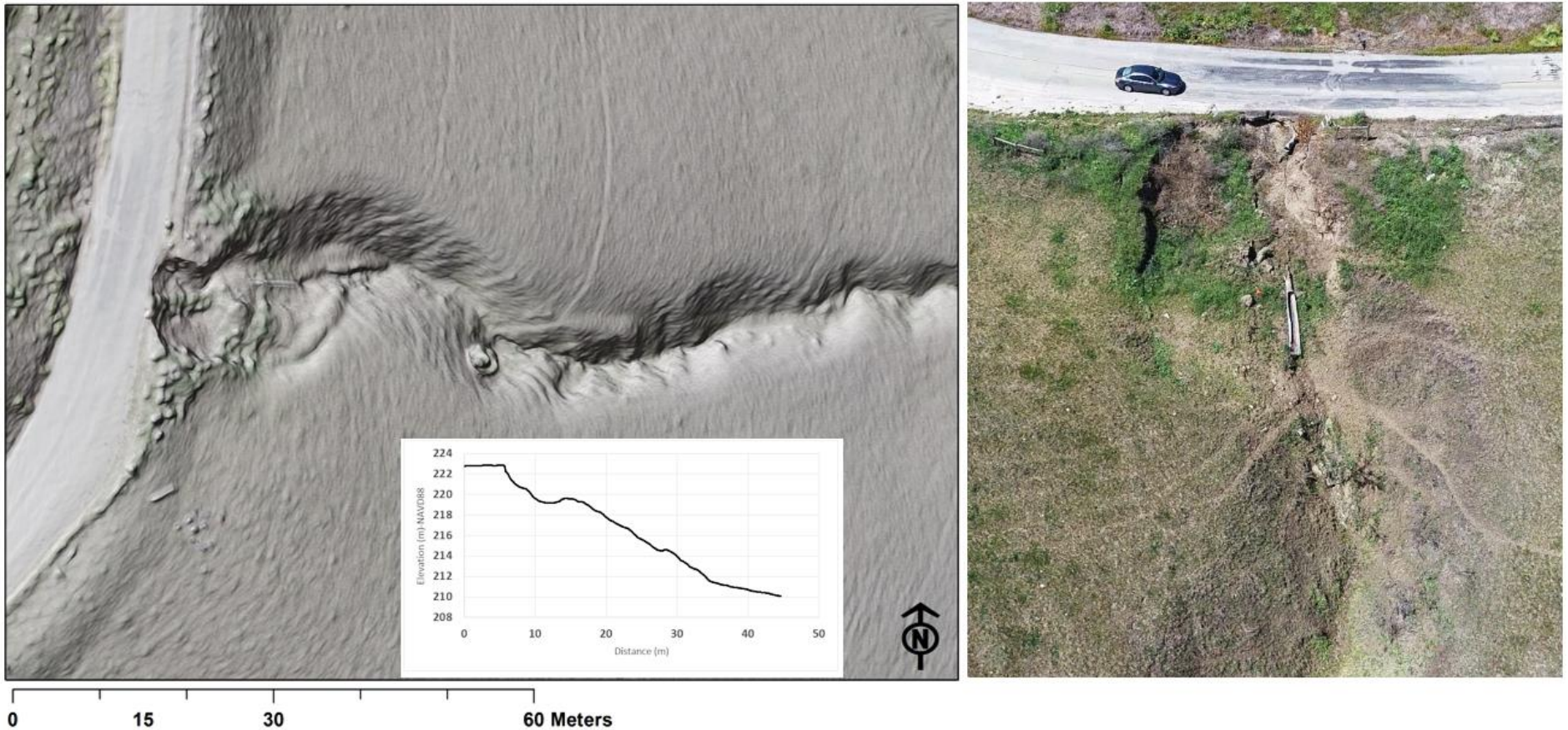


Figure 46. Hillshade and oblique sUAS aerial photograph of culvert-generated gully labeled “7” in Figure 36. Inset image is longitudinal profile of the upper reach of the gully, starting from the road surface.

3.3.6 Landslides and Colluvial Processes

The fine-grained bedrock east of the San Andreas Fault is very unstable on moderate to high slopes (Fig. 47). The substrate fails in either slow earthflows or more rapid colluvial processes throughout the San Benito watershed where the substrate persists for 100's of square kilometers (Sheingross et al. 2012). Many landslides, with a wide range of ages are visible in a single view (Fig. 48). These slope failure features are part of the natural sediment transport system rather than related to OHV use. We selected two landslide systems (Colluvial Creek and Hudner Slide) to study in detail. We tried to determine the slope failure mechanisms and rates, and to assess whether the sediment produced by landslides is reaching Bird Creek on a time frame of interest to resource managers and the TMDL regulatory process.

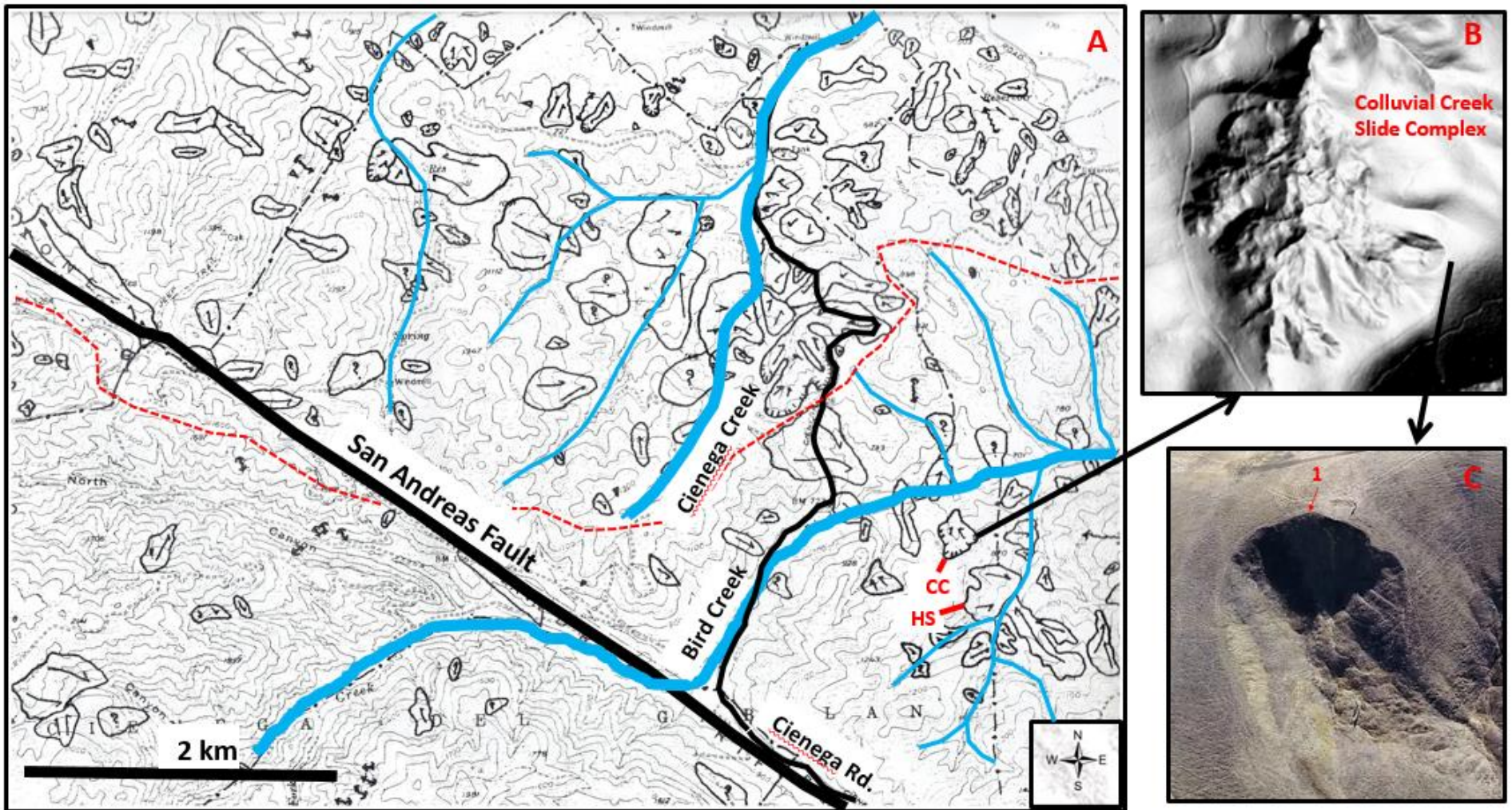


Figure 47 A) Landslide map showing approximately 80 slope failure features in the clay soils of the Bird Creek and Cienega Creek watersheds. Landslides are enclosed areas with arrows showing earthflow direction. Red dotted line is ridge dividing Bird Creek from Cienega Creek. CC is location of Colluvial Creek landslide complex. HS is Hudner slide. Modified excerpt from 1993 draft of Majmunder (1994). B) DEM of Colluvial Creek slide complex. C) Individual slump unit within the Colluvial Creek slide complex.



Figure 48. Low altitude oblique aerial view of unstable slopes in study area (foreground) and in the region, beyond. Red arrows point to a subset of slope failure features (typically “slumps”) present in the region. Foreground shows a subset of slump features in the Colluvial Creek complex. HS is headwall of Hudner Slide. OS is an example of a geomorphically “older” slide.

3.3.6.1 Colluvial Creek Slide Complex

Colluvial Creek is a small tributary to Bird creek located downstream of the Hudner stream gage and Hudner cross section reach (Fig. 10). The upper watershed is ringed with slumps (Fig. 49) and the lower watershed is a low-gradient colluvial valley and small, incised canyon-mouth fan (Fig. 49). The transition is a steep-walled, V-shaped ravine (Fig. 49).

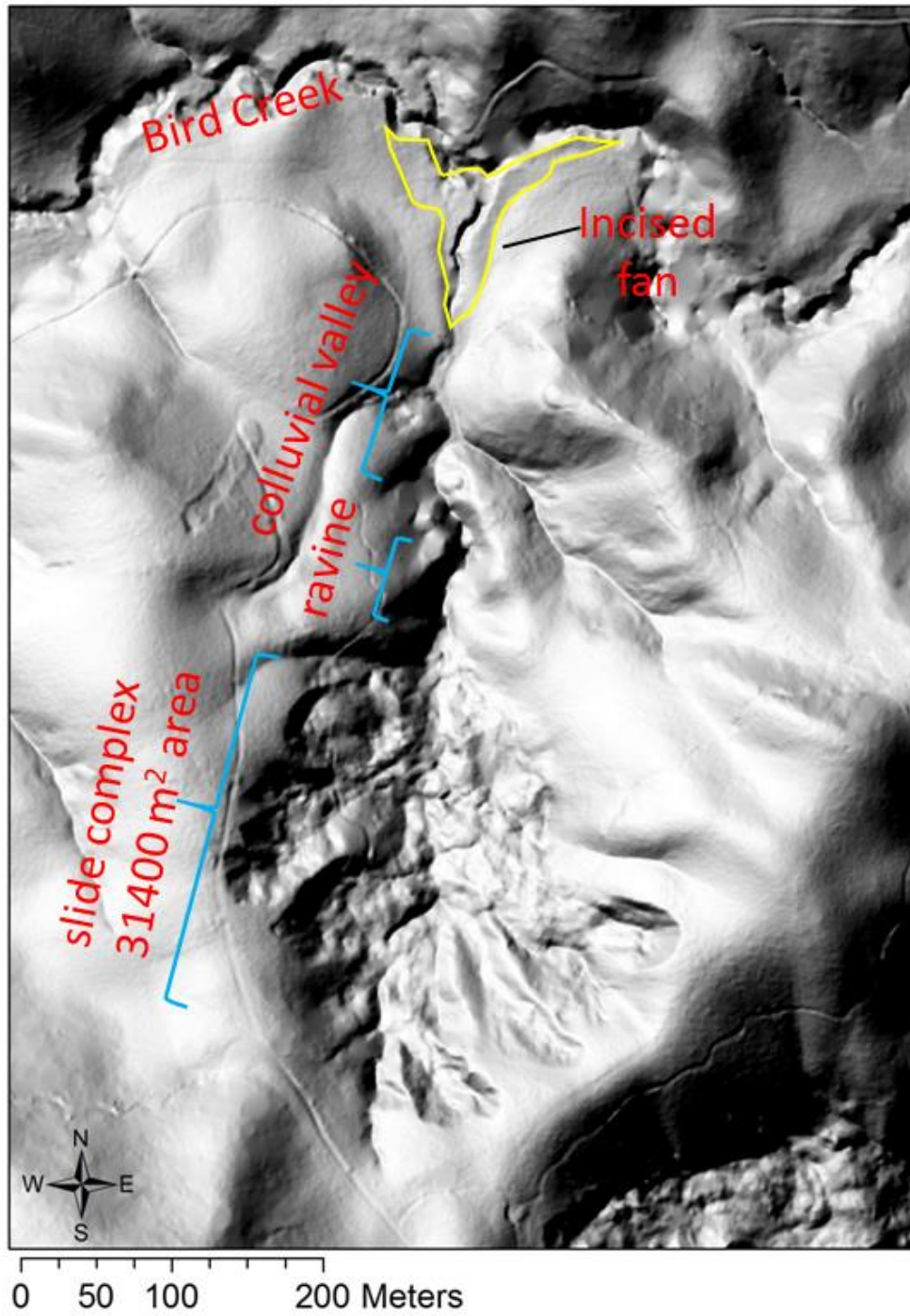


Figure 49. Key geomorphic elements of the Colluvial Creek landslide system. Location in Figure 47.

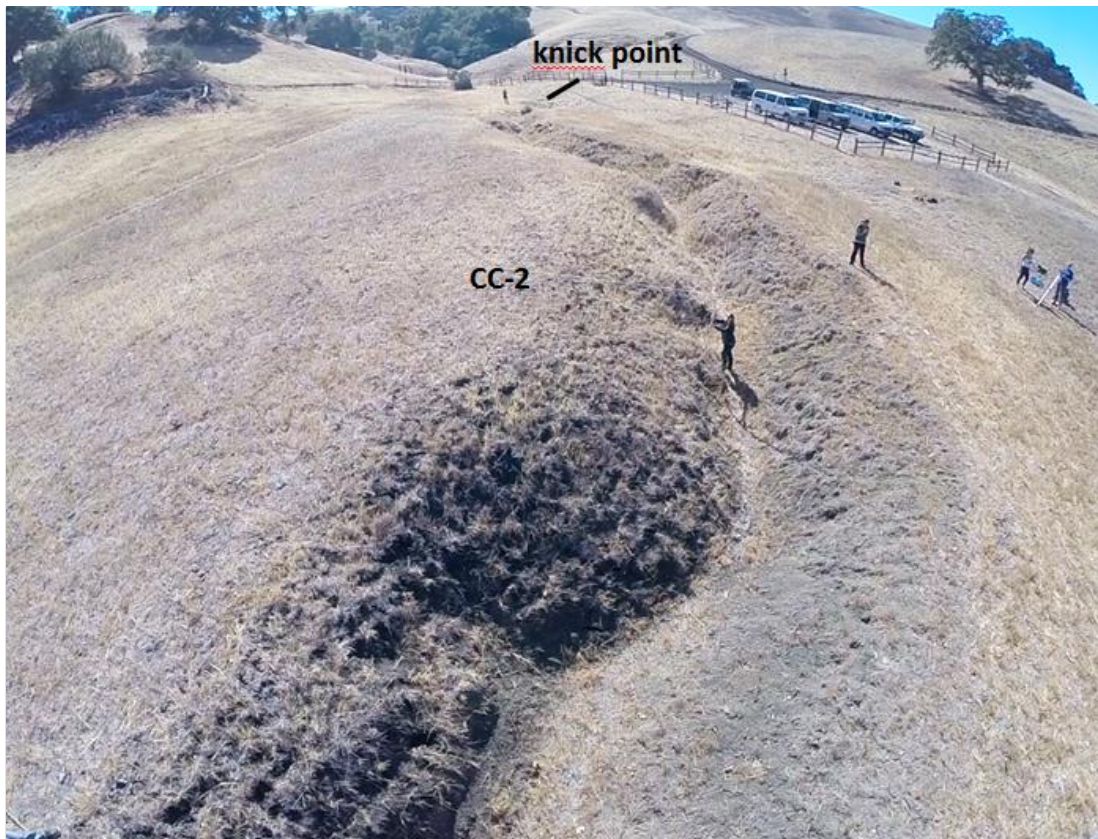


Figure 50. Oblique wide-angle view of incised canyon-mouth fan. View is up gradient from near Bird Creek. The knick point is the transition to the unchannelized colluvial valley (Fig. 49). CC-2 is location of cross section CC-2.

The general processes occurring in each part of the system can be deduced by reconnaissance level investigation, and with reference to geological cross sections (Fig. 51). In general,

- 1) earthflows in the upper watershed transport material downward until it is impeded where the watershed narrows (approximate location of “ravine” in Figure 51);
- 2) the slide material is then reworked via knick points that hydraulically connect the slide body to the ravine where material is transported by dilute alluvial flow down the steep ravine;
- 3) when the transported material reaches the break in slope at the mouth of the ravine, the dilute flows become less competent as they spread out to fill the wider space of the unchannelized valley bottom, and the material is deposited in a laterally confined fan emanating from the ravine; and
- 4) the aggrading valley fill is then gradually reworked directly to Bird Creek via a second knick point that is eroding the fan, leaving a steep-sided” V”-shaped gully.

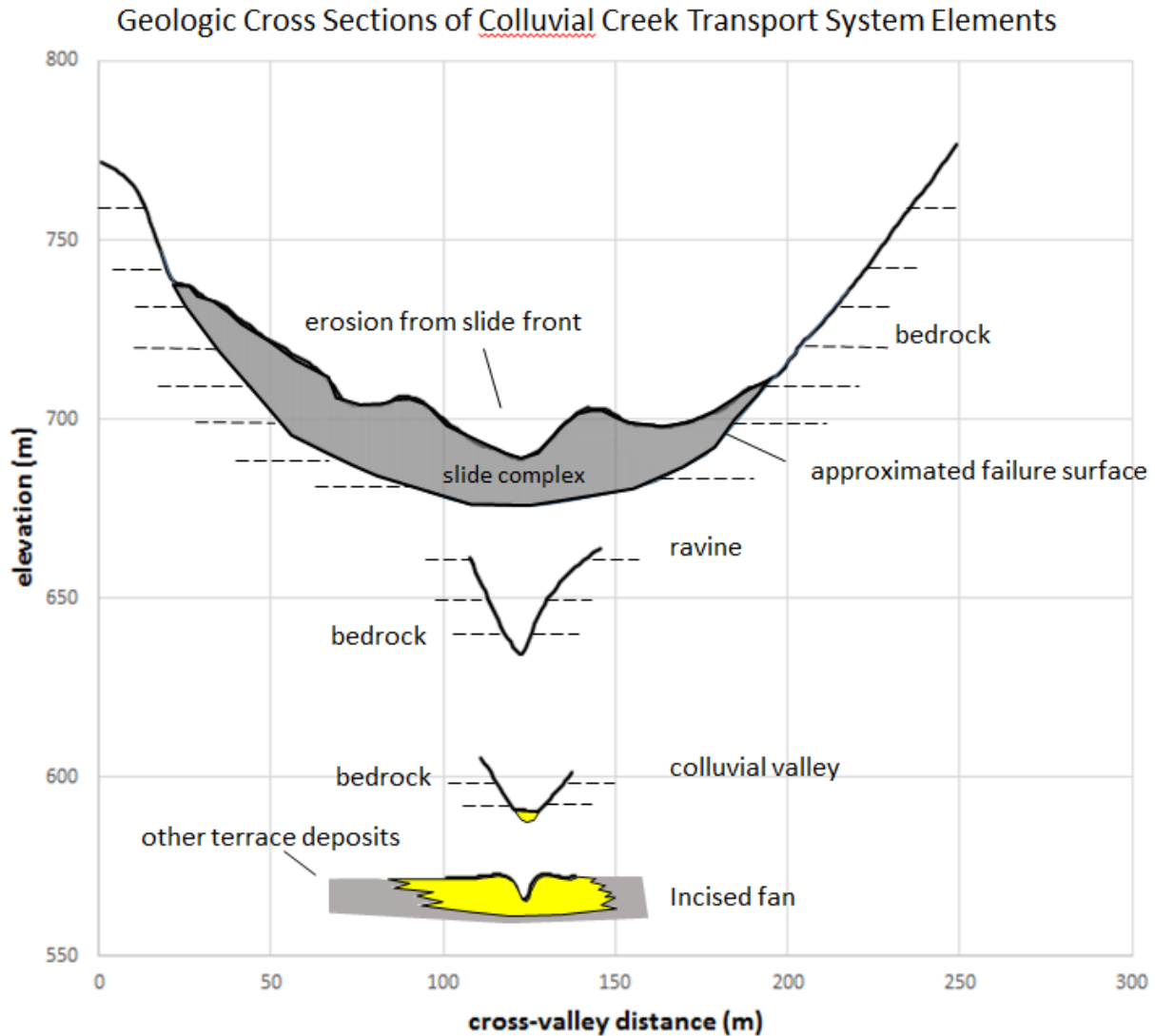


Figure 51. Scaled geologic cross sections illustrating components of the Colluvial Creek sediment transport system. View is down valley. Long term storage (grey) occurs in the slide complex; no sediment is stored in the steep-gradient ravine; a small volume of alluvial fill (yellow) is stored beneath the unchanneled colluvial valley bottom; and moderate-term material storage and transport occurs in the incised fan. Surface profiles from LiDAR-derived, 1 m pixel DEM. Figure 49 shows map-view spatial distribution of features.

Adding complexity to the process is the recognition that separate parts of the system do not operate synchronously, and not at the same rate. The mass (M) of material in the slide complex can be estimated as:

$$M = (\rho_s)(V) = (\rho_s)(A)(T),$$

where ρ_s is the density of the mudstone slide body (estimated at 2.07 tonnes/m³), V is the volume (m³), and A and T are estimates of the slide complex area and average thickness respectively. The area is approximately 31400 m² (Fig. 49), and the average thickness is somewhere between 10 m and 20 m (Fig. 52). Therefore, the slide complex embodies between 650,000 tonnes and 1,300,000 tonnes of regolith that is progressing downslope to Bird Creek.

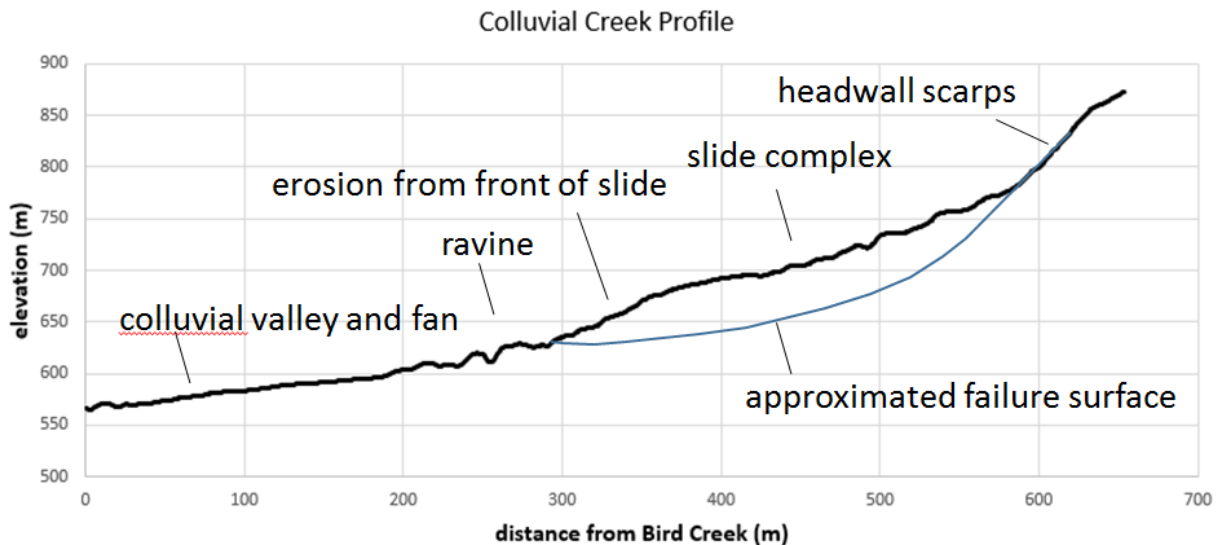


Figure 52. Longitudinal profile through LiDAR-based DEM of Colluvial Creek landslide system. Bird Creek is located 10 m down gradient of the plotted profile.

The slip rate of the slide bodies was determined by driving and surveying four iron rods in each of 5 slide bodies of the Colluvial Creek slide complex (Fig. 53). Peg displacement is visible in more detailed maps (Figs. 54 and 55). Slip rates for the slide bodies (Table 10; Fig. 56) show that the slides move each year, even during drought. All slides moved significantly more during the extremely wet year of 2017 (Fig. 56; Table 10).

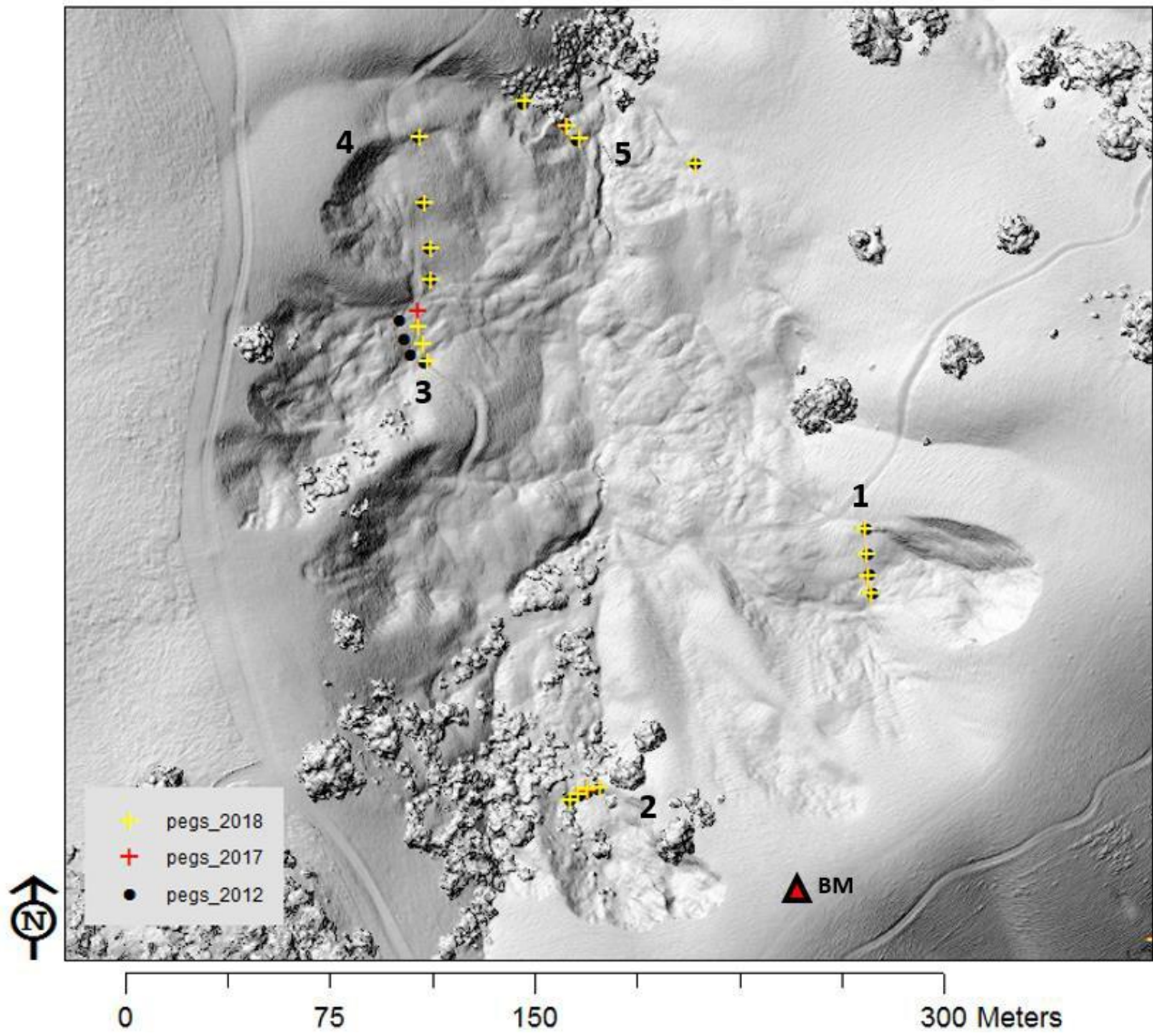


Figure 53. Twenty iron rods installed in the Colluvial Creek Slide in 2012 (black dots) were resurveyed to determine motion. The positions in 2017 (red cross) and 2018 (Yellow cross) positions are also plotted. Background is hillshade from 5/2/2018 low altitude photogrammetry.

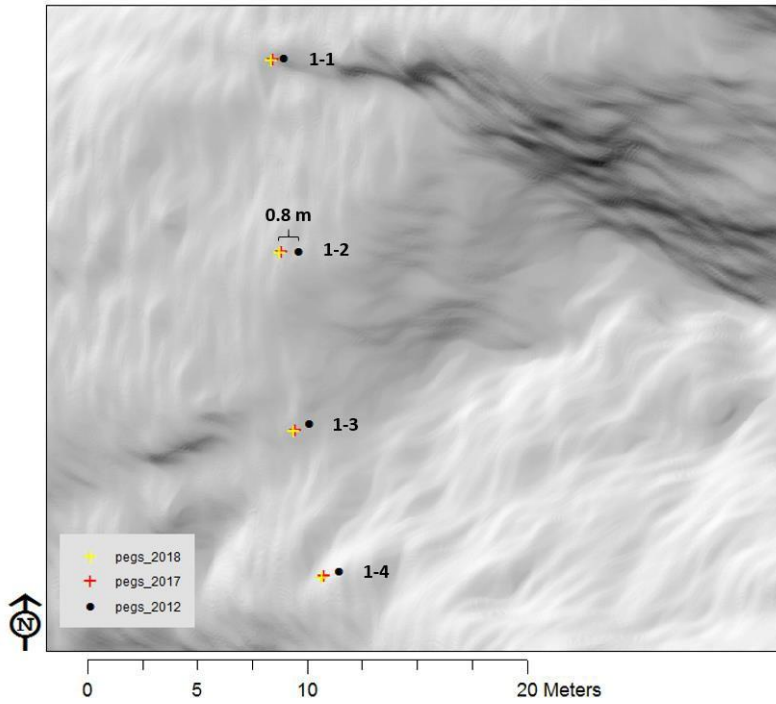


Figure 54. Close view of pegs in head of Colluvial Creek Slide number 1 (Fig. 53 for context).Background is hillshade from 5/2/2018 low altitude photogrammetry.

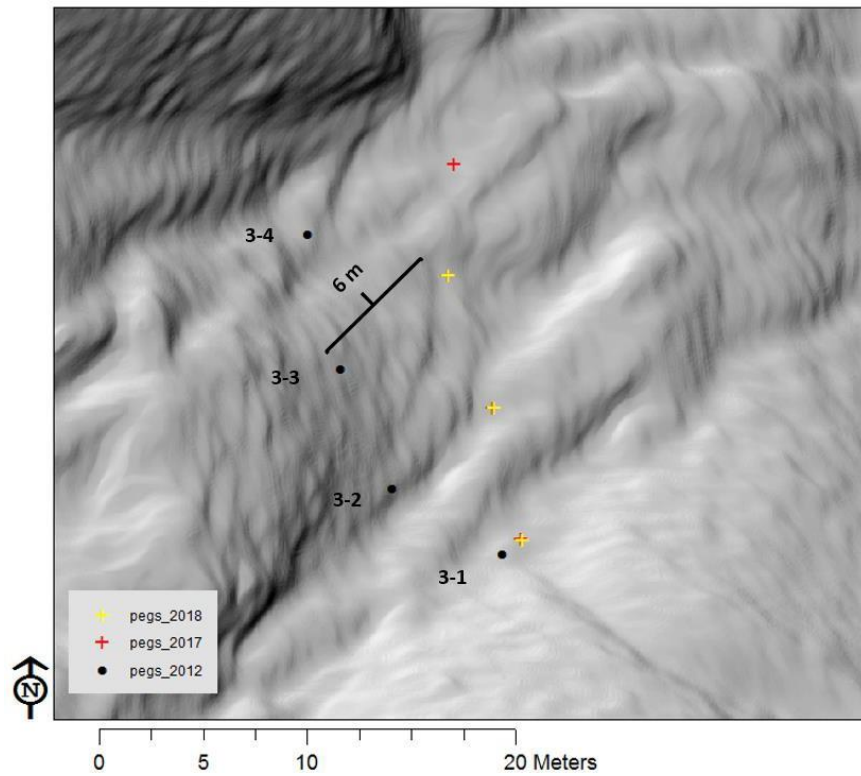


Figure 55. Close view of pegs in head of Colluvial Creek Slide number 3 (Fig. 53 for context).Background is hillshade from 5/2/2018 low altitude photogrammetry.

Table 10. Colluvial Creek landslide incremental pin movement between January 2012 and June 2021.

| Colluvial Creek Slide Average Slide Movement Since 2012 (m) | | | | | | | | |
|---|--------|--------|--------|--------|--------|--------|--------|--------|
| slide | Apr-12 | Oct-12 | Oct-13 | Jul-16 | Oct-17 | Nov-18 | Jun-19 | Jun-21 |
| 1 | 0.01 | 0.10 | 0.19 | 0.31 | 0.80 | 0.89 | 0.46 | 0.19 |
| 2 | 0.02 | 0.11 | 0.30 | 0.56 | 0.93 | 1.00 | 0.09 | 0.29 |
| 3 | 0.20 | 0.24 | | 0.53 | 5.90 | 5.95 | 0.05 | 0.10 |
| 4 | 0.05 | | 0.17 | 0.33 | 0.52 | 0.61 | 0.21 | 0.09 |
| 5 | 0.01 | | 0.27 | 0.57 | 0.92 | 1.01 | 0.10 | 0.07 |

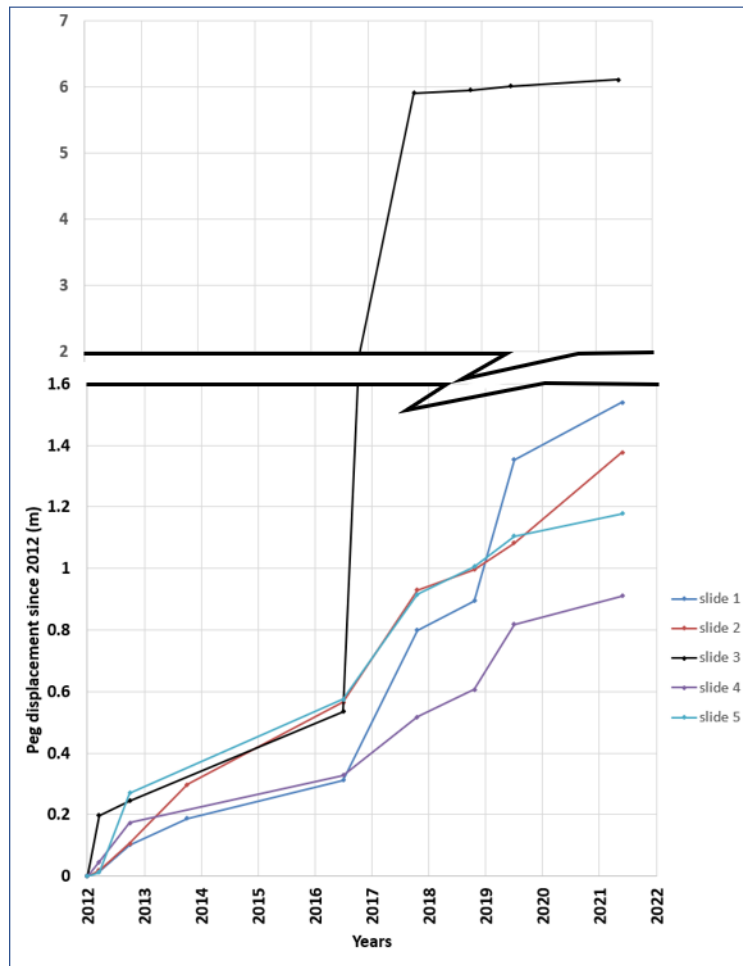


Figure 56. Cumulative slip of the Colluvial Creek landslide pins (site average). Note scale change for slide 3 at 1.6 m.

Regressing the slide trajectories in Figure 56 provides slip rates ranging from 0.093 to 0.16 m/yr, excluding the extreme event in slide 3. That range is not far from 0.2 m/yr, which is the typical velocity for earthflows in this region, as measured by interferometric synthetic aperture radar (Scheingross et al. 2012).

Eight benchmarked cross sections were surveyed between 2011 and 2021 to assess sediment transport from the active colluvial Creek slide complex to Bird Creek (Fig. 57). While the slide complex has been active during the study period, visual inspection and benchmarked cross sections (Fig. 58) of the ravine (CC-7 and CC-8), colluvial valley (CC-5 and CC-6), fan (CC-4), and incised fan (CC-1 to CC-3) indicate that those elements have been relatively inactive. In particular, we have seen no change in the location of the main

knick point at the head of the incised fan gully (CC-4). However, the age of the fan fill is young (decades), as indicated by buried ranch artifacts now exposed in the gully walls (Fig. 50), and a 1979 USDA aerial photograph of the site indicates that the fan incision is younger than 1979. These processes that transport material from landslide toes toward Bird Creek act on a decadal scale, which is of interest to resource managers. During the 11 years of our study, there was no contribution of sediment to Bird Creek from the Colluvial Creek slide complex.

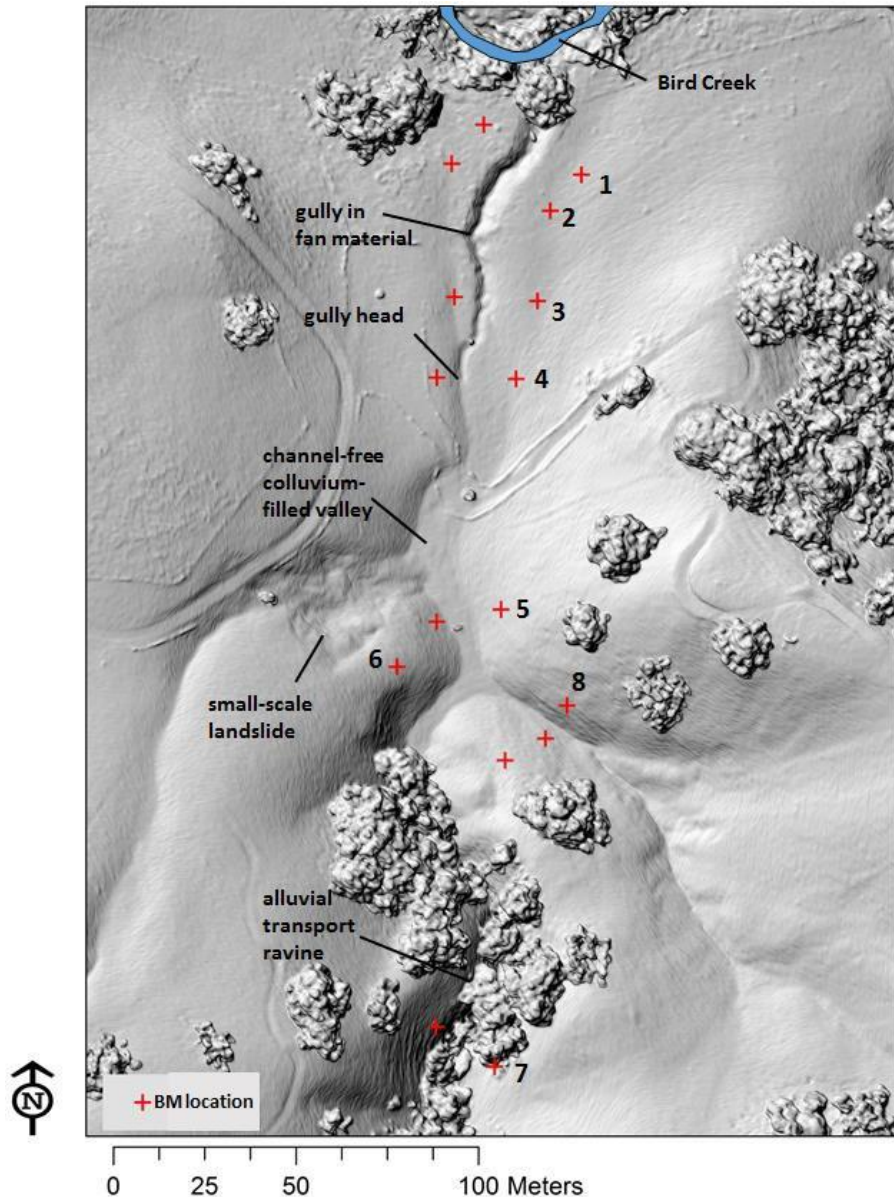


Figure 57. Benchmark locations for Colluvial Creek cross sections shown in Figure 58. Background is hillshade from 5/2/2018 low-attitude photogrammetry.

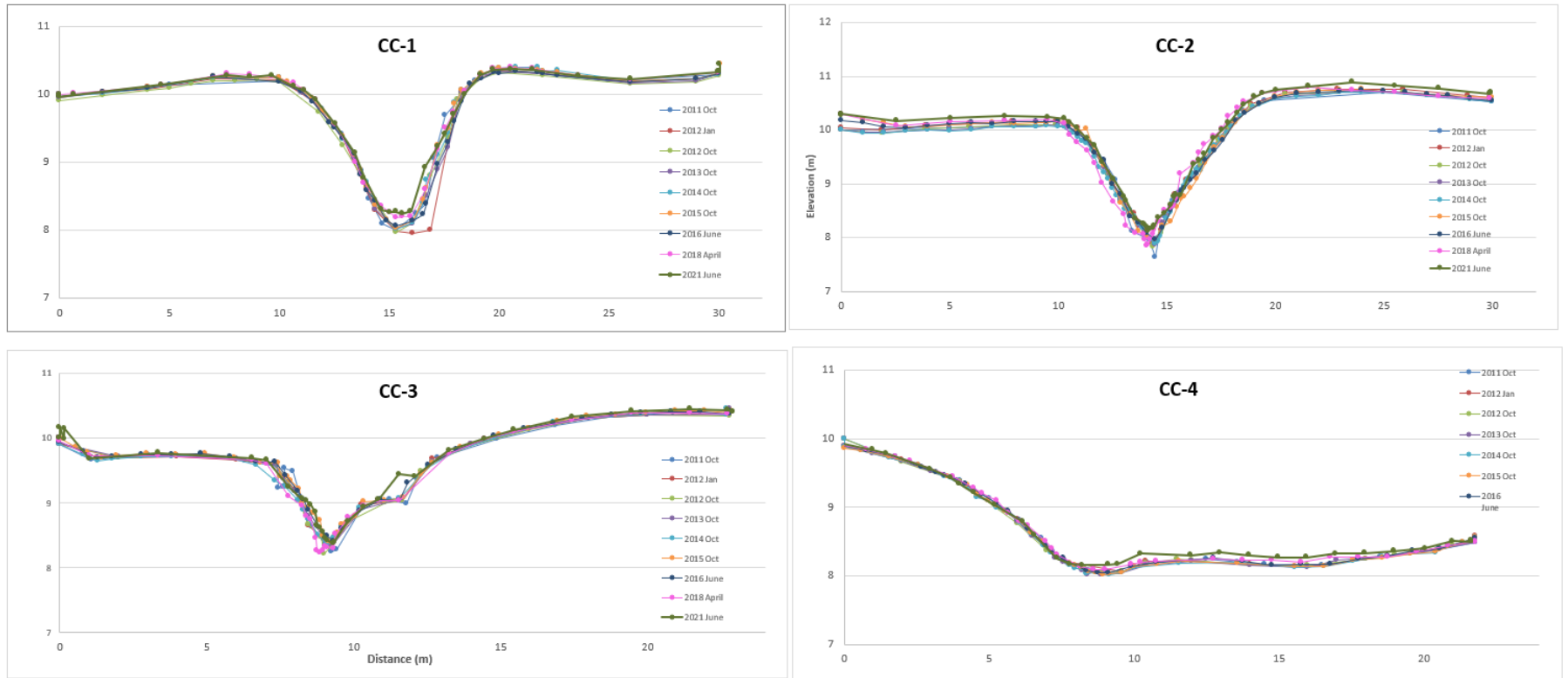


Figure 58. Time-series cross sections of Colluvial Creek. Horizontal axes are distance (m) from left benchmark. Vertical axes are elevation (m) relative to 10 m assigned to left benchmark. See Figure 57 for locations.

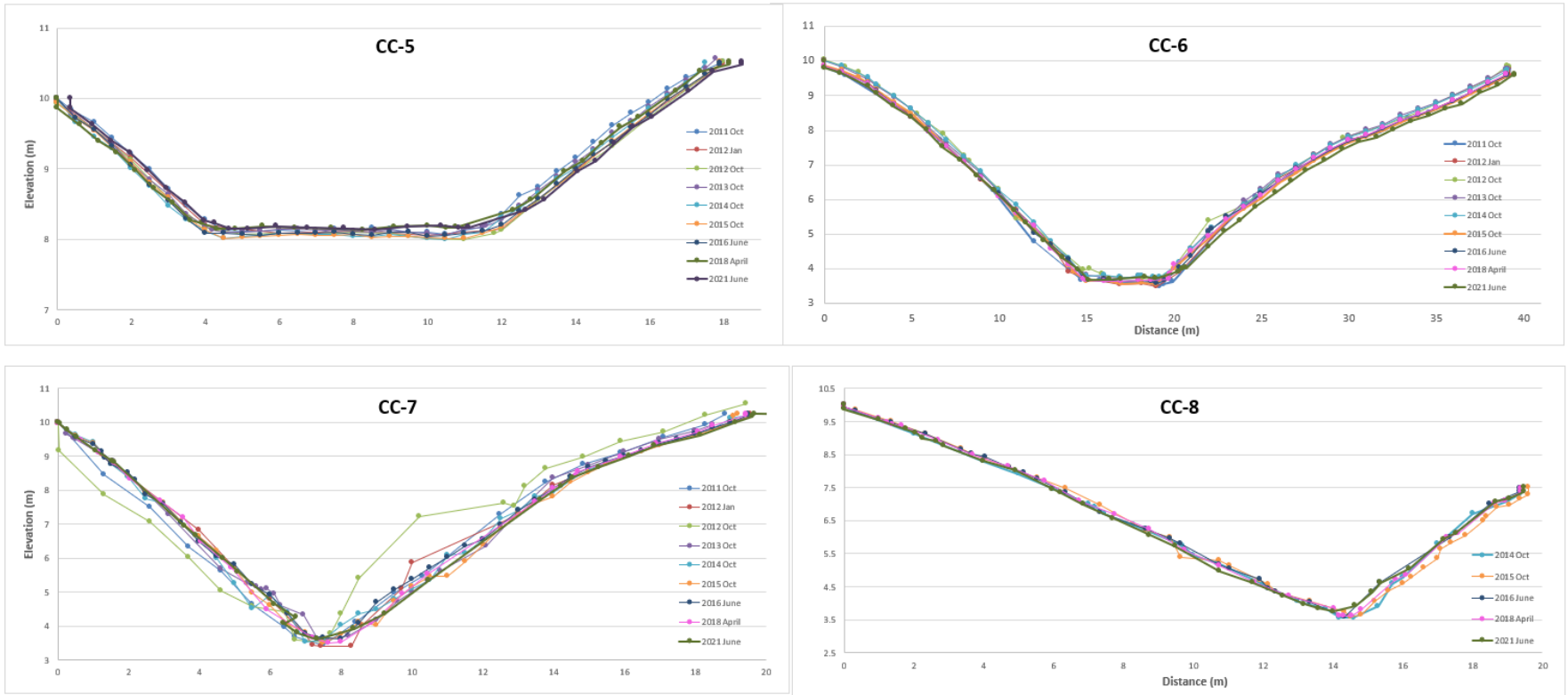


Figure 58 continued. Time-series cross sections of Colluvial Creek. Horizontal axes are distance (m) from left benchmark. Vertical axes are elevation (m) relative to 10 m assigned to left benchmark. See Figure 57 for locations.



Fig. 59. Ranch implements, including partially-buried glass bottles, fluid storage tank, and tires, only several decades old, are exposed by erosion of the fan fill. Up gradient wide-angle photo view of cross sections CC-1 and CC-2 (Fig. 58).

3.3.6.2 *Hudner Slide Complex*

Hudner Creek is a small tributary to Bird Creek. The watershed is mostly HHSVRA property, but the mouth joins Bird Creek downstream of the property line and downstream of the Hudner stream gage (Figs. 10 and 47). The upper watershed includes widespread slope failure, like that described in Colluvial Creek. Slide material has filled the valley bottom from both sides (Fig. 60). The Hudner Slide complex includes several superimposed slope failures that head near the divide with Colluvial Creek. The toe of the slide dammed the valley when it became very active sometime after 1979 (determined from aerial photographs), forcing aggradation and the development of a poorly-drained wet meadow (“Eroding fill” in Fig. 60).

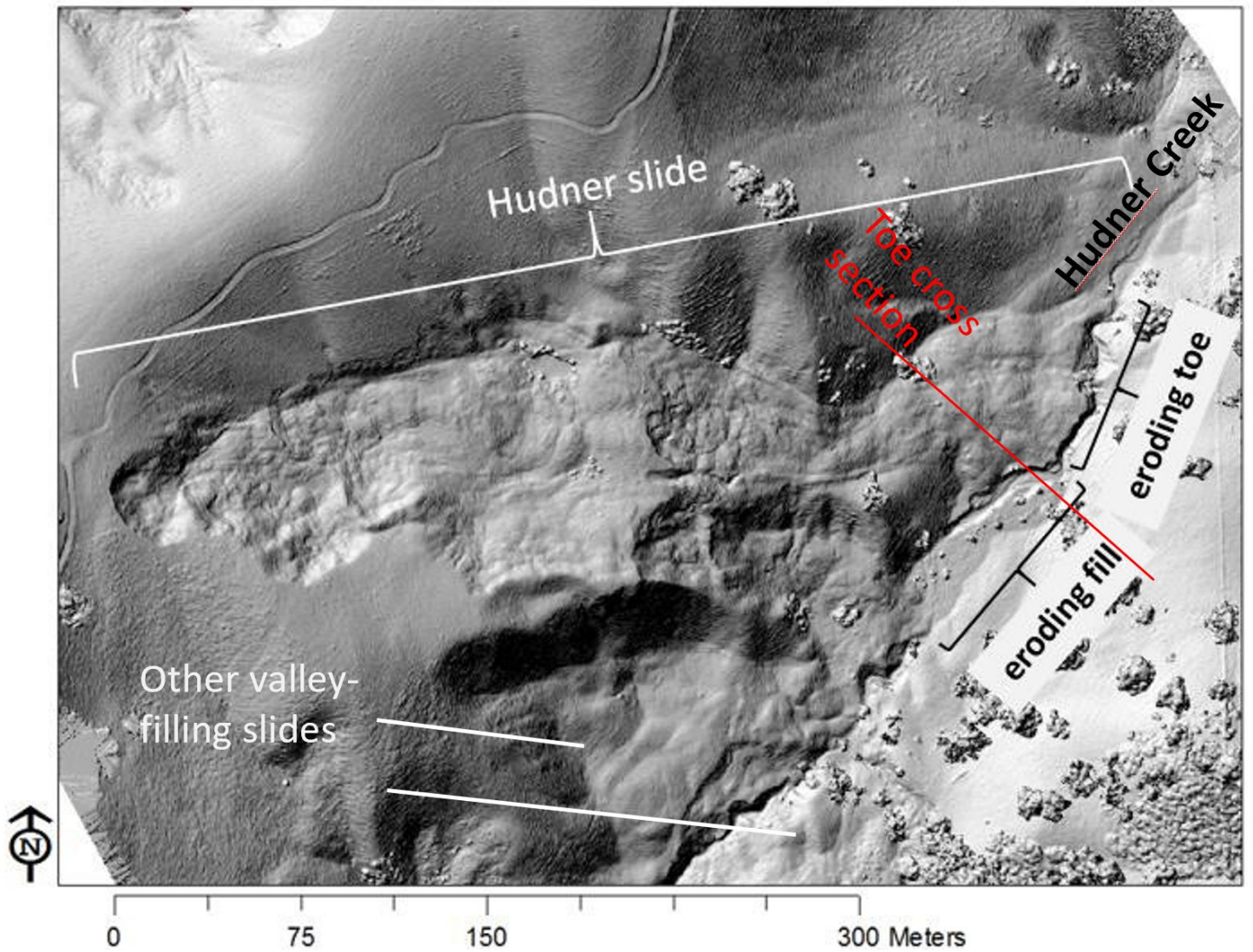


Figure 60. Key geomorphic elements of the Hudner landslide system shown in a 1 m DEM from 2010. Red line is section line for Figure 61.

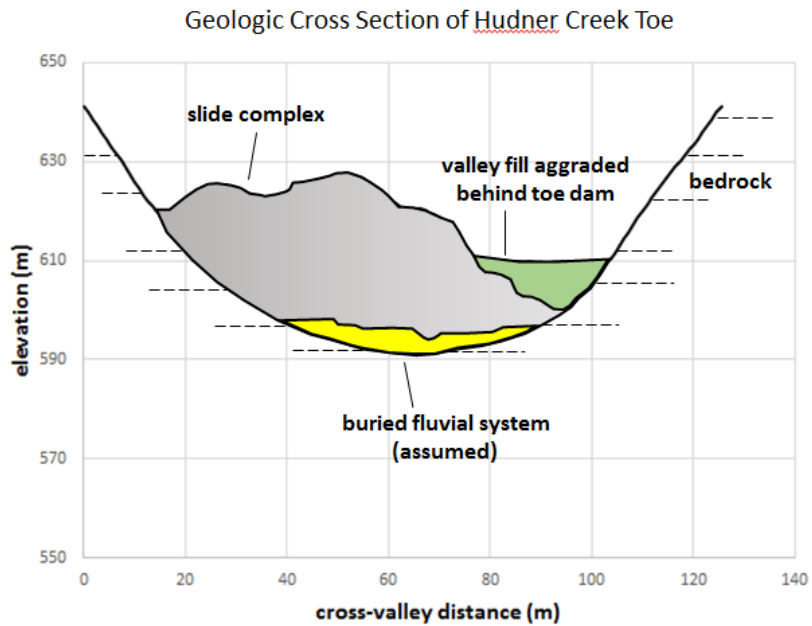


Figure 61. Scaled geologic cross section illustrating components of the Hudner Creek alluvial valley. View is down valley. Long term storage occurs in the slide complex (grey) that buried the Hudner Creek fluvial system (yellow); the slide toe dammed the valley, forcing sediment to aggrade as a ponded, channel-free valley fill (green). Surface profiles from LiDAR-derived 1 m DEM. Figure 60 shows map spatial distribution of features.

The Hudner Slide was a 25 m wide earthflow identifiable by subtle geomorphic features in a 1979 aerial photograph. The slide body had expanded to over 60 m wide, and had become more complex by 1998, as seen in Google Earth imagery. The headwall scarp had a very youthful appearance in 2012, indicated by steep to overhanging headwall with vegetation-free soil (Fig. 62). The HHSVRA District Superintendent noted that the fresh scarp appeared in the few months immediately preceding a park-wide aerial photography and LiDAR mission in fall 2010 (personal communication Mr. Matthew Allen). Comparing the 2010 orthophotos with those flown in 2014 indicates that the headwall is still adjusting (Fig. 63).

Twenty rebar pegs placed in rows in the slide captured slide motion between 2016 and 2018 (Fig. 64; Table 11).



Figure 62. Hudner Slide headwall scarp in spring 2012. Lack of vegetation and sharp (locally overhanging) top corner on the headwall scarp indicates that the slide motion is young. Yellow arrow indicates approximately 6 m of displacement.

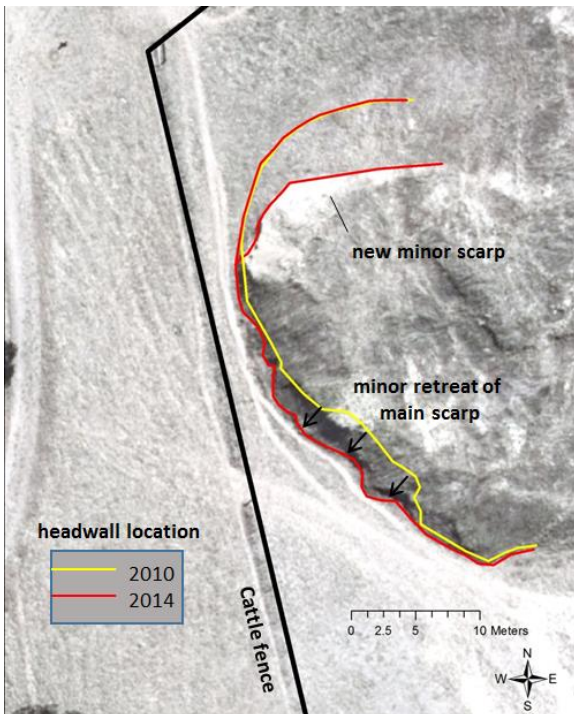


Figure 63. Location of the Hudner Slide headwall scarp has eroded headward approximately 3 m between 2010 and 2014 aerial photos. A new minor scarp formed on the north wall of the scarp during that time.

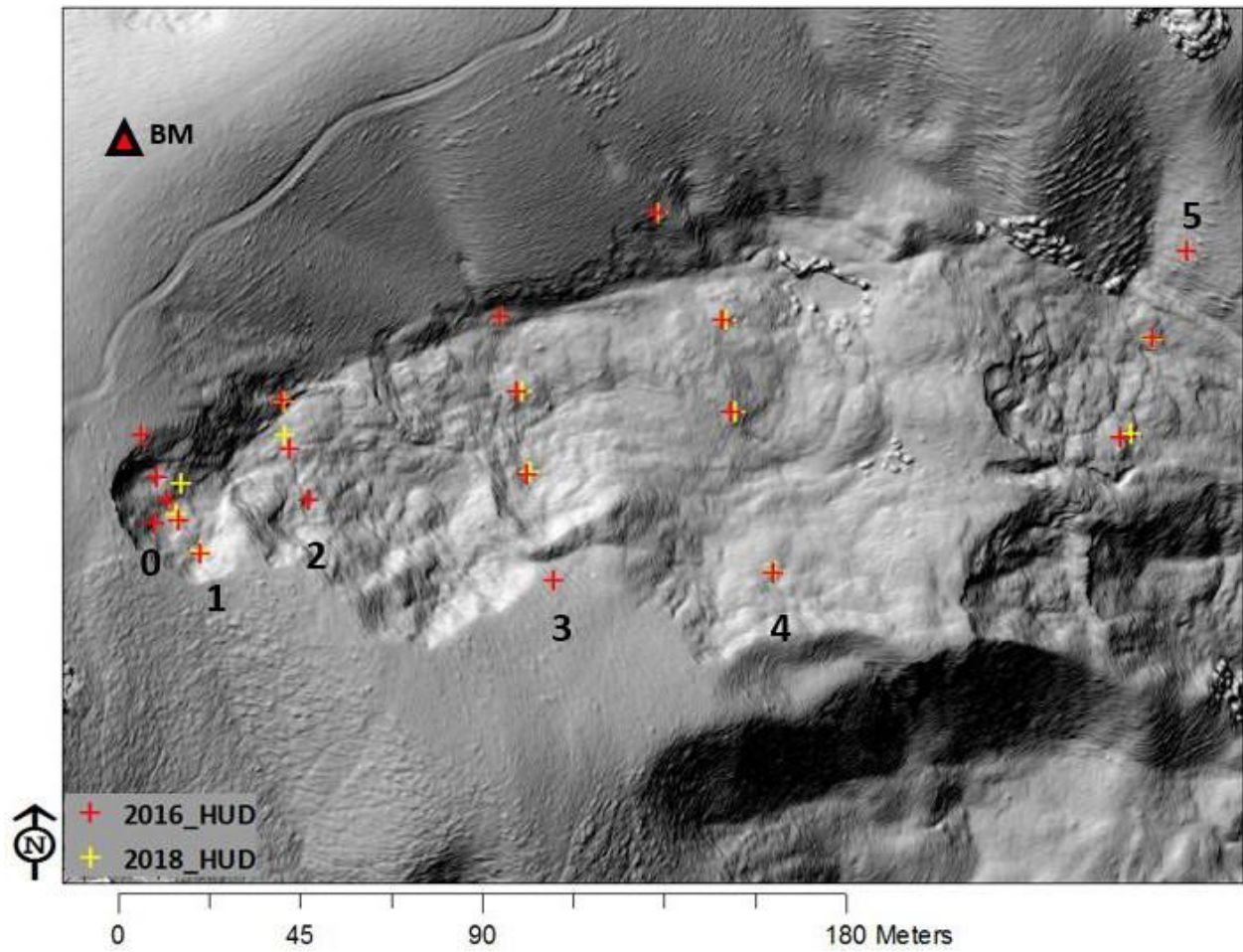


Figure 64. Twenty iron rods installed in the Hudner Slide in 2016 (red crosses) were resurveyed in 2018 (yellow crosses). Pegs are arranged in rows 0 through 5. Pegs are numbered sequentially from south to north in each row. Background is hillshade from 5/2/2018 low- altitude photogrammetry.

Table 11: Three-dimensional slip vector magnitudes of the Hudner Slide pegs measured from 2016 to 2018. “Average Slide” includes the pegs in the Hudner slide body; “Average Control” includes the pegs located in more stable ground outside the slide body (grey cells). Peg 4-1 was located in a tributary slide, adjacent to the main slide. See Figure 64 for peg locations. Blank entries indicate pegs that were present in 2016 that were likely buried beyond the reach of a metal detector in 2018.

| Peg | 3D |
|-----------------|------|
| 0-2 | |
| 1-1 | 0.65 |
| 1-3 | 2.74 |
| 1-4 | |
| 1-5 | 6.76 |
| 1-6 | 0.03 |
| 2-1 | |
| 2-2 | 3.79 |
| 2-3 | 0.33 |
| 3-1 | |
| 3-2 | 0.90 |
| 3-3 | 1.34 |
| 3-4 | 0.04 |
| 4-1 | 0.39 |
| 4-2 | 0.79 |
| 4-3 | 0.88 |
| 4-4 | 0.17 |
| 5-2 | 2.64 |
| 5-3 | 0.35 |
| 5-4 | 0.05 |
| Average Slide | 1.77 |
| Average Control | 0.08 |

The slide pegs placed in the hillslope adjacent to the slide (e.g., 3-1 and 3-4) are considered “experimental controls” in that they approximate expected motion of the ground if a landslide event were not triggered. Slide pegs moved an average of 1.77 m, in excess of the control pegs which moved just 0.08 m on average (Table 11). Peg motion in rows 3 and 4 are compatible with downslope motion of a single coherent slide body (Figs. 64 and 65). However, other peg movement indicates that slide motion was highly variable through space (Table 11; Fig. 64), leaving the average slide motion value less indicative of true overall sediment transport rates in landslide processes. The highly variable peg movement, including significant lateral (rather than directly downslope motion) indicates that the slide locally moved as an incoherent earthflow rather than as a coherent slide.

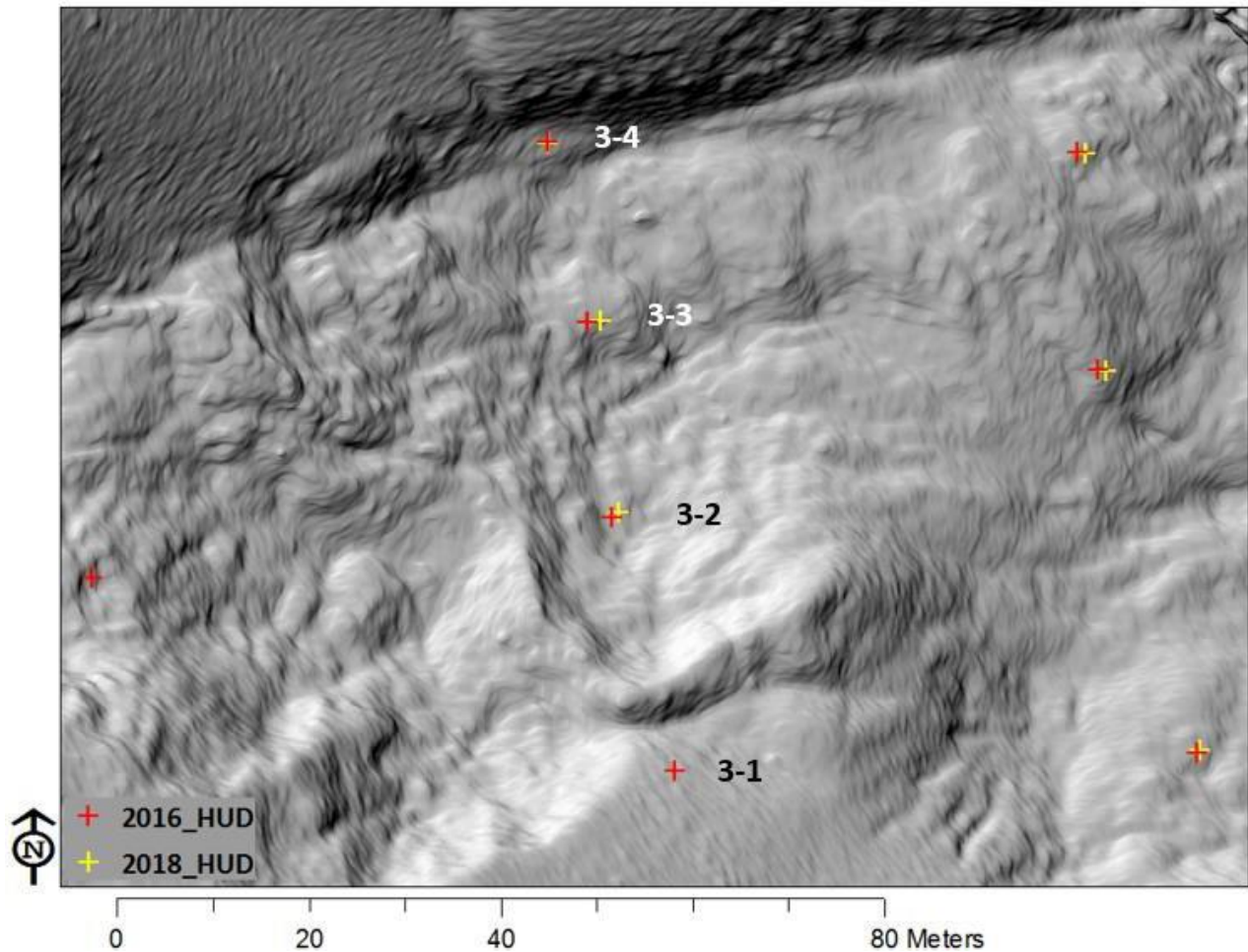


Figure 65. Third row of pegs in Hudner Slide installed in 2016 (red crosses) were resurveyed in 2018 (yellow crosses). Peg 3-1 was missing in 2018. Locations in Figure 64. Background is hillshade from 5/2/2018 low altitude photogrammetry.

The total two- year slide movement of 1.77 m provides an average movement of 0.89 m/yr. That value is certainly an over estimate because of the short time span that included the 2017 wet year.

Steep gullies cutting into a slide body are efficient sediment transport routes that can move sediment from the slide toward Bird Creek via Hudner Creek. Recent gulling is present within the Hudner slide body. For example, a gully is visible as a crease in the hillshade directly southwest of the southern peg of row 5 (Fig. 64).

A deep “V”-shaped ravine has incised the slide toe where it had over steepened the Hudner Creek valley floor (Figs. 60 and 66). The ravine transports slide material and aggraded A deep “V”-shaped ravine has incised the slide toe where it had over steepened the Hudner

Creek valley floor (Figs. 60 and 66). The ravine transports slide material and aggraded alluvium to the lower reach of Hudner Creek where it reaches Bird Creek below the park boundary through alluvial processes in wet years.



Figure 66. Oblique photo showing field relations between slide elements and valley sediment transport system. Meadow sediment filled in behind dam caused by slide toe. The creek eroded through the toe (see ravine) and advanced through the meadow in 2017.

The multiphase sediment transport process active in Hudner Slide includes gullying that liberates slide-related sediment from the slide toe and sediment trapped upstream of the slide toe (Figs. 66, 67 and 68). The volume of sediment released to Bird Creek through this gully system alone during the winter of 2017 is estimated to have been 1 100 m³ (1460 yd³), based upon 55 m of headward gully growth and a typical cross-sectional area of 20 m² (Fig. 68). That volume represents approximately 1 507 tonnes assuming an alluvium density

of 1370 kg/m³, which is the value measured in an “alluvial meadow” (Dumikh 2014). The volume and mass reported here are minimum contributions of sediment to Bird Creek from Hudner Creek because there are similar active gully systems located farther up the Hudner Creek valley.



Figure 67. Low-altitude oblique aerial photograph (5/2/18) of Hudner Creek gully incising toe and trapped alluvium at base of Hudner Slide. Dates are locations of gully head in 2016 and 2017.

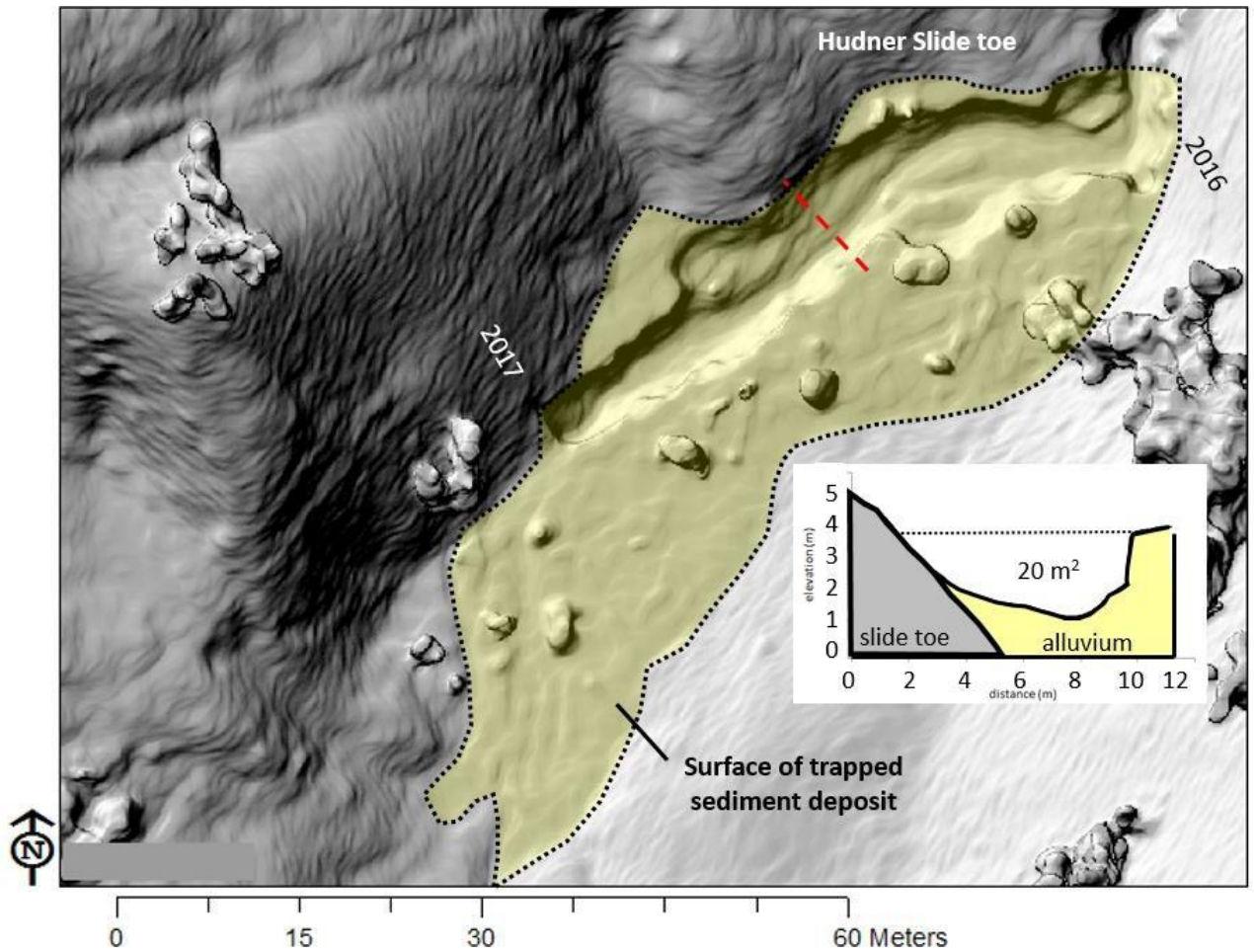


Figure 68 Hillshade shows gully at toe of Hudner Slide (5/2/18). Red dashed line is position of cross section inset. Cross section dimensions in meters. Dates are locations of gully head in 2016 and 2017.

3.3.7 Landslide Causes

Landslides are commonly triggered by either strong rains that saturate soils, strong transient earthquake accelerations, or both (earthquakes occurring in wet winter months). During the most recent 26 years there were 26 earthquakes above a magnitude of 4.0 within 20 km (12.5 miles) of Colluvial and Hudner Creeks, and only one that exceeded 5.0 (Fig. 69). The majority of the earthquakes occurred on, or within a few km of, the San Andreas Fault. Only 10 earthquakes occurred in the same years as a 10-year 24-hour rainfall event (NOAA). Major earthquakes and storms co-occurred in 1995,

1998, 2001, and 2016 (Table 12). The highest magnitude earthquake occurred within three kilometers of the park during the 1998 El Nino. There were no obvious triggers for the new headwall scarp that evolved sometime near 2010.

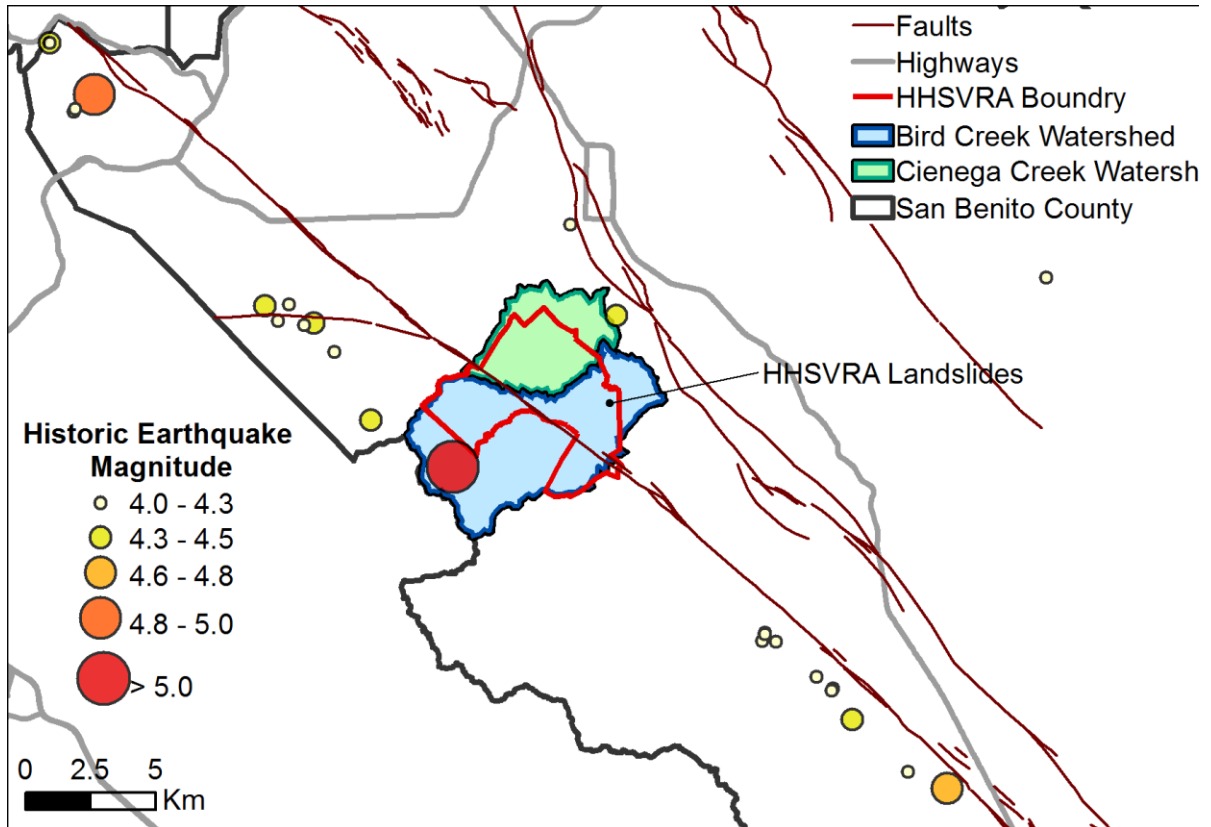


Figure 69. Historic earthquakes from 1990 - 2016 above a magnitude 4.0 and within 20 km of HHSVRA.

Table 12. Rainfall events larger than the 10-year 24-hour threshold and earthquakes greater than 4.0 magnitude within 20 km of HHSVRA between 1990 and 2016.

| Year | Rain Events | Earthquake Magnitude | | |
|------|-------------|----------------------|-----------|-------|
| | | 4.0 – 4.5 | 4.6 – 5.0 | > 5.0 |
| 1990 | | | | |
| 1991 | | | | |
| 1992 | | | | |
| 1993 | | | | |
| 1994 | 1 | | | |
| 1995 | 1 | 3 | | |
| 1996 | | | | |
| 1997 | | | | |
| 1998 | | 1 | | 1 |
| 1999 | | 2 | | |
| 2000 | | | | |
| 2001 | 3 | 5 | 1 | |
| 2002 | | | | |
| 2003 | | 1 | | |
| 2004 | | 1 | | |
| 2005 | | | | |
| 2006 | | 1 | | |
| 2007 | | | | |
| 2008 | | 1 | | |
| 2009 | | 1 | | |
| 2010 | | 1 | | |
| 2011 | | 1 | | |
| 2012 | | | | |
| 2013 | | | | |
| 2014 | | 1 | | |
| 2015 | | | | |
| 2016 | 1 | 1 | | |

While we have determined that the existing slides in HHSVRA accelerate downslope in response to wet winters, there is no obvious trigger for the major slip that produced the tall fresh scarp in 2010 (Fig. 62; Table 12). Apparently significant landslide events in the region can occur at random times. A recent study of slope failure features along the San Andreas Fault near the study area suggests that slow-moving earthflows like the Colluvial Creek and Hudner Creek complexes described above are triggered by winter rains saturating slopes underlain by fine-grained rocks along the San Andrea Fault

(Sheingross et al. 2012). Scheingross et al. (2012) further contend that the lack of strong seismicity along the “creeping” segment of the San Andreas Fault keeps the material on the slopes longer, fostering the low-velocity failure processes. The slope features in the study area therefore conform with the regional slope behavior.

3.4 Best Management Practices

3.4.1 Sediment Retention Basins

The park staff chose a subset of basins within the park to study between 2012 and 2018 (Fig. 70). Basins were chosen based on excavation status and if they were dry enough to survey. We surveyed the basins using a Real-Time Kinetic (RTK) Global Position System (GPS), total station, and drone photogrammetry methods to measure elevation changes within the selected basins. In sites with dense canopy cover, where GPS signal was not reliable, we used a Nikon 3” total station to survey topographic points.

Elevation points from RTK GPS or total station were used to make a DEM through interpolation in ArcMap. Data from drone photogrammetry were processed in Pix4D Cloud, using previously surveyed benchmarks as ground control points. Following winter runoff, we resurveyed several basins in different years using the same methodology. Net aggradation and degradation of sediment was determined using the Cut and Fill tool in ArcMap.

When sediment volume was too thin to quantify with standard survey methods, sediment accumulation was estimated by multiplying the average thickness of the new deposit (measured by penetration with a calibrated rod) by the area of the deposit (Teaby et al. 2013b).

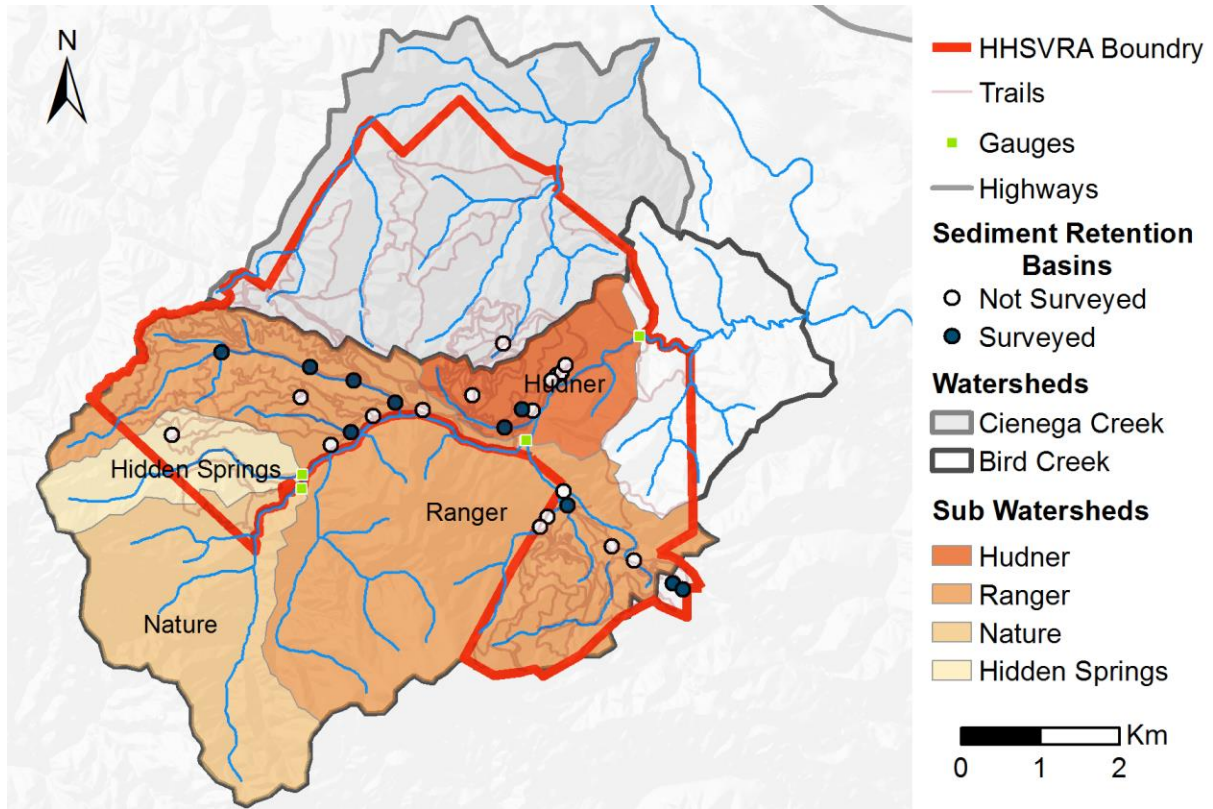


Figure 70. Sub-watershed and HHSVRA sediment retention basins located within the Bird Creek watershed.

Basins located in the clay soils receive mostly suspended sediment that is retained as thin silt and clay laminations (Fig. 71), while those in the granitic soils receive mostly sand and small gravel bedload with a smaller proportion of suspended sediment (Fig. 72). We surveyed 6 basins to determine the volume of retained sediment.



Figure 71. Superhill sediment basin receives runoff from clay soils east of the San Andreas Fault. Little bedload is present. Inset is a close-up view of laminated fine-grained deposits. Small color blocks on scale are 0.005m.

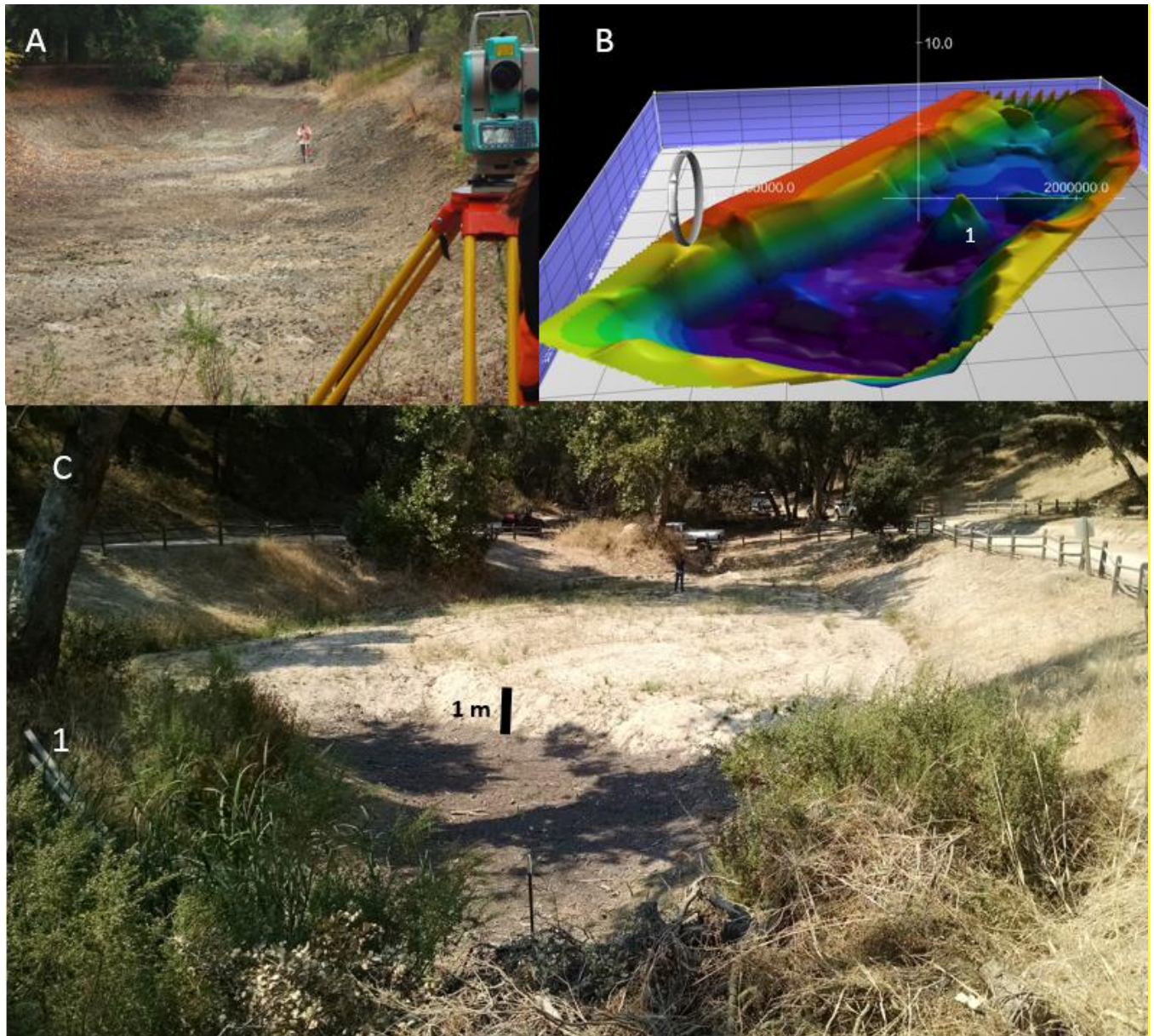


Fig 72. Sediment basin studies include surveying the shape with total station or survey-grade GPS (A), creating digital models (B), and resurveying after sedimentation (C). A) Gilmore Basin after cleanout in 2012. B) DEM of Woodwardia basin after cleanout in 2012. View is upstream. Island is labeled "1." C) Upstream view of Woodwardia basin in fall 2016 showing a 1 m thick sand deposit. Island is labeled "1 m."



Figure 73: Woodwardia Basin showing capacity for sediment (A), and sediment captured in 2017 (B). Note “do not enter” sign near letters and arrow showing the same tree.

Annual basin volume changes, including sediment capture and excavation, are shown in Table 13. The retention values, last surveyed in 2018, were summarized by substrate (granitic and clay soils) and then normalized to drainage area feeding the basin. That volumetric yield value was then extrapolated to the full set of basins in the HHSVRA (Fig. 74, Table 14).

Table 13: Calculation of weighted averages of annual retention per unit drainage area. Values are from basin surveys. See Figure 74 for method. Values in colored cells are used to extrapolate retention to unsurveyed basins in Table 14.

| Basin | Soil type | Survey start and end | Years | Sediment volume (m ³) | Sediment volume (yd ³) | Total volume/Total years (m ³ /yr) | Drainage area above basin (m ²) | Drainage area above basin (ac) | Retention per unit area (m ³ /m ²) | Retention per unit area (yd ³ /ac) |
|------------|--------------|----------------------|-------|-----------------------------------|------------------------------------|---|---|--------------------------------|---|---|
| | | | | | | | | | | |
| Gilmore | granite | 2012 to 2013 | 1 | 10 | 13 | 101.8 | 730507 | 180.5 | 0.000139 | 0.74 |
| | | 2013 to 2017 | 4 | 555 | 726 | | | | | |
| | | 2017 to 2018 | 1 | 46 | 60 | | | | | |
| GP1 | granite | 2012 to 2013 | 1 | 1 | 1 | 4.7 | 45221 | 11.2 | 0.000104 | 0.55 |
| | | 2014 to 2016 | 2 | 13 | 17 | | | | | |
| Scandia | granite | 2013 to 2016 | 3 | 342 | 447 | 86.5 | 1684860 | 416.3 | 0.000051 | 0.27 |
| | | 2017 to 2018 | 1 | 4 | 5 | | | | | |
| Superhill | clay | 2013 to 2016 | 3 | 67 | 88 | 22.3 | 72701 | 18.0 | 0.000307 | 1.62 |
| Office | clay/granite | 2012 to 2016 | 1 | 251 | 328 | 152 | 680000 | 168.0 | 0.000224 | 1.18 |
| | | 2017 to 2018 | 1 | 53 | 69 | | | | | |
| Woodwardia | granite | 2012 to 2016 | 4 | 39 | 51 | 160 | 1567480 | 387.3 | 0.000102 | 0.54 |
| | | 2016 to 2017 | 1 | 759 | 993 | | | | | |
| | | | | | | | weighted average | granite soil | 0.000107 | |
| | | | | | | | weighted average | clay soil | 0.000232 | |

Estimate total sediment retained in basins

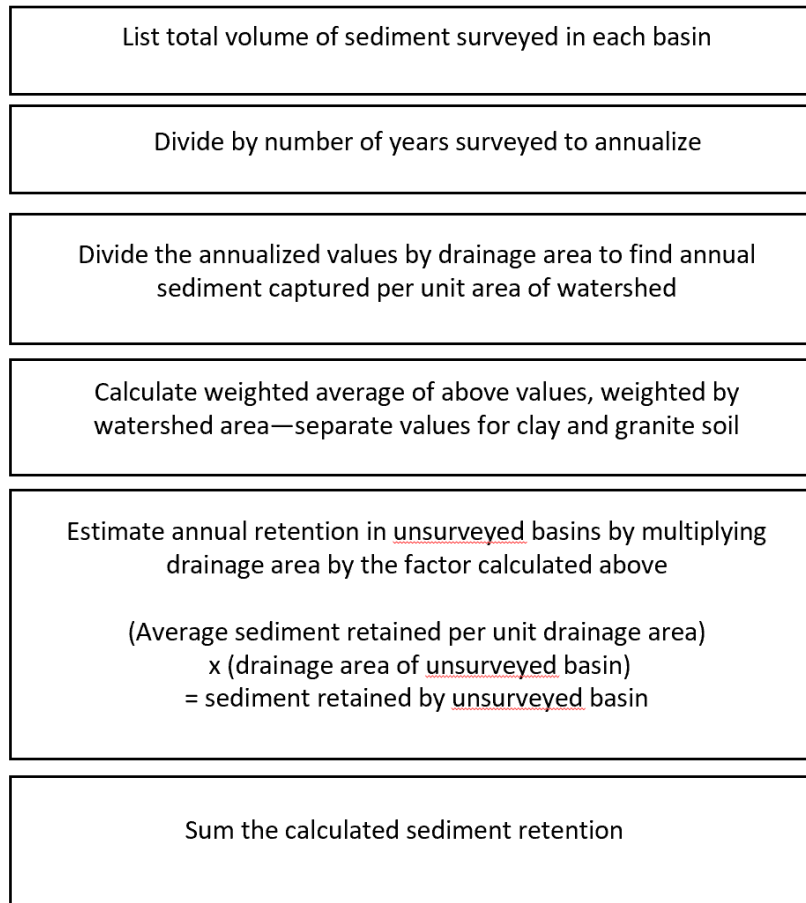


Figure 74: Calculation flow to extrapolate sediment basin retention survey data to entire park.

Table 14: Total sediment retained in Bird Creek watershed retention basins based upon sum of surveyed and unsurveyed basins.

| Basin | Soil type | Watershed | Drainage area above basin (m ²) | Calculated sediment retention (m ³ /yr) | Calculated sediment volume (yd ³ /yr) |
|--------------------------------|-----------|--------------|---|--|--|
| Woodwardia | granite | Bird | 1567480 | 159.6 | 208.7 |
| Whoopie-doo | granite | Bird | 671072 | 71.9 | 94.1 |
| Turtle | granite | Bird | 175052 | 18.8 | 24.5 |
| Sycamore | granite | Bird | 255541 | 27.4 | 35.8 |
| Scandia | granite | Bird | 1684860 | 86.5 | 113.1 |
| Madrone | granite | Bird | 41764 | 4.5 | 5.9 |
| Lodge | granite | Bird | 401968 | 43.1 | 56.3 |
| Bee | granite | Bird | 117782 | 12.6 | 16.5 |
| Tule Lake | granite | Hidden S. | 99220 | 10.6 | 13.9 |
| GP 2 | granite | Bird (Upper) | 108604 | 11.6 | 15.2 |
| Gilmore | granite | Bird (Upper) | 730507 | 101.8 | 133.2 |
| GarnerFlat | granite | Bird (Upper) | 1585600 | 169.9 | 222.3 |
| Area 5 | granite | Bird (Upper) | 2326610 | 538.9 | 704.8 |
| Office | clay | Bird | 680000 | 152.0 | 198.8 |
| GP 1 | clay | Bird (Upper) | 45221 | 4.7 | 6.1 |
| SuperHill | clay | Bird | 72701 | 22.3 | 29.2 |
| unnamed | clay | Bird | 160836 | 37.3 | 48.7 |
| Total sediment retained | | | | 1473.5 | 1927.3 |

The estimated mass of sediment retained in the basins relies on an estimate of density for the complex mixture of material and grain-sizes caught in the basin. We use a value of 1540 kg/m³ because it is an average of the density for sand and silty loam. That conversion factor indicates that approximately 2260 tonnes of sediment is captured by the basins in an average year.

The retained volumes in Table 13 are well constrained through modern survey methods, however there are considerable uncertainties in both the appropriate average density of basin fill and the relationship between drainage area and fill volume (Table 13).

In 2017, Woodwardia retained approximately 759 m³ (993 yd³) of sediment, the largest single-year retention during the study. This captured sediment, plus additional sediment, was excavated from Woodwardia in 2018, increasing the basin volume by

2520 m³ (3296 yd³). This excavation was estimated by HHSVRA staff to be 2724 yd³ of material, based on number of truckloads of sediment removed. The estimate by truckload underestimates the surveyed volume by approximately 18%.

3.4.2 Hidden Springs Sediment Inventory

Hidden Springs watershed occupies 678 acres in the headwaters of Bird Creek (Fig. 75). Of that total, 224 acres are both within the park and are north of Hidden Springs Creek, where public OHV is present. Thirty-two acres currently drain into two sediment basins, including Tule Lake (Fig. 76). The remaining 192 acres host 22.9 km of trails. We evaluated the need for a sediment retention basin in Bird Creek through a detailed geomorphic review of the watershed that culminated in an inventory of sediment sources, transport pathways, and sinks (Fig. 77). The map is based upon direct observation of all roads, trails and hill slopes in the watershed. Observations were augmented by low altitude sUAS reconnaissance video.

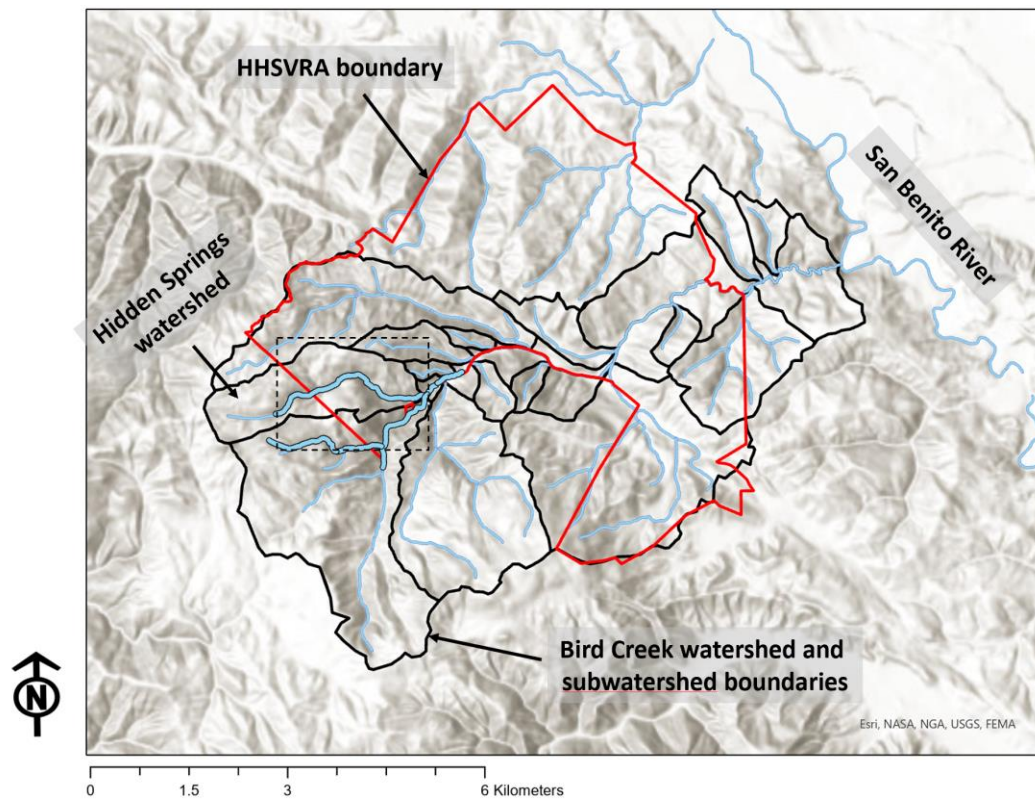


Figure 75. Hidden Creek watershed. Red outline is park boundary. Outer black line is Bird Creek watershed. Dashed box is region enlarged in Figure 76.

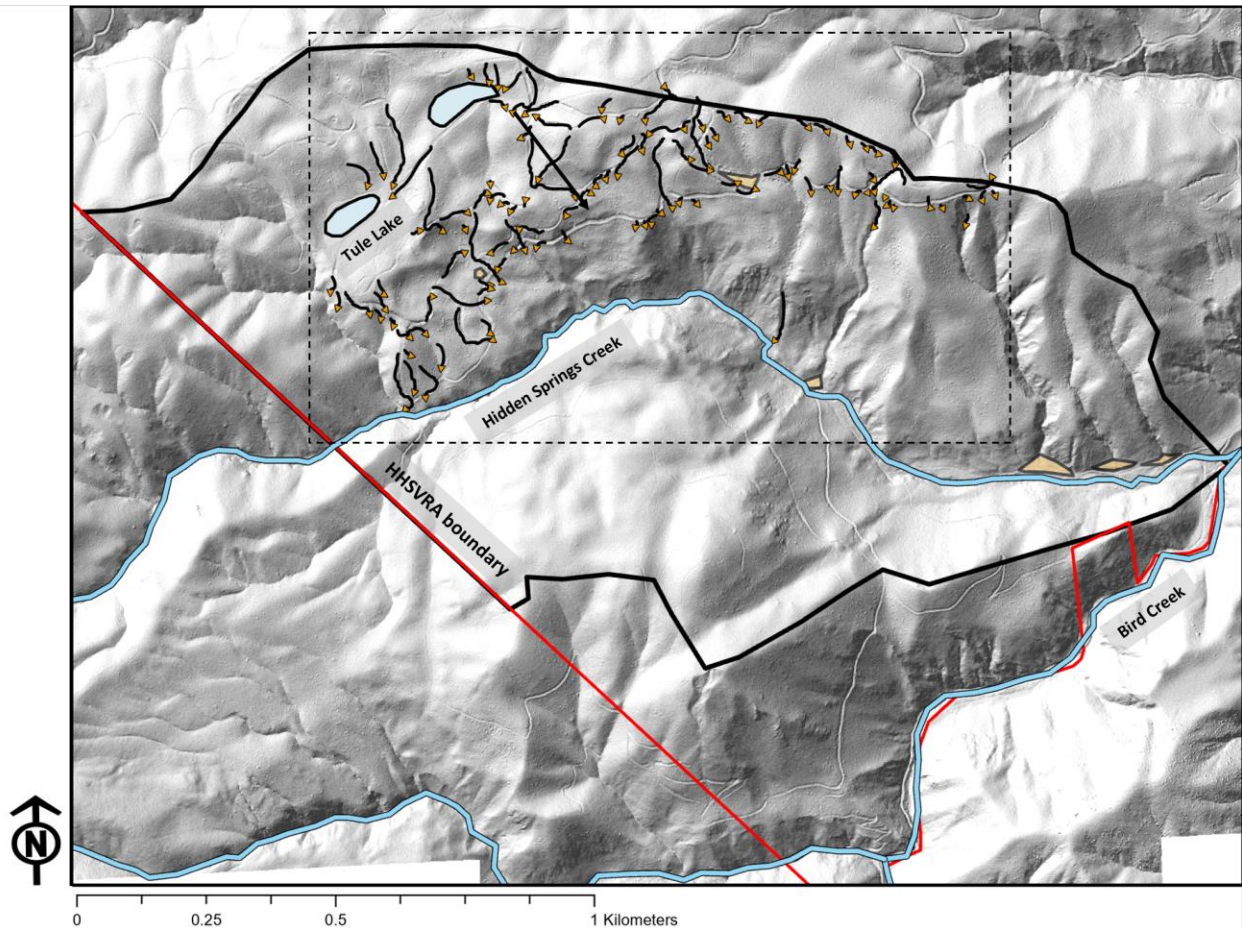


Figure. 76. Major sediment pathways mapped on a hillshade of Hidden Springs watershed. Blue regions are sediment retention basins. Brown regions with black outlines are natural sediment storage areas. Four inactive sediment fans are the storage areas mapped along Hidden Springs Creek. Dashed box is enlarged in Figure 77.

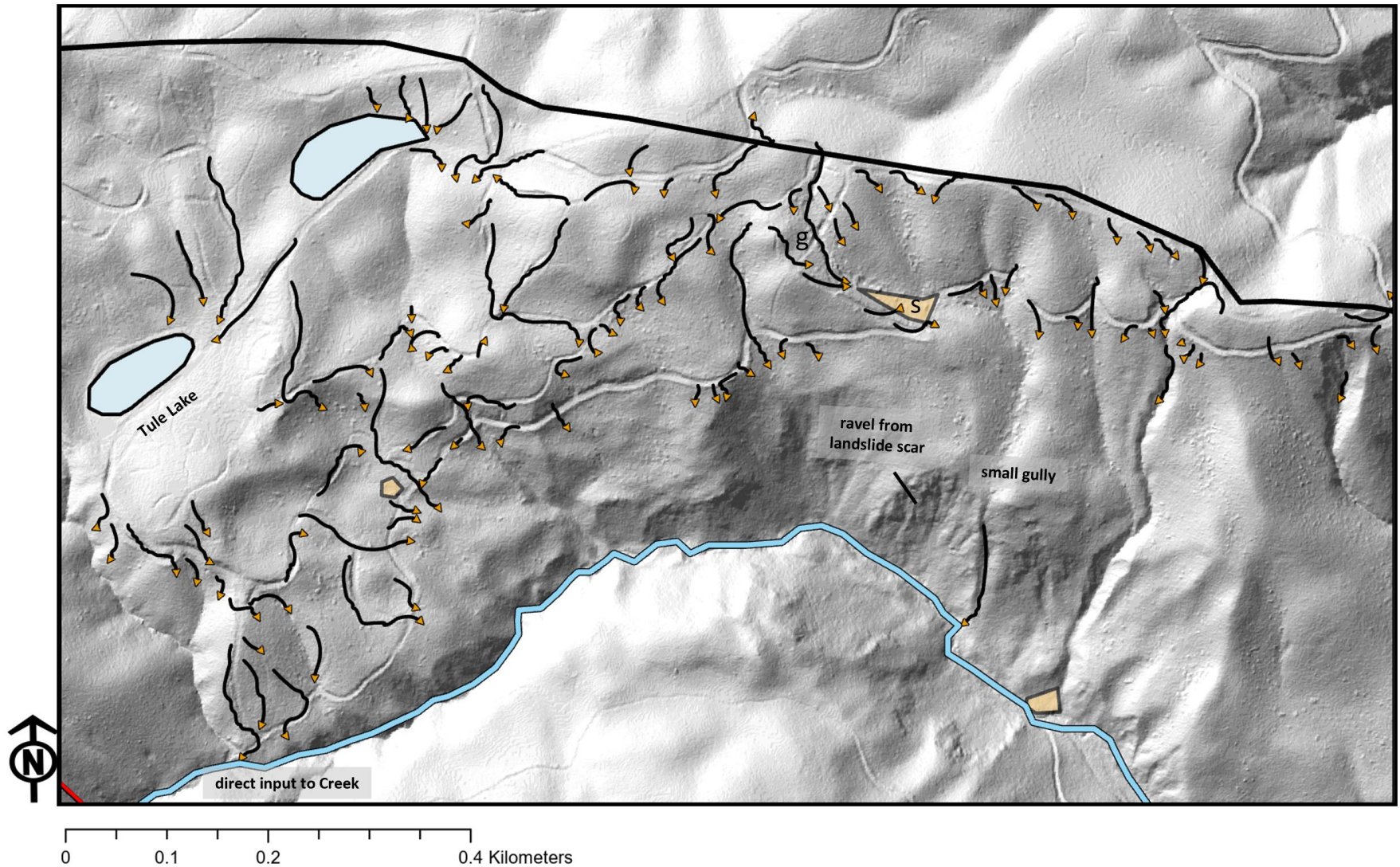


Figure. 77. Major sediment pathways mapped on a hillshade of Hidden Springs watershed. Arrow heads show approximate termination of each sediment pathway. Brown regions with black outline are natural sediment storage areas. "s" is major natural storage area below gully system (g). See Figure 76 for location.

The chief sediment sources include mapped and volunteer trails and a deep gully (“g” in Fig 77) in the upper watershed, and a small natural gully occupying an historic landslide scar near the channel (Fig. 77). The small gully was described in detail in Smith et al. (2016) because it produced a new chronic (but natural) source of small-gravel bedload to Bird Creek in 2012. The only instance of trail-sourced sediment directly entering Hidden Springs Creek is at the upstream end, where a steep decommissioned trail terminates near the channel (Fig. 77).

Sediment storage occurs on all hill slopes, in two naturally low-gradient locations, and in the inactive sediment fans at the downslope terminus of four ravines on the valley floor (Figs. 76 and 77). The ravines are generally inactive as evidenced by the mature vegetation, and sparse fresh sediment (and no incision) on the sediment fans.

The deep gully (“g” in Fig.77) has cut down through the deep granitic soil to more solid bedrock. The presence of bedrock in the invert has either arrested or greatly reduced the incision rate and consequent sediment production rate. Sediment leaving the gully is dispersed and stored on the local hillslope or is trapped in the natural storage area located farther downslope (“s” in Fig. 77). A small fraction traverses Olive Return Rd., where it is then trapped on a the densely vegetated slope.

Most trail-sourced sediment is transported only several meters before being stored on adjacent hillslopes beneath the dense native scrub plant community. The process is fostered by long reaches of out-sloped roads and well-placed water bars that do not (in many cases) intersect erosional features down-gradient of the road. A small proportion of the sediment is transported farther downslope in small channels. The sediment is typically dispersed when the channels reach a low gradient facet (Fig. 77).

Using the very general relationship between trail length and trail erosion (Table 7: line 1), the 22900 m of unprotected trails in Hidden Springs annually generate 211 m³ of sediment. That translates to fewer than 1.5 yd³ per acre of hillslope each year. That volume of material is easily dispersed and stored as colluvium in the chaparral.

Given the low input of trail-derived sediment, we conclude that construction and maintenance of a sediment retention basin in the narrow confines of Hidden Springs Creek is unnecessary. Building on an observation in Smith (2016), Hidden Springs Creek has a very steep channel with steep canyon walls, so there should be a very short lag time between peri-channel erosion events and sediment transport into Bird Creek. Direct visual monitoring during almost all peak runoff events during the past 11 years confirms

the absence of chronic high sediment transport rate (bedload or suspended load) from the mouth of Hidden Springs.

Sediment BMP activities in the watershed could include:

- 1) Regrading and planting the steep trail that terminates near Bird Creek,
- 2) Narrowing and outsloping the wide trails (e.g., Olive Orchard Return)
- 3) Periodically moving the location of waterbars to prevent gullying on adjacent hillslopes.

While an obvious BMP would be to regrade the deep gully (“g” in Fig. 77), it is no longer a significant sediment source. The overall disturbance footprint of heavy machinery during mechanical restoration on granitic slopes exceeding 40% grade might produce more harm to the ambient vegetative ecosystem than leaving the dormant gully in place.

3.4.3 Gully Management: Example BMP

Of the many restoration BMPs active at the HHSVRA, we selected the newly constructed Coyote Trail restoration site to monitor because it posed a significant engineering challenge. The project was designed to mitigate gully erosion on a 20% grade, bare slope with coarse granular granitic soils that are naturally prone to gully erosion. The engineering measures included filling and regrading a deeply incised trail system (Fig. 78). Once the steep site was regraded, 27 rip-rap grade control structures were installed to manage future erosion. The site was revegetated with native plants selected for the site conditions.



Figure 78. View down Coyote Trail restoration project. A) Before decommissioning, circa 2009. B) After grading and placement of rock berms, but before revegetation in July 2011.

We monitored the restoration site from 2012 to 2021 to assess the gully treatment. The Coyote Trail erosion control project was monitored for general effectiveness and stability. Each berm and intervening slope facet were periodically inspected for signs of renewed erosion and geomorphic stability. Six berms were selected for further study. Six benchmarked cross sections were established at each of the six berms for a total 36 transects that were periodically resurveyed to monitor project success. Surveys were conducted with autolevel and meter tape. The site was also periodically inspected to evaluate vegetative recovery, with the final inspection in 2021.

Visual inspection, ground-based photography, and serial surveys of a subset of the berms indicate that some berms performed well (Fig. 79), while others underwent a period of adjustment. During the first surveys in 2012, many of the berms showed early signs of lateral and vertical failure. The 2014 inspection showed that several berms were compromised by erosion (Figs. 80 and 81). Revegetation efforts have been successful despite the drought. Reconnaissance and surveys performed in 2016 indicated that the site vegetation was very healthy, but cross section surveys indicated that the berm system was still evolving (Appendix A).



Figure 79. Berm-1: View up-gradient of a berm in the Coyote Trail gully restoration site in March 2014. The berms trapped sediment until the space behind the berms had filled with sediment. This berm is an example of successful sediment trapping and grade control.



Figure 80. View down-gradient of a berm in the Coyote Trail gully restoration site in March 2014. Some berms provided incomplete grade control because lateral erosion outflanked the rock structure.



Figure 81. View up-gradient of a berm in the Coyote Trail gully restoration site in March 2014. While major gullying has been stopped, some berms provided incomplete grade control because of undercutting that bypassed the berm footers.

By 2021, 10 years after construction, the restoration site had a dense cover of deep-rooted native plants representing the plant community on the adjacent hill slopes (Fig. 82). The site had also geomorphically stabilized. Although one small gully is still present (Fig. 83), the site no longer has pervasive erosion noted in previous visits. Any sediment that leaves the site is caught in the sediment basins locate down valley.

Despite the early indications that the site might not stabilize, the restoration effort eventually returned a deeply scarred landscape (Fig. 78) to near natural conditions. Future restoration designs on steep granitic soils might have earlier success by employing closer-spaced berms that are keyed deeper into the bed and banks. Figure 9, and the Coyote Trail study illustrate that native revegetation is challenging in the drought-prone regional climate; restoration sites might take a decade to fully mature.



Figure 82: Coyote Trail restoration site in 2021. Native plants have stabilized the soil between the berms.



Figure 83: A gully in the Coyote Trail restoration site in 2021. Vegetation in the invert indicates that the feature may be stabilizing.

4 Discussion

We studied sediment sources, transport and BMPs at HHSVRA for eleven years. While OHV activity at the park might have been average during that span, it is unclear whether our measured parameters represent long-term average climate conditions. For example, only one year had near “average” rainfall and there were 6 drought years where Bird Creek has little to no runoff. Further, sediment transport reported at the gages in 2017 are almost certainly minimum values. While there are limitations to the data, this study represents the longest continuous sediment monitoring program in the SVRA system. Below, we use our spatially-extrapolated data sets to estimate a broader sediment budget for the park.

The sediment budget for Bird Creek may be stated as,

$$\text{Inputs} - \text{Outputs} = \text{Change in Storage} + \text{Error}.$$

That budget can be expressed in the following variables,

$$(S_a + S_{nsb} + S_{in}) - S_{out} = (S_{ret} + S_c) + S_e$$

S_a is the total mass of anthropogenic sediment sources we estimated

S_{nsb} is the portion of natural input upstream of Hudner gage (streambank erosion)

S_{in} is the mass of sediment entering the system as measured at the Nature gage

S_{out} is the mass of sediment leaving the system as measured at the Hudner gage

S_{ret} is the mass of sediment retained in the basins

S_c is the unmeasured mass of sediment stored in hillslope colluvium

S_e is the error in the budget.

Rearranging the terms, we sum all the un-estimated values on the right side of the equation to calculate the net residual unmeasured mass (Table 15):

$$(S_a + S_{nsb} + S_{in}) - S_{out} - S_{ret} = S_c + S_e.$$

Table 15. Sediment budget for Bird Creek Watershed Above Hudner Gage

| Variable | Symbol | Mass (tonnes) | Data source | Confidence |
|---|---|---------------|---|---|
| OHV roads and trails | S_a | 3390 | Extrapolated from 7 years of local trail erosion surveys. | Moderately-well constrained. Assumptions in report. |
| County Roads | S_a | 5 | San Juan Grade erosion captured by basins. Cienega Road has active gullies and soil slips | Poorly constrained |
| Cattle | S_a | 2 | Difficult to quantify distributed impacts | Poorly constrained |
| Campgrounds | S_a | <1 | Anecdotal observations | Poorly constrained |
| Landslides | This input (and output) occurs below Hudner gage. | 136 | Episodic high input (1500 tonne) measured by sUAS averaged over the 11-year study. Value not added to "Total Inputs" because it enters Bird Creek below the Hudner Gage. | Annual average value is poorly constrained. |
| Natural erosion from stream banks | S_{nsb} | 109 | Input from stream bank pins east of San Andreas Fault and no other input from stream channels | Minimum value. Not extrapolated to total watershed. |
| Stream channels | S_{nsb} | -58 | Repeat surveys show storage of locally-derived landslide material | High confidence |
| Sed entering system | S_{in} | 6 | 11 year average Nature Gage | Confident to order of magnitude. 2017 underestimated |
| Total inputs | S_a $+S_{nsb}$ $+S_{in}$ | ≈3457 | Does not include Hudner Slide | |
| Sed leaving system | S_{out} | 45 | 11 year average (w/0 2017) Hudner gage | Confident to order of magnitude. 2017 underestimated |
| Basin retention | S_{ret} | 2262 | Extrapolated basin capture. Extrapolation based upon drainage area above basin. Basins stratified by granitic or clayey soils. | Extrapolation based upon sparse data. Average bulk density of basin fill is between sand and silty loam (1.54 tonnes/m ³) |
| Change in storage - unmeasured natural erosion + Errors | $S_c + S_e$ | ≈1151 | Net residual mass that is either stored on slopes (S_c) or does not exist (S_e) | |

The overarching goal of the sediment retention basins in the park is to capture the sediment eroded by OHV use. The difference between the estimated OHV erosion (3392 tonnes) and basin retention (2262 tonnes) is 1130 tonnes. That difference can be interpreted as the amount of eroded sediment that was not “accounted for” in the basins, and likely represents hillslope storage. The last term of the budget sums the unmeasured hillslope storage S_c and measurement error S_e . Given that the sum is 1150 tonnes, we interpret that 1130 tonnes can be ascribed to unmeasured hillslope storage, leaving a total estimated error of just 20 tonnes.

The sediment sources located downstream of sediment basins include, cattle, campgrounds, stream banks, and stream channels. When estimates of those sources are added to the amount entering the park in Bird Creek (Nature gage), the annualized value is 60 tonnes. The annualized value leaving the park (Hudner gage) is 45 tonnes. These values are reasonably close, given the uncertainties in estimating sources or measuring sediment transport. We note that the stream gage values are minima because of the estimates made in 2017. The difference between the expected sediment mass leaving the park (60 tonnes) and the amount measured (45 tonnes) is 15 tonnes. This discrepancy is very close to the overall estimated error of the budget (20 tonnes).

The TMDL for the San Benito River watershed sets an eventual goal of 93,460 tonnes/yr of suspended sediment from all sources by the year 2050 (RWQCB 2005). It is not likely that the Regional Board or designees will directly measure suspended sediment in the main San Benito channel. It is a conceptual goal that can be indirectly monitored through periodic suspended sediment concentration measurements (RWQCB 2005). If we simplistically assume that all parts of the San Benito River watershed would contribute equally to that future goal, then Bird Creek upstream from the Hudner gage can be ascribed 2.2% of the load (2060 tonnes/yr), since it occupies approximately that much of the San Benito watershed. However, the highest annual load Bird Creek produced during our study was only 180 tonnes, in 2011, and our estimate of the annual average is 45 tonnes/yr (underestimated in 2017). Sediment management in the HHSVRA is keeping the total watershed yield well below the target value, perhaps by trapping both the anthropogenic and natural suspended sediment loads that are generated within the park boundary. The Hudner landslide produced 50% of the target on its own in 2017, so landslide processes are clearly an important sediment source to consider in estimating sediment load contributions from the regional watersheds.

Figure 84 represents our general understanding of the relative importance of the various sediment sources within the Bird Creek Watershed.

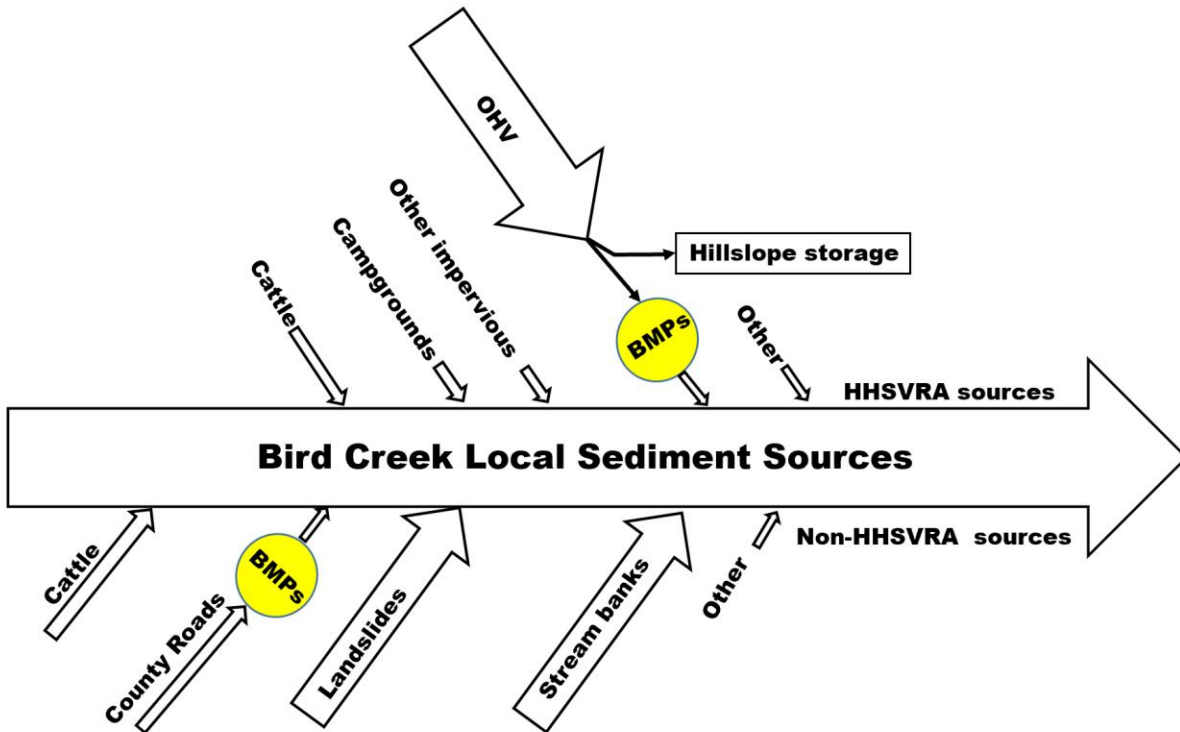


Figure 60. Bird Creek sediment sources. Arrows are qualitatively scaled to indicate our opinion about their relative volumetric importance. Upper sources are those related to State Park land. Lower sources are from other portions of the Bird Creek watershed. Some landslides contribute a very large proportion of sediment on a decadal to centennial time frame. BMPs are shown to decrease the impact of sources located upstream of sediment retention basins.

5 References

- Bedrossian T, Reynolds S. 2007a. Development of a Soil Conservation Standard and Guidelines for OHV Recreation Management in California. *Environmental & Engineering Geoscience* [Internet]. [2007 August; cited 2012 March 12]; 13 (3). Available from: <http://eeg.geoscienceworld.org/content/13/3/241.abstract>
- Bedrossian TL, Reynolds SD. 2007b. Guidelines of a soil conservation standard and guidelines for OHV recreation management in California. *The Geological Society of America* 13(3): p.241–253.
- Bogdan M, Smith D, Klein J, Somilleda N, and Soares S. 2019. Hollister Hills SVRA Trail Erosion Surveys: Summer 2019. The Watershed Institute, California State Monterey Bay, Publication No. WI–2019–06, 39 pp.
- [CA] California State Bill 249. 2017. California State Legislature. https://leginfo.legislature.ca.gov/faces/billTextClient.xhtml?bill_id=201720180SB249
- [CDOT] California Department of Transportation. 2014. Highway design manual. California Department of Transportation [Internet]. Available from: http://www.dot.ca.gov/hq/oppd/hdm/pdf/english/HDM_Complete_07Mar2014.pdf.
- California State Parks. 2009. California State Parks Off–Highway Motor Vehicle Recreation Division Strategic Plan. Available from: <http://ohv.parks.ca.gov/pages/25010/files/ohmvr%20strategic%20plan.pdf>
- [CDPR] State of California Department of Parks and Recreation (United States) Hollister Hills State Vehicular Recreation Area. Non–Motorized Buffer Trails Project. Sacramento (CA): State of California– Department of Parks and Recreation Off–Highway Motor Vehicle Recreation Division; 2012 Jan. 127 p. Available from: Department of Parks and Recreation Sacramento, CA. [Internet]. [cited 2012 Jan 25]; 56(4): 356–374. Available from: <http://www.jstor.org/stable/27828327>
- Chow, K, Luna, L, Smith D, and Silveus, J. 2015. Hollister Hills SVRA Trail Erosion Surveys: Summer 2015. The Watershed Institute, California State Monterey Bay, Publication No. WI–2015–04, 34 pp.

- Chow, K, Luna, L, Conlen, A, and Smith D. 2016. Hollister Hills SVRA Trail Erosion Surveys: Summer 2016. The Watershed Institute, California State Monterey Bay, Publication No. WI-2016-06.
- Chow, K, Luna, L, and Smith D. 2017. Hollister Hills SVRA Sediment Basin Volumes: Water Year 2016. The Watershed Institute, California State Monterey Bay, Publication No. WI-2017-02, 40 pp.
- Davies TRG, Korup O. 2006. Persistent alluvial fanhead trenching resulting from large, infrequent sediment inputs. *Earth Surface Processes and Landforms*, 32(5): 725–742.
- Dikau, R., Brunsden, D., Schrott, L. and Ibsen, M–L. (eds.) 1996. *Landslide recognition, identification, movement, and causes*. New York: John Wiley and Sons.
- [GEOL 460], CSUMB Class. Allan, J., Chaney, M., Chen, A., Demetre, J., Hurdle, M., Jew, N., Latham, B., Layne, M., Medina, M., Muratore, D., Odermatt, S., Rothwell, R., Suwada, J. and Smith D. 2014. Hollister Hills SVRA Sediment Sources and Erosion Control: San Juan Canyon Road, Coyote Trail, and Hidden Springs Watershed. CSUMB Division of Science and Environmental Policy Senior Thesis Report, 64pp.
- [GEOL 460], CSUMB Class. Davis, B., DeLay, C., Franco, D., Gonnerman, M., Grinstead, C., Hamblin, D., Haug, A., Hill, C., Kwan, R., McCullough, E., Pefok, M., Potter, T., Reynolds, D., Rogers, S., Santoyo, J., Vernon, M., Williams, C., Williams, J., and Smith. D. 2012. Partitioning Sediment Sources at the Hollister Hills State Vehicular Recreation Area. The Watershed Institute, California State Monterey Bay, Publication No. WI-2012-04, 74 pp.
- Graymer RW, Moring BC, Saucedo GJ, Wentworth CM, Brabb EE, and Knudsen KL. 2006. Geologic Map of the San Francisco Bay Region. US Geological Survey Scientific Investigations Map 2918. <http://pubs.usgs.gov/sim/2006/2918/>. Last accessed 10/04/2016.
- Griggs GB, Walsh BL. 1981. The impact, control, and mitigation of off-road vehicle activity in Hungry Valley, California. *Environmental Geology*. 3:229–243.
- Harden DR, Stenner H, Blatz I. 2001. The Calaveras and San Andreas Faults In and Around Hollister. Field Trip 6. Available from: <http://pubs.usgs.gov/bul/b2188/b2188ch6.pdf>

- Harrelson C, Potyonty J, Rawlins C. 1994. Stream Channel Reference Sites: An illustrated guide to field technique. General Technical Report RM-245. Fort Collins, CO: United States Department of Agriculture, Forest Service. 61 p.
- Harvey M and Watson C. 1986. Fluvial processes and morphological thresholds in incised channel restoration. *Water Resources Bulletin of the American Water Resources Association*, v.22, p.359-368.
- Hawley R, Bledsoe J, Stein E, and Haines B. 2012. Channel evolution model of semiarid stream response to urban-induced hydromodification. *Journal of the American Water Resources Association*. P. 1-3. DOI:10.1111/j.1752-1688.2012.00645.x.
- [HHSVRA] Hollister Hills SVRA Natural Resources Staff. 2012. 2012 Trail Assessment Report, Hollister Hills District. 115pp.
- Klein J, Bogdan M, Steinmetz C, Kwan-Davis R, Price M, Smith D. 2019. Hollister Hills SVRA Sediment Basin Volumes: Water Years 2017-2018. The Watershed Institute, California State University Monterey Bay, Publication No. WI-2019-04, 38 pp.
- Leopold, L.B., Wolman, M.G., and Miller, J.P. 1964. *Fluvial Processes in Geomorphology*: W.H. Freeman, San Francisco, 520pp.
- Luce CH, Wemple BC. 2001. Introduction to the special issue on hydrologic and geomorphic effects of forest roads. *Earth Surface Processes and Landforms* 26(2): 111-113.
- Majmundar H. 1994. *Landslide Hazards in the Hollister Area, San Benito County California, 1994: Landslide Hazard Identification Map No. 30 (DMG Open-File Report 94-02)*
- Minella JPG, Merten GH, Reichert JM, Clarke RT. 2008. Estimating suspended sediment concentrations from turbidity measurements and the calibration problem. *Hydrological Processes* 22: 1819-1830.
- Montgomery DR. 1994. Road surface drainage, channel initiation, and slope instability. *Water Resources Research* 30(6): 1925-1932. Available from: <http://onlinelibrary.wiley.com.library2.csumb.edu:2048/doi/10.1029/94WR00538/pdf>

- Morris, M., Smith, D., Pentecost, M., & Chow, K. 2018. Hollister Hills SVRA Trail Erosion Surveys: Summer 2017. The Watershed Institute, California State Monterey Bay, Publication No. WI-2018-04, 32 pp.
- Nicol C, Smith D, Nitayangkul K, Williams C, Moreland S. 2011. Hollister Hills SVRA Sediment Budget: Water year 2010-2011. The Watershed Institute, California State Monterey Bay, Publication No. WI-2011-04b, 25 pp.
- Nolan, K. M. and Shields, R. R., 2000, Measurement of stream discharge by wading, U. S. Geological Survey WRI 2003-4103, CD-ROM, various pages.
- [NRCS] Soil Survey Staff, Natural Resources Conservation Service, United States Department of Agriculture. Soil Survey Geographic (SSURGO) Database for [San Benito County, CA]. Available online at <http://soildatamart.nrcs.usda.gov>. Accessed [Feb 2011].
- Ouren DS, Haas C, Melcher CP, Stewart SC, Ponds PD, Sexton NR, Burris L, Fancher T, and Bowen ZH. 2007, Environmental effects of off-highway vehicles on Bureau of Land Management lands: A literature synthesis, annotated bibliographies, extensive bibliographies, and internet resources: U.S. Geological Survey, Open-File Report 2007-1353, 225 p.
- ESA PWA. 2013. Pajaro and San Benito Rivers Sediment Study and Transport Model Update. Memorandum from Gragg and Collinson to Guitierrez Consultants and AMBAG. https://prwfpa.planeteria-development.com/sites/default/files/2021-05/prwfpa_transport_sediment_study_2014_0.pdf
- PRISM Climate Group, Oregon State University, <http://prism.oregonstate.edu>, created 4 Feb 2004.
- Prosser I.P., Hughes A.O., Rutherford I.D. 2000. Bank erosion of an incised upland channel by sub aerial processes: Tasmania, Australia. *Earth Surface Processes and Landforms*; 25: 1085-1101.
- Ritter, D., Kochel, R., Miller, J. 2011. *Process geomorphology* (5th edition). Waveland Press Inc., Long Grove. 652 pp.

- [RWQCB] Region 3 Water Quality Control Board 2005. Pajaro River Total Maximum Daily Loads for Sediment (including Llagas Creek, Rider Creek, and San Benito River). 74 pp. http://www.waterboards.ca.gov/centralcoast/water_issues/programs/tmdl/docs/pajaro/sediment/paj_sed_tmdl_project_report.pdf . Accessed [December 2016].
- [RWQCB] Region 3 Water Quality Control Board 2006. Resolution No. R3-2005-0132 Amending the water quality control plan for the central coast basin to include Pajaro River total maximum daily loads and implementation plan for sediment including Llagas Creek, Rider Creek, and San Benito River and a land disturbance prohibition. 11 pp. http://www.swrcb.ca.gov/rwqcb3/water_issues/programs/tmdl/docs/pajaro/sediment/paj_sed_tmdl_resoln+bpa.pdf. Accessed [October 2016].
- Scheingross J, Minchew B, Mackey B, Simons M, Lamb M. and Hensley S. 2012. Fault-zone controls on the spatial distribution of slow-moving landslides. *GSA Bulletin*. V. 125, p. 473-489. Doi: 10.1130/B30719.1.
- Schnieders J., Smith D., Somilleda, N., and Soares, S. 2020. Hollister Hills SVRA Trail Erosion Surveys: Summer 2020. The Watershed Institute, California State Monterey Bay, Publication No. WI-2021-01, 38 pp.
- Silveus, J, Teaby A, and Smith D. 2014. Hollister Hills SVRA Trail Erosion Surveys: Spring 2014. The Watershed Institute, California State Monterey Bay, Publication No. WI-2014-09, 20 pp.
- Smith D., Chow, K, and Luna, L. 2016. Six Year Summary of Watershed Studies at Hollister Hills State Recreational Vehicle Area: Fall 2010 to Fall 2016. The Watershed Institute, California State Monterey Bay, Publication No. WI-2016-12, 94pp.
- Smith D, Bogdan M, Klein J, Terzulli A, Soares S, and Somilleda N. 2019. Hollister Hills SVRA Trail Erosion Surveys: Summer 2018. The Watershed Institute, California State Monterey Bay, Publication No. WI-2019-01, 40 pp
- Smith D, Klein J, Bogdan M, Steinmetz C, Kwan-Davis R, and Price M. 2019. Landslide, Channel, and Road Culvert Sediment sources at Hollister Hills State Recreational

- Vehicle Area – 2018 Report. The Watershed Institute, California State Monterey Bay, Publication No. WI-2019-03, pp 43.
- Smith, D. Schnieders, J., Marshall, L., Melchor, K., Wolfe, S., Campbell, D., French, A. Randolph, J., Whitaker, M., Klein, J., Steinmentz, C., and Kwan, R. 2021. Influence of a Post-dam Sediment Pulse and Post-fire Debris Flows on Steelhead Spawning Gravel in the Carmel River, California. *Frontiers in Earth Sciences–Biogeosciences*. DOI: 10.3389/feart.2021.802825.
- Teaby A, Silveus, J, and Smith D. 2013a. Hollister Hills SVRA Trail Erosion Surveys: Spring 2013. The Watershed Institute, California State Monterey Bay, Publication No. WI-2013-07, 32 pp.
- Teaby A, Silveus, J, Smith D. 2013b. Hollister Hills SVRA Sediment Basin Volumes: Water year 2012–2013. The Watershed Institute, California State Monterey Bay, Publication No. WI-2014-12, 27 pp.
- Trimble SW, Mendel AC. 1995. The cow as a geomorphic agent – A critical review. *Geomorphology*. 13: 233–253.
- Turton DJ, Smolen MD, Stebler E. 2009. Effective BMPS in reducing sediment from unpaved roads in the Stillwater creek, Oklahoma Watershed. *Journal of the American Water Resources Association* 45(6): 1343–1351.
- Tuttle M, Griggs G. 1987. Soil erosion and management recommendations at three state vehicular recreation areas, California. *Environmental Geology and Water Science*. V.10. P.111–123
- Wagner DL, Greene G, Saucedo GJ, and Pridmore CL. 2002. Geologic Map of the Monterey 30' X 60 'Quadrangle and Adjacent Areas, California. California Geological Survey Regional Geologic Map No. 1, 1:100,00 scale. <http://www.quake.ca.gov/gmaps/rgm/monterey/monterey.html>. Last accessed 10/04/2016
- Wass PD, Marks SD, Finch JW, Leeks GJL, Ingram JK. 1997. Monitoring and preliminary interpretation of in-river turbidity and remote sensed imagery for suspended sediment transport studies in the Humber catchment. *The Science of the Total Environment* 194: 263–283.

Western Weather Group [Internet]. c 2021. Hollister SVRA Weather Information and Data. cited 2021 Oct 1. Available from: <http://westernwx.com/hollisterhills/>.

Wynn, T. and Mostaghimi, S. 2006. The Effects of Vegetation and Soil Type on Streambank Subaerial Processes in Southwestern Virginia, USA. *Earth Surface Processes and Landforms*. 31: 399–413.

6 Appendix A

Cross sections from berm 26 of the Coyote Trail restoration site. The site showed typical behavior of the surveyed berms.

